CHARACTERISTICS OF BYZANTINE PERIOD BUILDING BRICKS USED IN ST. JEAN BASILICA (AYASULUK HILL) AND ANAIA CHURCH (KADIKALESİ)

A Thesis Submitted to
the Graduate School of Engineering and Science of
İzmir Institute of Technology
in Partial Fulfilment of the Requirements for the Degree of

MASTER OF SCIENCE

in Architectural Restoration

by
Elif ÇAM

July 2022
İZMİR

ACKNOWLEDGMENTS

Foremost, I would like to express my sincere thanks to my supervisor, Assoc. Prof. Dr. Elif Uğurlu Sağın for her great guidance and support throughout the study. This thesis could not have been made possible without her knowledge and encouragement. Her geniality and endless patience with our questions were what enhanced my motivation to research and sense of curiosity. I feel so lucky to be her one of the first master's degree students.

I specially would like to thank Prof. Dr. Başak İpekoğlu for her help and contacts in determining the study subject and Prof. Dr. Hasan Böke for his valuable suggestions and criticisms. I am also thankful to Inst. Dr. Kerem Şerifaki for sharing his knowledge and experiences, and Assoc. Prof. Dr. Hasan Engin Duran for his support in IBM SPSS.

I owe a debt of gratitude to the Kadıkalesi/Anaia and Ayasuluk Hill and St. Jean Basilica Excavation Teams, particularly Prof. Dr. Zeynep Mercangöz and Assoc. Prof. Dr. Sinan Mimaroğlu, for sharing the excavation materials and archives, also for their warm hospitality.

I would like to thank the examining committee members, Assoc. Prof. Dr. Sinan Mimaroğlu and Assoc. Prof. Dr. Hasan Engin Duran for kindly participation in my thesis defence seminar.

I would like to show my acknowledgement to lecturers of the IZTECH Center for Materials Research (MAM) who spent their time on SEM-EDS, XRD, MTM and TGA analyses. I am grateful that IZTECH-BAP financially supported the TGA and MTM analyses of this study.

I would like to express my gratitude to my dear friends Ayşegül Demir, Tuğçe Tekin, Nihan Bulut, Zeynep Özkaya, and Rabia Nur Bilekli for their uplifting friendships. The times I spend with them are so precious. My special thanks to my dear friend and companion Tuğçe Işık for being with me in every difficulty during this process. I consider myself fortunate to have a friend like her with whom I have shared field surveys and laboratory processes.

Last but not least, I wish to express my heartfelt gratitude to my dear parents, Yasemen and İsmail Çam, and my beloved sister, Bilge Çam, for their unending love and support throughout every stage of my life.

ABSTRACT

CHARACTERISTICS OF BYZANTINE PERIOD BUILDING BRICKS USED IN ST. JEAN BASILICA (AYASULUK HILL) AND ANAIA CHURCH (KADIKALESİ)

Fired bricks, one of the oldest man-made building materials, are historical documents that reflect the production technologies of their periods and the raw material characteristics of the geography they were located. Characterization of bricks is essential for revealing production techniques of their times and contributing to conservation works on monuments built with this material to pass through next generations.

The fired bricks were frequently used as one of the important building materials in Byzantine Architecture. In this study, the fired bricks collected from the different construction periods of St. Jean Basilica, Ayasuluk Hill and Anaia Church, Kadıkalesi, which belong to the Byzantine Period, were investigated to determine material properties, periodical differences, and production technologies. The properties of Byzantine bricks were determined by standard test methods, compression tests, SEM-EDS, XRD, FTIR, and TGA analyses.

According to the results, brick samples taken from both areas were highly porous and low-dense materials. Ca-poor clay source was used in producing St. Jean Basilica bricks, while Anaia Church bricks were produced with Ca-rich clay sources. This situation was decisive in the colour of bricks, and St. Jean Basilica bricks were in reddish colours, while Anaia Church bricks were in brown/beige colours. Also, raw material was extracted from a single source in the production of all St. Jean Basilica bricks, while two different sources were utilized for Anaia Church bricks throughout the three construction periods. Besides, the bricks of both churches were found to be fired at low temperatures (700–900°C) due to the technology of Byzantine kilns. Despite low firing temperatures, the majority of the bricks did not possess pozzolanic properties since they did not contain a sufficient amount of clay minerals. The highest mechanical strength was determined in the bricks with higher firing temperature and bricks with the higher calcium content. The properties of fired bricks were differentiated based on production technologies; contrary, a distinctive difference was not observed depending on their periods.

ÖZET

ST. JEAN BAZİLİKA (AYASULUK TEPESİ) VE ANAİA KİLİSESİ'NDE (KADIKALESİ) KULLANILAN BİZANS DÖNEMİ YAPI TUĞLALARININ ÖZELLİKLERİ

İnsan eliyle üretilmiş en eski yapı malzemelerinden biri olan pişmiş tuğlalar, ait oldukları dönemin üretim teknolojilerini ve bulundukları coğrafyanın hammadde özelliklerini yansıtan tarihi belgelerdir. Pişmiş tuğlaların özelliklerinin belirlenmesi, dönemlerinin üretim tekniklerinin açığa çıkarılmasının yanında bu malzemeyle inşa edilmiş anıtların gelecek nesillere aktarılması için yürütülecek olan koruma çalışmalarına katkı sağlanması açısından önemlidir.

Pişmiş tuğla, Bizans Mimarisinin önemli yapı malzemelerinden biri olarak bu dönem yapılarında sıklıkla kullanılmıştır. Bu çalışmada, Bizans Dönemi'ne ait Ayasuluk Tepesi, St. Jean Bazilikası ve Kadıkalesi, Anaia Kilisesi'nin farklı yapım dönemlerinden alınan pişmiş tuğlalar, malzeme özelliklerinin belirlenmesi, dönemsel farklıların ve üretim teknolojilerinin saptanması amacıyla incelenmiştir. Tuğlaların özellikleri, standart test metotları, basınç testleri, SEM-EDS, XRD, FTIR ve TGA analizleriyle saptanmıştır.

Analiz sonuçlarına göre, iki alandan alınan tuğla örnekler yüksek gözenekli ve düşük yoğunluklu malzemelerdir. St. Jean Bazilikası tuğlalarının kalsiyum oranı düşük kil kaynağı, Anaia Kilisesi tuğlalarının ise kalsiyumca zengin kil kaynağı kullanılarak üretildikleri saptanmıştır. Bu durumun tuğlaların renklerinde belirleyici rol oynadığı ve St. Jean Bazilikası tuğlaları kırmızımsı renkte iken, Anaia Kilisesi tuğlalarının kahverengi/bej tonlarında olduğu belirlenmiştir. St. Jean Bazilikası tuğlalarının tamamının üretiminde hammadde için tek bir kaynak kullanılmış, Anaia Kilisesi tuğlaları için üç dönem boyunca iki farklı kaynaktan yararlanılmıştır. Ayrıca, Bizans Dönemi fırın teknolojisinden dolayı, iki yapının tuğlalarının da düşük sıcaklıklarda pişirildikleri (700–900°C) saptanmıştır. Düşük sıcaklıklarda pişirilmiş olmalarına rağmen tuğlaların büyük çoğunluğunun puzolanik özellik göstermemesi yeterli miktarda kil minerali içermediklerini ortaya koymuştur. En yüksek mekanik dayanıma yüksek sıcaklıklarda pişirilmiş veya kalsiyum oranı en yüksek olan tuğlaların sahip olduğu belirlenmiştir. Tuğlaların özellikleri, üretim yöntemlerine bağlı olarak farklılaşmasına karşın dönemsel olarak belirgin bir fark tespit edilmemiştir.

To my dear family...

TABLE OF CONTENTS

LIST OF FIGURES viii

LIST OF TABLES xi

CHAPTER 1. INTRODUCTION 1
1.1. Problem Definition 2
1.2. Aim and Scope of the Study 3
1.3. Methods of the Study 3

CHAPTER 2. PRODUCTION AND PROPERTIES OF HISTORICAL BRICKS 5
2.1. A Brief History of Brick Material 5
2.2. Production Technologies of Brick Material 8
2.3. Recent Studies on Historical Bricks 11
2.3.1. Basic Physical Properties 12
2.3.2. Mechanical Properties 14
2.3.3. Chemical Compositions and Pozzolanic Properties 18
2.3.4. Mineralogical Compositions 21

CHAPTER 3. HISTORICAL, GEOGRAPHICAL AND ARCHITECTURAL FEATURES OF STUDY AREAS 25
3.1. St. Jean Basilica, Ayasuluk Hill 27
3.2. Anaia Church, Kadıkalesi 33

CHAPTER 4. EXPERIMENTAL STUDIES 40
4.1. Sampling 40
4.2. Experimental Studies 47
4.2.1. Determination of Basic Physical Properties 47
4.2.2. Determination of Mineralogical and Chemical Compositions, Microstructural Properties, Thermogravimetric Analyses 50
4.2.3. Colour Measurements 51
4.2.4. Determination of Pozzolanic Activities 52

4.2.5. Determination of Mechanical Properties 53

CHAPTER 5. RESULTS & DISCUSSION 55
5.1. Basic Physical Properties 55
5.2. Chemical Compositions 61
5.3. Mineralogical Compositions 66
5.4. Thermogravimetric Analyses 81
5.5. Colour Identification 84
5.6. Pozzolanic Activities 88
5.7. Microstructural Properties 89
5.8. Mechanical Properties 93

CHAPTER 6. CONCLUSION 97

REFERENCES 100

LIST OF FIGURES

Figure **Page**

Figure 2.1. a: Hagia Sophia, b: Hagia Irene, c: Kariye Museum, d: Myrelaion Monastery 6

Figure 2.2. Recessed brick technique, a: Northern façade of Anaia Church, b: Detail of squared area shows recessed bricks, c: Elevation sketch of the technique, d: Section sketch of the technique..... 7

Figure 2.3. Examples of cloisonne technique, a: Monasteries of Daphni, Greece, b: A bastion of Kadıkalesi, c: Fortification wall of Ayasuluk Hill..... 8

Figure 2.4. Representative sketches of fired brick production, a: Extraction and preparation of clay, b: Moulding and drying, c: Firing in a kiln 8

Figure 2.5. In-situ bricks from Anaia Church, Kadıkalesi with scratches on the surfaces 9

Figure 2.6. Sketch of a brick kiln..... 10

Figure 3.1. Map of Aegean Region shows locations of study areas (Dashed line area is enlarged on Figure 3.2) 25

Figure 3.2. Locations of study areas with neighbouring provinces..... 26

Figure 3.3. Aerial view of Ayasuluk Hill and St. Jean Basilica with their surrounding 27

Figure 3.4. Locations of the city centres of Ephesus 29

Figure 3.5. Plan of St. Jean Basilica showing the construction phases 30

Figure 3.6. Baptistery pool and wall structures from 1st period 31

Figure 3.7. Photo of southern nave with outer brick wall on the left and stone columns and pillars on the right..... 31

Figure 3.8. Photo of the exterior arched walls of substructure and the atrium built on top of it..... 32

Figure 3.9. Different wall bonding types from the northern transept (Right side of the wall was a part of 1st phase, and the left side was built in later periods)..... 32

Figure 3.10. Anaia Church and other structures placed within Kadıkalesi (Two aerial photos taken in 2018 and 2021 from Kadıkalesi/Anaia Excavation Archive were overlapped to show the Church without top shelter.)..... 33

Figure 3.11. Plan of Anaia Church 36

Figure **Page**

Figure 3.12. Photo of Anaia Church showing the spaces and their construction periods (Colours indicating the periods were expressed in Figure 3.11) 37
Figure 3.13. Substructure from 1st phase with brick vault and arches 37
Figure 3.14. Photo of the wall between naos and inner narthex, buttresses from 2nd phase (blue dashed lines) supports the wall from 1st phase (green dashed lines) 38
Figure 3.15. The wall between naos and southern nave, walls added in 3rd period (purple dashed lines) between piers from 1st period (green dashed lines) ... 38
Figure 3.16. A buttress on the northern façade dated to the 3rd phase 39
Figure 3.17. Photo of the cistern in the west corner of the Church showing the remains of arches and domes 39
Figure 4.1. Sample labelling method 41
Figure 4.2. a: Substructure plan, b: General plan of St. Jean Basilica, Ayasuluk Hill and photos show where samples were taken 42
Figure 4.3. a: Substructure plan, b: General plan of Anaia Church, Kadıkalesi and photos show where samples were taken 44
Figure 4.4. a: Weight measurements, b: Samples in vacuum oven, c: Measurements of Archimedes weight 48
Figure 4.5. Brick samples during drying cycle in room condition for determination of drying rate 49
Figure 4.6. a: Munsell Hue scale, b: Munsell colour system 52
Figure 4.7. a: Mixing $Ca(OH)_2$ and brick powder, b: Measurement of electrical conductivity 53
Figure 4.8. a: Photo of Shimadzu AG-I mechanical test instrument, b: Process of loading force to a brick sample 54
Figure 5.1. Porosity (%) and apparent density (g/cm^3) values of St. Jean Basilica samples from different construction periods 56
Figure 5.2. Porosity (%) and apparent density (g/cm^3) values of Anaia Church samples from different construction periods 57
Figure 5.3. Drying rates of bricks from St. Jean Basilica, Ayasuluk Hill 60
Figure 5.4. Drying rates of bricks from Anaia Church, Kadıkalesi 60
Figure 5.5. Dendrogram of Hierarchical Cluster Analysis 65

Figure **Page**

Figure 5.6. XRD spectra of bricks from 1st phase (AR1, AR2, AG) of St. Jean Basilica 68
Figure 5.7. XRD spectrum of bricks from 2nd phase (AB1, AB2, AT1, AT2) and 3rd phase (AI, AN, AS) of St. Jean Basilica 69
Figure 5.8. XRD spectrum of bricks from 1st phase (KS1, KS2, KS3, KS4, KBa2, KBa3, KBa4) of Anaia Church 70
Figure 5.9. XRD spectrum of bricks from 1st phase (KN3, KN5) and 2nd phase (KN1, KN2, KN6, KI1) of Anaia Church 71
Figure 5.10. XRD spectrum of bricks from 3rd phase (KI2, KN4, KBa1, KP, KO1, KO2, KC1) of Anaia Church 72
Figure 5.11. FTIR spectra of brick samples from 1st (AR1, AR2, AG), 2nd (AB1, AB2, AT1, AT2) and 3rd (AI) periods of St. Jean Basilica 75
Figure 5.12. FTIR spectra of brick samples from 3rd period (AN, AS) of St. Jean Basilica and 1st period (KS1, KS2, KS3, KS4, KBa2) of Anaia Church 76
Figure 5.13. FTIR spectra of brick samples from 1st (KBa3, KBa4, KN3, KN5) and 2nd (KN1, KN2, KN6, KI1) period of Anaia Church 77
Figure 5.14. FTIR spectra of brick samples from 3rd period (KI2, KN4, KBa1, KO1, KO2, KP, KC1) of Anaia Church 78
Figure 5.15. TGA graphs of St. Jean Basilica bricks 83
Figure 5.16. TGA graphs of Anaia Church bricks 84
Figure 5.17. SEM (BSE) images of bricks (x1000), a: KN4 (Cluster 1, 700–800°C), b: AB2 (Cluster 2, 700–800°C), c: KO1 (Cluster 3, 700–800°C) 90
Figure 5.18. SEM (BSE) images of bricks (x1000), a: KS2 (Cluster 1, 850–870°C), b: AT1 (Cluster 2, 850–870°C), c: KBa4 (Cluster 3, 800–850°C) 91
Figure 5.19. SEM (BSE) images of bricks (x1000), a: KS3 (Cluster 1, ~900°C), b: AN (Cluster 2, ~900°C) 92
Figure 5.20. SEM image (150x) and EDX results of grog in the brick matrix (KS2) 93
Figure 5.21. Behaviour of AR2 during the mechanical test 93
Figure 5.22. Behaviour of AN during the mechanical test 94
Figure 5.23. Behaviour of KN5 during the mechanical test 94

LIST OF TABLES

Table **Page**

Table 2.1. Basic physical and mechanical properties of historical bricks determined by previous studies 15

Table 2.2. Chemical compositions and pozzolanic properties of historical bricks determined by previous studies 20

Table 2.3. Mineralogical compositions and estimated firing temperatures of historical bricks determined by previous studies 24

Table 4.1. Brick samples from St. Jean Church, Ayasuluk Hill 43

Table 4.2. Brick samples from Anaia Church, Kadıkalesi 45

Table 5.1. Porosity and apparent density of bricks investigated by recent studies 57

Table 5.2. Porosity (P), apparent density (D), saturation coefficient (S), and pore interconnectivity (Ax) values of St. Jean Basilica and Anaia Church bricks 59

Table 5.3. Chemical compositions (%) of brick samples determined by SEM-EDS 62

Table 5.4. Chemical compositions of bricks investigated by recent studies 63

Table 5.5. Mean, F and P values obtained by ANOVA test (P-value is represented with *** if it was lower than 0.01, ** if it was lower than 0.05, and * if it was lower than 0.1) 65

Table 5.6. Temperature thresholds of mineralogical transformations 67

Table 5.7. Functional groups and their vibrational wavenumbers (cm^{-1}) determined in FTIR spectra of brick samples 74

Table 5.8. Mineralogical compositions and estimated firing temperatures of bricks 80

Table 5.9. Weight losses (%) in particular temperature ranges (°C) 81

Table 5.10. Colour of bricks determined by using Munsell Soil Colour Chart 86

Table 5.11. The colour classification of bricks based on chemical clusters and firing temperatures 87

Table 5.12. Electrical conductivity differences and pozzolanicity classification of bricks 89

Table 5.13. Uniaxial compressive strength and modulus of elasticity values of bricks with porosity percentages 96

CHAPTER 1

INTRODUCTION

The fired brick was one of the oldest building materials that were manufactured deliberately, reflecting the technology of humanity. The fired bricks were found to be produced and used firstly in Mesopotamia around 3500 BC (Bakırer 1981; Wright 2009). Accordingly, the usage of fired bricks passed through the civilizations in Anatolia and Europe. Despite the fact that the fired bricks took part in Greek Architecture, their usage predominantly occurred during the Roman Period and continued in Byzantium. The fired bricks were frequently used in Byzantine architecture for structural and ornamental purposes, especially in Anatolia, Balkans, and Italy (Mango 1985).

The properties of the fired bricks are associated with the properties of natural raw material source and the production technologies, which include shaping and firing processes. Historical bricks were produced within several stages. The determination and extraction of suitable raw material were conducted in the first stage. Accordingly, the raw material was mixed with water and shaped by hands in timber moulds. Then, the bricks were dried under the sun and fired in the kilns (Fernandes, Lourenço, and Castro 2010).

The properties of raw material with its additives, such as sand, straw, reeds, etc., defined the chemical and mineralogical composition of the final product and also caused changes in its physical properties, like colour and pore structure (Davey 1961; Riccardi, Messiga, and Duminuco 1999; Elert et al. 2003; Cardiano et al. 2004). The shaping methods lead to alterations in physical properties; the bricks shaped by traditional methods had more porous structures than those produced by modern shaping methods applied with high pressure. Also, the firing was the process that caused crucial modifications in the mineralogical compositions and physical properties and thus played a decisive role in the properties of bricks. At high firing temperatures (>900°C), new mineralogical phases begin to form; and the durability of bricks increases due to the reduction in total porosity, number of micropores and pore connectivity (Cultrone et al. 2004; Lopez-Arce and Garcia-Guinea 2005; Benavente et al. 2006; Uğurlu Sağın and Böke 2013). However, the temperature distribution could not be achieved homogeneously because of the ancient kiln technology, and most bricks were fired at low temperatures.

Consequently, determining the characteristics of fired bricks provides information about craftsmanship and ancient production technologies. Since the brick materials reflect the knowledge and technologies of their times, they should all be conserved as historical documents. Also, determining the characteristics of historical fired bricks has great importance within the conservation practice to maintain the integrity of the monument with its original materials and also for the selection and production of new materials compatible with historical bricks.

1.1. Problem Definition

The characterization of historical brick materials was investigated in several studies. There is an abundance of studies focused on the bricks from the Roman Period. On the contrary, bricks from Byzantine Period were subjected to limited studies.

Furthermore, the recent research on the characterization of fired bricks from Byzantium were mostly focused on bricks of some monuments from İstanbul, and only a few studied Byzantine bricks from Anatolia. Since only a few studies have been conducted on Byzantine bricks in Western Anatolia, there is a lack of knowledge on this subject.

Also, there is insufficient knowledge about whether there was a variation in the production and properties of fired bricks produced in different centuries during the Byzantine Era in Anatolia.

Within this context, in this thesis, characteristics of building bricks used in two important Byzantine churches in Western Anatolia, St. Jean Basilica and Anaia Church, were studied. On these monuments chosen for study cases, brick properties have not been studied before. It is unknown whether the bricks of the monuments, which were built close to each other, were produced at the same site, with the same raw material, or separately. Also, it has not been determined whether the manufacturing methods of the monuments' bricks were sustained constantly over the centuries or changed with construction periods.

Furthermore, the mechanical properties of bricks were determined in a few studies because it is challenging to get bricks from historical structures in the sizes required for mechanical tests. In this study, the mechanical properties were investigated, unlike most studies. Additionally, different from previous studies, colourimetric properties of brick

samples were examined apart from basic physical properties, and their relations with chemical and mineralogical composition and firing temperatures were evaluated.

1.2. Aim and Scope of the Study

The aim of this study is to determine the characteristics of Byzantine bricks from different construction periods of two archaeological monuments located in Western Anatolia for evaluation of the production technologies of Byzantium and to investigate the periodical differences in terms of raw materials and kiln conditions. The other purpose is to contribute conservation works to be carried out in these monuments regarding the material characteristics.

In the scope of the study, two Byzantine churches, which are St. Jean Basilica in Ayasuluk Hill (Selçuk, İzmir), and Anaia Church in Kadıkalesi (Kuşadası, Aydın), were chosen. Those monuments were selected since they were brick masonries dated to similar periods of Byzantine and were located close to each other. They had similar architectural features, such as material usage, construction technique and spatial organization. Also, they were the structures which were undergone several interventions throughout the Byzantine Period. Accordingly, the churches are important examples as they represent Byzantine brick production and use in different centuries.

Furthermore, Ayasuluk Hill and Anaia city acted as the important religious centers of the region. The fact that churches are located in religious centers is important in terms of both having similar religious status and historical values in the Byzantine Period.

The similarities of St. Jean Basilica and Anaia Church in terms of constructional, periodical and value were effective in the selection of them for the study cases.

1.3. Method and Content of the Study

The study consisted of field survey, literature review, experimental studies, and evaluation of the results. The field survey, which included documentation and sampling, was carried out in July 2020. The locations and construction periods of the brick samples were documented with photographs and sketches. The brick samples were collected from several spaces of the monuments according to their construction periods.

In the experimental studies, the samples were analysed with laboratory investigations between September 2020 and December 2021 to determine the physical and mechanical properties, chemical and mineralogical compositions, pozzolanic activities, and microstructural properties of bricks. The basic physical and pozzolanic properties and mineralogical compositions by FTIR analyses were conducted in the IZTECH Material Conservation Laboratory. SEM-EDS, XRD, TGA, and mechanical analyses were carried out in the IZTECH Center of Materials Research. The results of the analyses were discussed and compared between the buildings and the construction periods within the buildings and evaluated together with other studies on historical building bricks.

The thesis consisted of six chapters. The general information about the history of brick material usage, its ancient production technologies, and the recent studies on historical fired bricks were mentioned in the second chapter. The third chapter included the geographical, historical, and architectural information of case areas. The sampling of the bricks and the methods of experimental studies, which were the determination of basic physical properties, chemical and mineralogical compositions, thermogravimetric analysis, colour identification, pozzolanic, microstructural, and mechanical properties, were explained under chapter four. In the fifth chapter, the results of these experimental studies were given and discussed in correlation with each other. As the final, the results were evaluated and concluded in the sixth chapter.

CHAPTER 2

PRODUCTION AND PROPERTIES OF HISTORICAL BRICKS

2.1. A Brief History of Brick Material

Brick has been one of the initial building materials used since ancient civilizations. It is known that the first bricks were produced by shaping a mixture of mud and straw into ovals and used in Mesopotamia around the 8th millennium BC (Bakırer 1981; Wright 2005, 2009). The oval-shaped mud bricks evolved into a rectangular shape with the introduction of moulds (Davey 1961; Bakırer 1981). During that period, buildings generally consisted of small-scale structures, like houses, and the owners of the buildings manufactured the mudbricks for their needs. However, with urban development, more durable building materials than mud bricks were required since the durability, and mechanical properties of mud bricks were not capable enough for construction works, especially for larger-scale public buildings (Bakırer 1981; Wright 2005). In order to overcome these disadvantages of mud bricks, bricks were started to be fired in kilns with the experience of ceramic production (Bakırer 1981; Adam 2005).

Fired bricks were first manufactured and used in Mesopotamia in the 4th millennium BC (Bakırer 1981; Wright 2009). Since the cost and time required to manufacture fired bricks were significantly higher than those of mud bricks, mud and fired bricks were frequently used together in constructions (Davey 1961; Bakırer 1981; Wright 2005). The Mesopotamian civilizations, like the Sumerians, Babylonians, Assyrians and Akkadians, used fired bricks, especially in parts of the buildings directly exposed to moisture like foundations and lower parts of the walls (Davey 1961; Moorey 1999). Thousands of years after Mesopotamian civilizations, fired clay products like terra-cotta pipes, roof tiles, etc., occurred from the 7th century BC; and fired bricks began to be used after the 4th century BC in Greek architecture. Nevertheless, brick was not widely used in Greek architecture, and its rise to prominence as a primary building material occurred during the Roman period (Davey 1961; Malacrino 2010; Tucci 2015).

In Roman times, construction techniques were transformed by the invention of Roman concrete, and fired bricks started to be also used as a rendering material. Roman concrete facing with fired bricks, namely *opus testaceum*, became a common technique in the 1st century AD (Davey 1961; Bakırer 1981; Wright 2005; Tucci 2015). Therefore, brick production increased and became an important industry in the Roman Empire (Helen 1975; Scalenghe et al. 2015; Tucci 2015). The brick sizes and shapes were standardised in this period (Davey 1961; MacDonald 1982). The bricks were generally manufactured in square shapes with the sizes of 19.7 cm (two-thirds of a foot), 29.6 cm (one foot), 44.4 cm (one and a half feet), and 59.2 cm (two feet) (Malacrino 2010). There were also bricks in rectangular, triangular, and circular forms (Davey 1961).

Afterwards, brick material continued to be widely used in the Byzantine Period. However, the use of bricks as facing materials disappeared, and they became the main materials of masonries. Brick masonry buildings were defined as "*the central tradition of Byzantine Architecture*" since brick masonries were constructed especially in Constantinople, the capital of the Empire (Mango 1985). Hagia Sophia, Hagia Irene, Kariye Museum, and Myrelaion Monastery are some of the significant examples of Byzantine brick architecture in Constantinople (Krautheimer 1986) (Figure 2.1).



Figure 2.1. a: Hagia Sophia, b: Hagia Irene, c: Kariye Museum, d: Myrelaion Monastery (Source: "Türkiye Kültür Portalı" n.d.)

In Byzantine architecture, the walls were constructed with solid bricks or alternating bonds of bricks and stones (Eyice 1963; Mango 1985; Ousterhout 1999; Jeffreys, Haldon, and Cormack 2008), whereas the construction of domes, arches and vaults were solid brick works (Mango 1985). In the walls constructed with alternating bonds, brick courses were laid on the stone rows that were faced by rough-cut stone and filled with mortared rubble stone. Thus, bricks acted as the determinants of wall thicknesses (Mango 1985; Ousterhout 1999). The Byzantine construction systems were sustained without any distinction of periods; only around the 11th century, the recessed brick technique and cloisonne technique were used on façades of buildings (Eyice 1963; Ousterhout 1999). The recessed brick technique, used for either structural or ornamental purposes, was formed by leaving one of two successive rows of bricks behind surface and filling the space with mortar (Mango 1985; Ousterhout 1999) (Figure 2.2). The cloisonne technique was an organisation of bricks vertically and horizontally around stones on the wall façade (Ousterhout 1999; Jeffreys, Haldon, and Cormack 2008) (Figure 2.3).



Figure 2.2. Recessed brick technique, a: Northern façade of Anaia Church (Photo: E. Çam, 2020), b: Detail of squared area shows recessed bricks (Source: Kanmaz 2015), c: Elevation sketch of the technique (Source: Ousterhout 1999, 174), d: Section sketch of the technique (Source: Ousterhout 1999, 174)



Figure 2.3. Examples of cloisonne technique, a: Monasteries of Daphni, Greece (Source: "Monasteries of Daphni, Hosios Loukas and Nea Moni of Chios - Gallery - UNESCO World Heritage Centre" n.d.) b: A bastion of Kadıkalesi (Photo: E. Çam, 2021), c: Fortification wall of Ayasuluk Hill (Photo: E. Çam, 2020)

After Byzantium, bricks continued to be used during the Seljuk and Ottoman periods. For centuries, the availability of clay material, convenience of its usage, and development of durability through firing led to the continuity of bricks. Eventually, fired bricks still have an important place in today's architecture.

2.2. Production Technologies of Brick Material

Antique production techniques of fired brick materials were basically comprised of four main stages, which were the preparation of raw materials, shaping, drying, and firing (MacDonald 1982; Fernandes, Lourenço, and Castro 2010) (Figure 2.4).

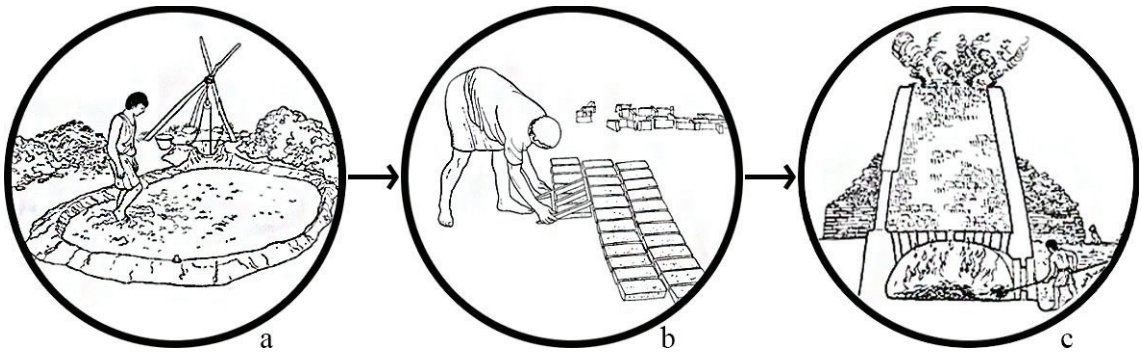


Figure 2.4. Representative sketches of fired brick production, a: Extraction and preparation of clay, b: Moulding and drying, c: Firing in a kiln (Source of sketches: Adam 2005, 107, 109, 110)

In the first stage, clay was extracted from the source and accumulated in the working area. The source was preferred to be as close as possible to the working area due to the difficulties of transporting raw material in ancient times (Kahya 1992; Fernandes, Lourenço, and Castro 2010; Scalenghe et al. 2015). This situation may have brought along the necessity and risk of using clays with unideal properties for brick production in some areas. Vitruvius stated that the clay which was going to be used to make bricks should not be sandy or pebbly clay or fine gravel. White and chalky or red clays were recommended by him as they were smooth, light, and durable (Vitruvius 1914). In cases where this type of clay was not available, early producers were making some additions to improve the quality. For instance, adding water provided plasticity to clay and facilitated working with it (Davey 1961; Adam 2005; Wright 2005; Fernandes, Lourenço, and Castro 2010). If water was used excessively, the clays liquefied, so sand was added to keep the consistency. Also, sand reduced shrinkage and avoided cracking and disintegration. (Kahya 1992; Adam 2005; Wright 2005; Fernandes, Lourenço, and Castro 2010). Following these additions, the clay was kneaded to homogenise, mostly by hand, and became ready for shaping (Davey 1961) (Figure 2.4).

The shaping was achieved by the four-sided wooden or metal moulds (Ousterhout 1999). Clay mixture was placed into moulds, and trimmed to remove the excess material (Davey 1961; Adam 2005; Wright 2005; Fernandes, Lourenço, and Castro 2010; Malacrino 2010) (Figure 2.4). Producers sometimes made scratches on the surfaces of fresh bricks by hand to increase the surface area and thus to provide a better bond between brick and mortar (Figure 2.5).



Figure 2.5. In-situ bricks from Anaia Church, Kadıkalesi with scratches on the surfaces

Following the shaping process, the bricks were left to dry for several days in a sheltered place in order to keep them away from external factors (Davey 1961; Ousterhout 1999; Fernandes, Lourenço, and Castro 2010). It was noticed that bricks should not be exposed to direct sunlight since drying occurs faster in warm climates, causing cracks in the bricks, and also that they should not be exposed to rain because the drying rate slows down in humid climates (Adam 2005; Wright 2005; Fernandes, Lourenço, and Castro 2010). In this regard, the production of bricks was recommended to be carried out in Spring or Autumn by Vitruvius (1914).

Thereafter, the firing process took place in order to provide durability and strength to the dried bricks (Figure 2.4). There were two options for firing: using brick kilns or firing without kilns, known as open-hearth firing (Ousterhout 1999; Malacrino 2010). Brick kilns consisted of two parts, basically. The lower part was the combustion chamber, which involved an opening for fuelling the fire during the process. The other part placed on the combustion chamber was the charging chamber in which bricks were loaded. These two chambers were separated from each other by a plate with several holes that allowed the heat to pass through (Davey 1961; Adam 2005; Wright 2005) (Figure 2.6). The temperature in the kilns was decreasing with the distance from the fire, resulting in the uneven firing of bricks. In the kilns, the temperature could reach 1000°C at the bottom parts close to the fire; but the temperature could decrease even to 550-600°C at the upper parts (Davey 1961; Scalenghe et al. 2015).

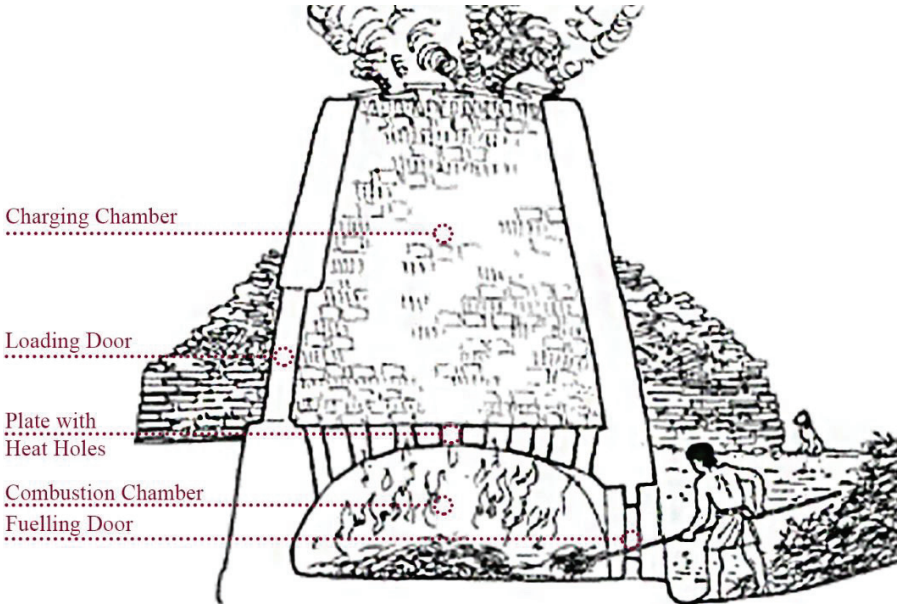


Figure 2.6. Sketch of a brick kiln

(Source of sketch: Adam 2005, 110)

In the open-hearth firing, bricks were stacked in a pit, and the fire was set directly in the middle. At the end of the process, no evidence was left from the firing yard since bricks were taken away (Ousterhout 1999; Wright 2005). Although the second type ensured the firing of large quantities at once, the firing happened at low temperatures, and the quality of bricks was reduced proportionally (Ousterhout 1999; Wright 2005; Malacrino 2010).

Brick production became a common practice in Byzantium (Eyice 1963). The bricks were manufactured on the construction sites locally due to expenses of transportation (Ousterhout 1999; Eroğlu and Akyol 2017). The construction of a building required thousands of bricks, so several kilns had to be worked simultaneously. The location of kilns was regulated by Exabiblos, a law text written in 14th-century Byzantium (Ousterhout 1999). It was stated that kilns must be constructed outside the cities because of the large space necessity and the air pollution caused by the kilns. They must be away from the houses by forty steps in the north and west directions, and twenty-five steps in the south and east directions, and the kilns should not be close to each other (Ousterhout 1999). Furthermore, the workers in brick production were named by their jobs in Exabiblos; clay workers as *ostrakarioi* and brick-makers as *keramopoioi* (Ousterhout 1999). They were seasonal workers and were changing their locations where they were needed for construction (Kahya 1992; Ousterhout 1999).

The brick production techniques proceeded without any significant change until industrialization started within the 19th century (Papayianni and Stefanidou 2000). With the mechanization, shaping and firing methods were developed. Bricks started to be shaped by vacuum and fired at high temperatures exceeding 1100 °C in homogenous kiln conditions. Accordingly, modern bricks are less porous materials with superior mechanical properties compared to historical bricks.

2.3. Recent Studies on Historical Bricks

Studies on historical bricks mostly focus on the characterization of bricks used in several structures by ancient civilizations, the manufacturing process and its effects on the material, and the deterioration mechanisms of bricks. Under this heading, recent studies about the characterization of historical building bricks were investigated in terms

of their basic physical and mechanical properties, chemical compositions and pozzolanic properties, and mineralogical compositions.

There is a limited number of studies on the properties of Byzantine bricks. In addition, most of them focused on the bricks from monuments in İstanbul (Kahya 1992; Moropoulou, Çakmak, and Polikreti 2002; Ballato et al. 2005; Kurugöl and Tekin 2010; Ulukaya et al. 2017; Taranto et al. 2019), and only a few investigated bricks from Anatolia (Kurugöl and Tekin 2010; Özyıldırım and Akyol 2016; Eroğlu and Akyol 2017).

Thus, studies on historical bricks from the Roman (Calliari et al. 2001; Lopez-Arce and Garcia-Guinea 2005; Aslan Özkaya and Böke 2009; Oguz, Turker, and Kockal 2014; Stefanidou, Papayianni, and Pachta 2015; Scalenghe et al. 2015; Uğurlu Sağın 2017; Scatigno et al. 2018) and Ottoman Periods (Kahya 1992; Çizer 2004; Ballato et al. 2005; Kurugöl 2009; Uğurlu Sağın and Böke 2013; Gürhan, Uğurlu Sağın, and Böke 2017) were also examined, apart from the studies on Byzantine Period (Kahya 1992; Papayianni and Stefanidou 2000; Cardiano et al. 2004; Ballato et al. 2005; Tekin and Kurugöl 2011; Stefanidou, Papayianni, and Pachta 2015; Özyıldırım and Akyol 2016; Eroğlu and Akyol 2017; Ulukaya et al. 2017; Taranto et al. 2019).

The general aims of these studies were to determine the characteristics of historical bricks and ancient production technologies and to contribute to the conservation and restoration process of historic buildings. The results of the recent studies were given below (Table 2.1, Table 2.2, Table 2.3)

2.3.1. Basic Physical Properties

Basic physical properties of historical bricks were identified mainly according to their density and porosity values. Besides, other parameters associated with porosity and moisture content of bricks, such as pore size distribution and water absorption, were investigated to determine brick structure in some cases (Table 2.1). Those values were calculated by using standard test methods.

Density and porosity values of Roman bricks used in Serapis Temple were found 1.65 g/cm^3 and 35.0 % by Aslan Özkaya and Böke (2009), and between 1.63–1.73 g/cm^3 and 28.90–32.65 % by Uğurlu Sağın (2017). Further, Uğurlu Sağın (2017) determined density values 1.71 g/cm^3 in bricks from Aigai and between 1.32–1.63 g/cm^3 in bricks from Nysa, and porosity 29.58 % in bricks from Aigai and between 44.53–47.69 % in

bricks from Nysa. In other studies, the density and porosity of Roman bricks were determined between 1.9–2.0 g/cm^3 and 22.2–25.1 % for Toledo city (Lopez-Arce and Garcia-Guinea 2005), 1.80–1.86 g/cm^3 and 26.0–34.0 % for Era Bath (Oguz, Turker, and Kockal 2014), and 1.63–1.84 g/cm^3 for monuments from Greece (Stefanidou, Papayianni, and Pachta 2015).

For the Byzantine bricks, density values were found in the range of 1.46–1.84 g/cm^3 by Stefanidou, Papayianni and Pachta (2015), 1.38–1.88 g/cm^3 by Papayianni and Stefanidou (2000), 1.55–1.81 g/cm^3 by Eroğlu and Akyol (2017), 1.73 g/cm^3 by Özyıldırım and Akyol (2016), 1.70 g/cm^3 by Ulukaya et al. (2017) and 1.52–1.72 g/cm^3 by Cardiano et al. (2004), whereas porosity percentages were obtained between 14.96–34.87 by Papayianni and Stefanidou (2000), 26.80–35.77 by Eroğlu and Akyol (2017), 31.67 by Özyıldırım and Akyol (2016), 31.4–35.3 by Ulukaya et al. (2017), and 31.4–42.6 by Cardiano et al. (2004). In the studies of Kurugöl and Tekin (2010) and Kahya (1992), different structures and different centuries of the Byzantine Period were investigated. Density and porosity values were obtained between 1.33–2.05 g/cm^3 and 20.1–47.4% by Kurugöl and Tekin (2010) and 1.55–1.89 g/cm^3 and 20.3–39.0% by Kahya (1992). The study of Kahya (1992) revealed that Byzantine bricks differentiated according to periods, and an improvement was observed in the properties of bricks from the 8th century. This improvement was stopped, and decline was observed in the properties of bricks from 11th and 12th centuries (Kahya 1992).

Furthermore, densities of bricks from the Ottoman Period were found between 1.73–1.89 g/cm^3 by Kahya (1992), 1.67–1.80 g/cm^3 by Çizer (2004), 1.7–1.8 g/cm^3 by Uğurlu Sağın and Böke (2013), and between 1.53–1.64 g/cm^3 by Kurugöl (2009). Porosity values were determined between 20.3–30.1% in the study of Kahya (1992), 29.4–36.0% by Çizer (2004), 33.0–37.0% by Uğurlu Sağın and Böke (2013), and between 32.6–37.5% by Kurugöl (2009) (Table 2.1).

Water absorption percentage is another parameter determined for the evaluation of basic physical properties of brick materials in most of the studies (Kahya 1992; Lopez-Arce and Garcia-Guinea 2005; Kurugöl 2009; Tekin and Kurugöl 2011; Oguz, Turker, and Kockal 2014; Stefanidou, Papayianni, and Pachta 2015; Özyıldırım and Akyol 2016; Eroğlu and Akyol 2017). In the studies, water absorption of Roman bricks was observed in the range of 6.7–12.6 % by Lopez-Arce and Garcia-Guinea (2005), 13.3–16.7 % by Oguz, Turker and Kockal (2014), and 14.3–22.4% by Stefanidou, Papayianni and Pachta (2015). For Byzantine bricks, the value was found between 16.0–29.8 % by Stefanidou,

Papayianni and Pachta (2015), between 14.8–23.1 % by Eroğlu and Akyol (2017), ranging between 10.5–34.8 % by Kurugöl and Tekin (2010), as 18.3 % by Özyıldırım and Akyol (2016), and ranging between 13.1–25.2 % by Kahya (1992). Besides for Ottoman bricks, Kahya (1992) determined water absorption between 11.2–17.4 %, and Kurugöl (2009) found it between 19.9–24.5 % (Table 2.1).

Pore size distribution was determined in some of the studies (Papayianni and Stefanidou 2000; Cardiano et al. 2004; Lopez-Arce and Garcia-Guinea 2005; Uğurlu Sağın and Böke 2013). The pore size distribution of Roman bricks was found in the range of 0.07–0.33 μm in the study of Lopez-Arce and Garcia-Guinea (2005). In the case of Byzantine bricks, Papayianni and Stefanidou (2000) determined the main pore volume between 70–250 μm, and Cardiano, et al. (2004) indicated the pore size distribution of bricks between 0.20–0.83 μm. Besides, the radius of pores present in Ottoman bricks was mostly under 5 μm, according to the study of Uğurlu Sağın and Böke (2013) (Table 2.1).

2.3.2. Mechanical Properties

The mechanical properties of historical bricks were investigated in a limited number of studies (Kahya 1992; Papayianni and Stefanidou 2000; Lopez-Arce and Garcia-Guinea 2005; Aslan Özkaya and Böke 2009; Kurugöl 2009; Kurugöl and Tekin 2010; Oguz, Turker, and Kockal 2014; Stefanidou, Papayianni, and Pachta 2015; Ulukaya et al. 2017), probably since it is hard to take brick samples from monuments as much as required sizes determined by the standards for mechanical tests. Compressive strength and modulus of elasticity were used to define mechanical properties in most of the studies. Aslan Özkaya and Böke (2009) found the compressive strength of Roman brick as 6.0 MPa, while in the other studies, compressive strengths were found between 21.2–44.0 MPa (Lopez-Arce and Garcia-Guinea 2005) and 20.0–47.8 MPa (Oguz, Turker, and Kockal 2014). In the study of Stefanidou Papayianni and Pachta (2015), Roman bricks were observed to have compressive strength between 4.6–20.7 MPa and modulus of elasticity between 2.78–5.20 GPa, whereas Byzantine bricks were observed to have compressive strength between 4.5–16.1 MPa and modulus of elasticity between 2.86–9.20 GPa. Another study by Papayianni and Stefanidou (2000) obtained compressive strength and modulus of elasticity of Byzantine bricks from Greece between 9.8–17.6 MPa and between 2.59–10.83 GPa, respectively. In the other studies, the compressive

strength of Byzantine bricks was found between 7.9–33.0 MPa for castles in Turkey by Kurugöl and Tekin (2010), between 9.2–11.0 MPa by Ulukaya et al. (2017), and between 16.9–34.7 MPa for monuments in Istanbul by Kahya (1992). In the case of Ottoman bricks, compressive strength was found ranging between 8.7–14.0 MPa by Kahya (1992). Also, Kurugöl (2009) determined compressive strength between 4.1–5.2 MPa and modulus of elasticity between 3.6–7.0 GPa, respectively.

Table 2.1. Basic physical and mechanical properties of historical bricks determined by previous studies

Location-Reference		Period of Bricks Samples	Basic Physical Properties				Mechanical Properties	
			Appearent Density (g/cm^3)	Porosity (%)	Pore size distribution (µm)	Water absorption (%)	Compressive Strength (MPa)	Modulus of Elasticity (GPa)
Serapis Temple, Bergama/Turkey (Aslan Özkaya and Böke 2009)		Helenistic and Roman Periods	1.65	35.00	-	-	6.00	-
Some archaeological sites of Turkey (Uğurlu Sağın 2017)	Bergama	Roman	1.63-1.73	28.90-32.65	-	-	-	-
	Aigai	Roman	1.71	29.58				
	Nysa	Roman	1.32-1.63	44.53-47.69				
Toledo/Spain (Lopez-Arce and Garcia-Guinea 2005)		Roman (1st-4th c.)	2.0-1.9	22.2-25.1	0.07-0.33	6.7-12.6	21.18-44.01	
Era Bath, Myra/Turkey (Oguz, Turker and Kockal 2014)		Roman (3rd c.)	1.80-1.86	26-34	-	13.26-16.68	20.0-47.8	-
Greece (Stefanidou, Papayianni and Pachta 2015)		Roman (2nd-4th)	1.63-1.84	-	-	14.28-22.38	4.62-20.72	2.78-5.20
		Byzantine (7th-14th)	1.46-1.84			16.02-29.8	4.50-16.08	2.86-9.20
Greece (Papayianni and Stefanidou 2000)		Byzantine periods	1.38-1.88	14.96-34.87	70-250 µm (main pore volume)	-	9.80-17.65	2.59-10.83
Boğsak Island, Mersin/Turkey (Eroğlu and Akyol 2017)		Early Byzantine Period (3rd-7th c.)	1.55-1.81	26.80-35.77	-	14.85-23.10	-	-
Castles in Different Cities of Turkey (Kurugöl and Tekin 2010)	Kütahya	Byzantine (8th-14th)	1.33-1.60	32.0-47.4	-	20.0-34.8	7.9-17.4	-
	Amasra	Byzantine (9th-11th)	1.76-1.81	29.8-33.5		16.6-19.6	15.1-18.0	
	Trabzon	Byzantine(10th-12th)	1.67-2.05	20.1-34.3		10.5-20.5	10.6-33.0	
	İstanbul	Byzantine(13th-14th)	1.61-1.83	28.9-36.1		15.7-22.5	9.4-20.6	
Olba Monastery, Mersin/Turkey (Özyıldırım and Akyol 2016)		Byzantine	1.73	31.67	-	18.34	-	-
İstanbul/Turkey (Ulukaya, et al. 2017)		Late Byzantine Period	1.70	31.4-35.3	-	-	9.2-11.0	-

(cont. on next page)

Table 2.1. (cont.)

Location-Reference	Period of Bricks Samples	Basic Physical Properties				Mechanical Properties	
		Appearent Density (g/cm^3)	Porosity (%)	Pore size distribution (µm)	Water absorption (%)	Compressive Strength (MPa)	Modulus of Elasticity (GPa)
Monastery of San Filippo di Fragala, Sicily/Italy (Cardiano, et al. 2004)	Byzantine Period	1.52-1.72	31.4-42.6	0.20-0.83	-	-	-
İstanbul/Turkey (Kahya 1992)	Byzantine (4th-6th)	1.55-1.79	25.1-39.0	-	14.7-25.2	16.88-32.26	-
	Byzantine (8th-10th)	1.72-1.81	23.7-31.1		13.1-17.8	18.66-34.75	
	Byzantine (11th-12th)	1.63-1.64	30.9-33.0		19.0-20.1	24.82-27.13	
	Byzantine (14th)	1.86	28.4		15.4	26.29	
	Ottoman (15th c.)	1.73-1.89	20.3-30.1		11.2-17.4	8.72-13.99	
Bath buildings in İzmir/Turkey (Çizer 2004)	Ottoman (15th-16th)	1.67-1.80	29.45-35.96				
Bath buildings in İzmir/Turkey (Uğurlu Sağın and Böke 2013)	Ottoman Period	1.7-1.8	33-37	mostly r<5µm (SEM)	-	-	-
İstanbul/Turkey (Kurugöl 2009)	Ottoman (18th-19th)	1.53-1.64	32.6-37.5	-	19.9-24.5	4.1-5.2	3.6-7.0

2.3.3. Chemical Compositions and Pozzolanic Properties

Chemical composition is one of the essential features in the characterization of historical bricks since they provide information about the properties of raw materials and the provenance of clays. Major oxides and trace element compositions can be used to define chemical compositions. The clay types are generally defined as Ca-rich and Ca-poor clays based on their CaO percentage to be more or less than 6%, respectively (Riccardi, Messiga, and Duminuco 1999; Elert et al. 2003; Bartz and Chorowska 2016; Taranto et al. 2019).

The chemical compositions of Roman bricks were determined with Scanning Electron Microscope coupled with energy dispersive spectroscopy (SEM-EDS) by Aslan Özkaya and Böke (2009), and Oguz, Turker and Kockal (2014), and with X-ray Fluorescence (XRF) by Uğurlu Sağın (2017). The bricks of Serapis Temple (Aslan Özkaya and Böke 2009), Pergamon and Aigai (Uğurlu Sağın 2017) were found to be produced with Ca-poor clays. Furthermore, Ca-rich clay was used in the production of Nysa (Uğurlu Sağın 2017) and Era Bath bricks (Oguz, Turker, and Kockal 2014). Overall, Roman bricks contained high amounts of SiO_2 and Al_2O_3 and low amounts of MgO, Na_2O, K_2O and TiO_2. Besides, Fe_2O_3 was found in high percentages in Serapis Temple and Nysa bricks and in low percentages in Pergamon, Aigai and Era Bath bricks (Table 2.2).

The chemical compositions of Byzantine bricks were investigated in the studies by using XRF (Ballato et al. 2005; Ulukaya et al. 2017; Taranto et al. 2019), Inductively Coupled Plasma Atomic Emission Spectroscopy (ICP) (Cardiano et al. 2004; Tekin and Kurugöl 2011), and Instrumental Neutron Activation Analysis (INAA) (Cardiano et al. 2004) (Table 2.2). The chemical composition of Hagia Sophia bricks was determined to change according to the construction periods (Taranto et al. 2019). The Ca-rich clay source was used for manufacturing the bricks of Hagia Sophia, except for the 5^{th} century bricks. The Hagia Sophia bricks were composed of primarily SiO_2, Al_2O_3, and Fe_2O_3, with minor amounts of Na_2O, K_2O, TiO_2, MnO, and P_2O_5. Nevertheless, MgO content was observed in high percentages in the 6^{th} and 14^{th} century bricks and low percentages in those from the 4^{th} and 5^{th} centuries. Furthermore, Ca-rich clays were determined in Byzantine bricks from castles in Kütahya, Trabzon and İstanbul (Kurugöl and Tekin 2010), monuments in İstanbul (Ballato et al. 2005; Ulukaya et al. 2017) and Sicily

(Cardiano et al. 2004). Bricks were determined to have high amounts of SiO_2, Al_2O_3, and Fe_2O_3, and low amounts of MgO, Na_2O, K_2O, and TiO_2. On the other hand, Ca-poor bricks from Amasra castle were found to compose of high amounts of SiO_2 and Al_2O_3 and low amounts of Fe_2O_3, MgO, Na_2O, K_2O, TiO_2, MnO, P_2O_5, and Cr_2O_3 (Kurugöl and Tekin 2010).

The studies on Ottoman bricks determined the chemical compositions by using XRF (Ballato et al. 2005; Uğurlu Sağın and Böke 2013), SEM-EDS (Gürhan, Uğurlu Sağın, and Böke 2017), and ICP (Kurugöl 2009) (Table 2.2). It was indicated that Ottoman bricks were produced by using Ca-poor clays. The chemical compositions of Ottoman bricks from bath buildings in İzmir (Uğurlu Sağın and Böke 2013), Great Palace of Constantinople (Ballato et al. 2005) and from İstanbul (Kurugöl 2009) were in a similar range; they contained high amounts of SiO_2 and Al_2O_3, moderate amounts of Fe_2O_3, and low amounts of MgO, Na_2O, K_2O, TiO_2. The bricks from the Eski Bath in Aydın contained high amounts of SiO_2, Al_2O_3, and Fe_2O_3, moderate amounts of CaO, and low amounts of MgO, Na_2O, K_2O, and TiO_2 (Gürhan, Uğurlu Sağın, and Böke 2017) (Table 2.2).

Pozzolanic activities of building bricks were determined in the studies by different methods, such as measurement of electrical conductivity differences (Aslan Özkaya and Böke 2009; Uğurlu Sağın and Böke 2013; Oguz, Turker, and Kockal 2014; Gürhan, Uğurlu Sağın, and Böke 2017; Uğurlu Sağın 2017), compressive strength of mortars produced by the powder of studied bricks (TS 25) (Kurugöl 2009; Kurugöl and Tekin 2010), and Frattini test (Ulukaya et al. 2017). Roman bricks from Serapis Temple (Aslan Özkaya and Böke 2009), Pergamon, Aigai, Nysa (Uğurlu Sağın 2017), Era Bath (Oguz, Turker, and Kockal 2014), and Ottoman bricks from the bath buildings in İzmir (Uğurlu Sağın and Böke 2013) and Aydın (Gürhan, Uğurlu Sağın, and Böke 2017) were found non-pozzolanic according to the electrical conductivity measurement method (Luxan, Madruga, and Saavedra 1989) (Table 2.2). The Byzantine bricks from the castles in Turkey (Kurugöl and Tekin 2010) and from İstanbul (Ulukaya et al. 2017) showed pozzolanic activity (Table 2.2).

Table 2.2. Chemical compositions and pozzolanic properties of historical bricks determined by previous studies

Location-Reference		Period of Bricks Samples	Chemical Composition (%)									Pozzolanic activities
			Method	SiO_2	Al_2O_3	CaO	Fe_2O_3	MgO	Na_2O	K_2O	TiO_2	Other	
Serapis Temple, Bergama/Turkey (Aslan Özkaya and Böke 2009)		Helenistic and Roman Periods	SEM-EDS	56.0-58.1	17.0-17.8	3.8-4.4	9.7-11.4	3.1-4.0	2.4-3.4	3.3-4.6	-	-	non-pozzolanic
Some archaeological sites of Turkey (Uğurlu Sağın 2017)	Bergama	Roman	XRF	53.5-58.8	16.7-17.4	4.8-6.4	4.9-5.4	2.8-2.9	1.1-1.6	2.6-3.1	0.7-0.8	-	0.02-0.91 mS/cm non-pozzolanic
	Aigai	Roman		60.1	18.8	4.8	5.8	2	1.1	3.1	1.1	-	
	Nysa	Roman		48.0-50.3	18.4-22.5	4.5-10.4	6.2-8.3	3.2-5.1	0.5-0.8	2.9-3.9	0.9-1.0	-	
Era Bath, Myra/Turkey (Oguz, Turker and Kockal 2014)		Roman (3^{rd} c.)	SEM-EDS	45.5	16	22.8	6.9	4.3	1.8	2.4	-	-	0.09-0.41 mS/cm non-pozzolanic
Hagia Sophia, İstanbul/Turkey (Taranto, et al. 2019)		Byzantine (4^{th} c.)	XRF	48.7-55.4	15.5-20.0	4.8-8.1	7.5-9.6	3.0-5.5	0.8-1.2	2.3-3.3	0.9-1.0	0.2-2.9	-
		Byzantine (5^{th} c.)		51.7-62.0	15.4-19.4	1.5-5.4	7.1-10.0	3.1-6.4	0.8-1.8	1.9-2.5	1.0-1.1	0.2-0.3	
		Byzantine (6^{th} c.)		39.0-54.2	11.7-17.1	9.8-19.0	8.4-12.6	3.7-8.8	1.1-1.7	1.1-2.5	0.7-0.9	0.2-0.3	
		Byzantine (14^{th} c.)		49.6-57.7	12.5-16.2	8.2-12.5	8.0-9.5	5.7-8.6	1.1-1.4	1.3-2.1	0.8-0.9	0.2	
Castles in Different Cities of Turkey (Kurugöl and Tekin 2010)	Kütahya	Byzantine (8^{th}-14^{th})	ICP	49.1-50.4	15.3-19.3	7.8-9.7	5.3-6.4	4.1-5.6	0.6-0.8	3.2-3.6	0.7-0.8	0.2-0.3	pozzolanic
	Amasra	Byzantine (9^{th}-11^{th})		62.4	15.2	3.8	5.6	1.2	2.0	3.6	0.8	0.2	
	Trabzon	Byzantine(10^{th}-12^{th})		56.7-60.2	13.1-13.3	7.0-9.1	6.5-8.0	2.4-3.3	0.8-1.3	1.2-1.3	0.9-1.0	0.5-0.6	
	İstanbul	Byzantine(13^{th}-14^{th})		53.4	12.5	8.5	6.7	4.6	1.1	2.2	0.7	0.4	
İstanbul/Turkey (Ulukaya,et al. 2017)		Late Byzantine	XRF	48.4	14	23.1	7.7	2.4	1.1	2	-	-	pozzolanic
Monastery of San Filippo di Fragala, Sicily/Italy (Cardiano, et al. 2004)		Byzantine Period	ICP & INAA	50-60	15-19	1-12	5-8	1-2	~1	3-4	<1	-	-
Great Palace of Constantinople, İstanbul/Turkey (Ballato, et al. 2005)		Byzantine Period	XRF	52.8-60.9	15.3-16.3	5.5-13.8	6.1-9.1	2.9-7.3	1.2-2.4	2.0-3.1	0.8-0.9	0.1-0.2	-
		Ottoman Period		66.6-67.5	15.2-17.2	0.5-2.6	6.9-7.6	2.2-2.5	2.2-2.3	1.9-2.1	1.0-1.1	0.1	
Bath buildings in İzmir/Turkey (Uğurlu Sağın and Böke 2013)		Ottoman Period	XRF	59.8-69.0	15.1-18.8	0.5-3.0	6.2-6.9	1.6-2.5	0.3-0.4	1.9-3.0	0.6-0.8	0.04-0.1	0.2-0.7 mS/cm non-pozzolanic
Eski Bath, Aydın/Turkey (Gürhan, Uğurlu Sağın and Böke 2017)		Ottoman (16^{th}-17^{th})	SEM-EDS	49.2-51.1	24.4-21.8	5.4-7.2	9.8-10.8	4.5-4.7	1.1-1.2	4.0-4.1	1.0-1.8	-	0.72-0.86 mS/cm non-pozzolanic
İstanbul/Turkey (Kurugöl 2009)		Ottoman (18^{th}-19^{th})	ICP	67.65	14.2	3.42	6.08	1.77	2.39	1.97	0.88	0.29	pozzolanic

2.3.4. Mineralogical Compositions

Mineralogical compositions of bricks were used for their characterization and also for the estimation of firing temperatures. The most preferred method used in the studies was X-ray diffractometer (XRD) (Cardiano et al. 2004; Ballato et al. 2005; Lopez-Arce and Garcia-Guinea 2005; Aslan Özkaya and Böke 2009; Kurugöl 2009; Tekin and Kurugöl 2011; Uğurlu Sağın and Böke 2013; Oguz, Turker, and Kockal 2014; Stefanidou, Papayianni, and Pachta 2015; Gürhan, Uğurlu Sağın, and Böke 2017; Uğurlu Sağın 2017; Ulukaya et al. 2017; Taranto et al. 2019). In addition, optical microscopy (OM) (Özyıldırım and Akyol 2016; Eroğlu and Akyol 2017) and Fourier transformed infrared spectroscopy (FTIR) (Uğurlu Sağın 2017) were also used in the studies. The results were depicted in Table 2.3.

Aslan Özkaya and Böke (2009) specified that the Roman bricks of Serapis Temple contained quartz, albite, hematite, potassium feldspar and muscovite. Accordingly, the bricks were estimated to be fired at nearly 850˚C. The Roman bricks from Pergamon, Aigai and Nysa were mainly comprised of quartz, anorthite, and albite (Uğurlu Sağın 2017). Furthermore, muscovite was determined in Pergamon bricks; and calcite, hematite, and muscovite were determined in Nysa bricks. The firing temperatures of bricks were evaluated as between 850 and 900°C.

According to Lopez-Arce and Garcia-Guinea (2005), the bricks from Toledo, dated to the Roman Period, contained quartz, calcite, anorthite, albite, hematite, illite and diopside, and fired above 900°C.

The mineralogical composition of Era bath bricks from the Roman Period was found to consist of quartz, calcite, anorthite, hematite, potassium feldspar, and illite with a firing temperature of approximately 850°C (Oguz, Turker, and Kockal 2014).

In the study of Stefanidou, Papayianni and Pachta (2015), quartz, calcite, anorthite, albite, illite and gypsum were determined in the bricks that were collected from Roman and Byzantine monuments in Greece. However, firing temperatures were not evaluated within the scope of this study.

The Byzantine bricks from Boğsak Island studied by Eroğlu and Akyol (2017) consisted mainly of quartz, anorthite, albite and limestone, and chert was also found in some samples. They were estimated to be fired between 750–850°C.

The Hagia Sophia bricks were determined to have quartz, calcite, anorthite, albite, hematite, K-feldspar, muscovite, biotite, and pyroxene, and to be fired above 900°C (Taranto et al. 2019).

The bricks from various castles built during Byzantium were investigated by Kurugöl and Tekin (2010). Quartz and calcite were determined in brick samples from Kütahya, and some of the samples had anorthite, albite, hematite, and illite. Bricks from İstanbul were determined to comprise quartz, calcite, muscovite and illite. Accordingly, the firing temperature of samples from both areas was evaluated as between 800–850°C. Besides, quartz, hematite, K-feldspar, and labradorite were found in Amasra samples, and quartz, pyroxene, and sodium silicate were found in Trabzon samples. The firing temperatures were between 850–900°C and above 950°C, respectively.

The mineralogical compositions of Byzantine bricks of Olba Monastery in Mersin consisted of quartz, calcite, anorthite, albite, illite and limestone. The firing temperatures were estimated to be between 750 and 800°C (Özyıldırım and Akyol 2016).

Another study conducted on Byzantine bricks (Ulukaya et al. 2017) identified the mineralogical compositions of bricks from İstanbul as quartz, albite, potassium feldspar, and calcium silicate hydrate (CSH). It was stated that the firing temperatures might be between 850 and 900°C.

Byzantine bricks taken from a Monastery in Sicily were determined to have quartz, hematite, potassium feldspar and muscovite, also anorthite, gehlenite, and diopside presented in some. They were supposed to be fired at temperatures between 800–900°C (Cardiano et al. 2004).

The study of Ballato et al. (2005) compared Byzantine and Ottoman bricks from Great Palace of Constantinople. Byzantine bricks were composed of quartz, anorthite, albite, hematite, and diopside; in addition, calcite, muscovite, illite, gehlenite, zeolite, halite, and gypsum were detected in some. Ottoman bricks contained quartz, albite, hematite, muscovite, and illite mainly, and calcite, halite, and gypsum in some. However, firing temperature was not predicted within the scope of the study.

The mineralogical composition of Ottoman bricks from bath buildings in İzmir (Uğurlu Sağın and Böke 2013) and Aydın (Gürhan, Uğurlu Sağın, and Böke 2017) had similar mineralogical compositions. They were composed of quartz, calcite, albite, hematite, potassium feldspar, and muscovite; only some samples from İzmir did not include calcite and muscovite. It was mentioned that the bricks from İzmir were fired

around 850°C (Uğurlu Sağın and Böke 2013) and the firing temperature of samples from Aydın (Gürhan, Uğurlu Sağın, and Böke 2017) did not exceed 900°C.

Ottoman bricks from İstanbul were found to contain quartz, albite, hematite, chalcopyrite and CaO and their firing temperature was estimated between 800–900°C Kurugöl (2009).

Table 2.3. Mineralogical compositions and estimated firing temperatures of historical bricks determined by previous studies

Location-Reference		Period of Bricks Samples	Mineralogical Composition																	Estimated Firing T.
			Method	Q	C	A	Al	H	K	M	Do	Ill	Bi	G	Di	W	Mu	Cr	Sp	Other	
Serapis Temple, Bergama/Turkey (Aslan Özkaya and Böke 2009)		Helenistic and Roman Periods	XRD	X			X	X	X	X											~850 °C
Some arhaeological sites of Turkey (Uğurlu Sağın 2017)	Bergama	Roman	XRD FTIR	X		X	X			X											850-900 °C
	Aigai	Roman		X		X	X														850-900 °C
	Nysa	Roman		X	X	X	X	X		X											850-900 °C
Toledo/Spain (Lopez-Arce and Garcia-Guinea 2005)		Roman (1^{st}-4^{th} c.)	XRD	X	X	X	X	X				X			X						> 900 °C
Era Bath, Myra/Turkey (Oğuz, Türker and Koçkal 2014)		Roman (3^{rd} c.)	XRD	X	X	X		X	X			X									~850 °C
Greece (Stefanidou, Papayianni and Pachta 2015)		Roman (2^{nd}-4^{th})	XRD	X	X	X	X					X									-
		Byzantine (7^{th}-14^{th})																		gypsum	
Boğsak Island, Mersin/Turkey (Eroğlu and Akyol 2017)		Early Byzantine Period (3^{rd}-7^{th} c.)	OM	X		X	X													limestone, chert*	750-850 °C
Hagia Sophia, İstanbul/Turkey (Taranto, et al. 2019)		Byzantine (4^{th}-14^{th})	XRPD	X	X	X	X	X	X	X			X							pyroxene	> 900 °C
Castles in Different Cities of Turkey (Kurugöl and Tekin 2010)	Kütahya	Byzantine (8^{th}-14^{th})	XRD	X	X	X*	X*	X*				X*									800-850 °C
	Amasra	Byzantine (9^{th}-11^{th})		X				X	X											labradorite	850-900 °C
	Trabzon	Byzantine(10^{th}-12^{th})		X																pyroxene,sodiumsilicate	< 950 °C
	İstanbul	Byzantine (13^{th}-14^{th})		X	X					X		X									800-850 °C
Olba Monastery, Mersin/Turkey (Özyıldırım and Akyol 2016)		Byzantine	OM	X	X	X	X					X								limestone	750-800 °C
İstanbul/Turkey (Ulukaya,et al.2017)		Late Byzantine	XRD	X		X				X										CSH	850-900 °C
Monastery of San Filippo di Fragala, Sicily/Italy (Cardiano, et al. 2004)		Byzantine Period	XRD	X	X	X*		X	X	X				X*	X*						800-900 °C
Great Palace of Constantinople, Istanbul/Turkey (Ballato, et al. 2005)		Byzantine Period	XRD	X	X*	X	X	X		X*		X*		X*	X					zeolite*, halite*,gypsum*	-
		Ottoman Period		X	X*		X	X		X		X									
Bath buildings in İzmir/Turkey (Uğurlu Sağın and Böke 2013)		Ottoman Period	XRD	X	X*		X	X	X	X*											~850 °C
Eski Bath, Aydın/Turkey (Gürhan, Uğurlu Sağın and Böke 2017)		Ottoman (16^{th}-17^{th})	XRD	X	X		X	X	X	X											< 900 °C
İstanbul/Turkey (Kurugöl 2009)		Ottoman (18^{th}-19^{th})	XRD	X			X	X												chalcopyrite, CaO	800-900 °C

Q:Quartz, C:Calcite, A:Anorthite, Al:Albite, H:Hematite, K:K-feldspar, M:Muscovite, Do:Dolomite, Ill:Illite, Bi:Biotite, G:Gehlenite, Di:Diopside, W:Wollastonite, Mu:Mullite, Cr:Cristobalite, Sp:Spinel (* : present in some samples)

CHAPTER 3

HISTORICAL, GEOGRAPHICAL AND ARCHITECTURAL FEATURES OF STUDY AREAS

The Anaia Church in Kuşadası, Aydın and St. Jean Basilica in Selçuk, İzmir were chosen to determine the characteristics and manufacturing techniques of Byzantine period building bricks (Figure 3.1, 3.2). Their close-range locations, similar time periods of construction and usage during the Byzantine period, and brick material usage are the reasons for their selection as case areas of the study.

In this chapter, the historical and geographical background and architectural features of the study areas were given.



Figure 3.1. Map of Aegean Region shows locations of study areas (Dashed line area is enlarged on Figure 3.2) (Revised from Google Earth)



Figure 3.2. Locations of study areas with neighbouring provinces

(Revised from Google Earth)

3.1. St. Jean Basilica, Ayasuluk Hill

Ayasuluk Hill and St. Jean Basilica are located in Selçuk, İzmir. Selçuk is a historical town located in the southeast of İzmir city center and on the border with Aydın. The town is surrounded by Menderes and Torbalı on the north, Tire and Germencik on the east, Söke and Kuşadası on the south (Figure 3.2). Ayasuluk Hill is a mound placed on the northwest part of the Selçuk plain. The Hill surrounded by a fortress comprises the remains of several structures, such as St. Jean Basilica, Gate of Persecution, the citadel that involves houses, a villa, cisterns, a bath, and a mosque (Figure 3.3). St. Jean Basilica is an archaeological monument built during the Byzantine period (4^{th}-6^{th} centuries). The Hill and its monuments are the 1^{st}-degree archaeological site, and they were registered firstly on 11.12.1976 with the decision number A-262 by GEEAYK. Also, the Hill was declared as UNESCO's World Heritage Site along with Ephesus in 2015 ("Ephesus - UNESCO World Heritage Centre" 2015). Scientific excavations of Ayasuluk Hill and St. Jean Basilica were begun in 1921 by G. A. Sotiriou and had been continued by the Austrian Archaeological Institute between 1927-1930 and by the Ephesus Museum Directorate of Ministry of Culture between 1960-2006 (Mimaroğlu 2017; Mimaroğlu and Erdoğan 2018). Pamukkale University conducted the excavation from 2007 to 2019 under the supervision of Dr. Mustafa Büyükkolancı. Since 2020, excavations are proceeding under the supervision of Assoc. Prof. Dr. Sinan Mimaroğlu, Mustafa Kemal University.



Figure 3.3. Aerial view of Ayasuluk Hill and St. Jean Basilica with their surrounding (Revised from photo from Büyükkolancı 2016)

Ayasuluk Hill has a long history of settled life dating back to 3000 BC, the Early Bronze Age. In the second half of the 2nd millennium BC (Late Bronze Age), an important city named as "Apasas" was founded on the Ayasuluk Hill within the border of Arzawa Kingdom, according to Hittite written sources (Büyükkolancı 2008). "Apasas" is thought to be the origin of the name "Ephesus" (Büyükkolancı 2008; Ladstaetter et al. 2015; Baranaydın 2016). The city was conquered by the Lydians in 560 BC, and Lydian King forced the city to move from the Hill to surround of Artemis Temple (Figure 3.4) (Büyükkolancı 2008; Ladstaetter et al. 2015). The city center remained in that location during the Persian (386-334 BC) and Alexander the Great (334-323 BC) hegemonies (Bean 1979). Under the rule of Lysimakhos, who was one of the generals of Alexander the Great, Ephesus was relocated to its current location (Bean 1979; Ladstaetter et al. 2015) (Figure 3.4), and the city was designed as one of the Hellenic cities with a grid plan (Foss 1979). Ephesus gained importance in the Hellenistic and Roman Periods as a commercial port in the Mediterranean and became the capital of the Asian State of the Roman Empire. However, there is little information about the settlement in Ayasuluk during this period. According to the Christian faith, St. Jean, one of the Apostles of Jesus Christ and writer of the Bible, came to Ephesus in the 1st century AD and stayed here until the end of his life and was buried in the Ayasuluk Hill (Mercangöz 1997; Ladstaetter et al. 2015). Consequently, the Hill regained importance with the effect of spreading Christianity and became the 4th city center of Ephesus in the Byzantine Period (Figure 3.4). Ayasuluk Hill was conquered by Aydınoğulları at the beginning of the 14th century and became the capital city of the principality in 1348 (Büyükkolancı 2001). In 1390, it came under the rule of the Ottoman Empire (Büyükkolancı 2001; Ladstaetter et al. 2015). The hill was estimated to maintain its importance until the end of the reign of Fatih Sultan Mehmet (Büyükkolancı 2001).

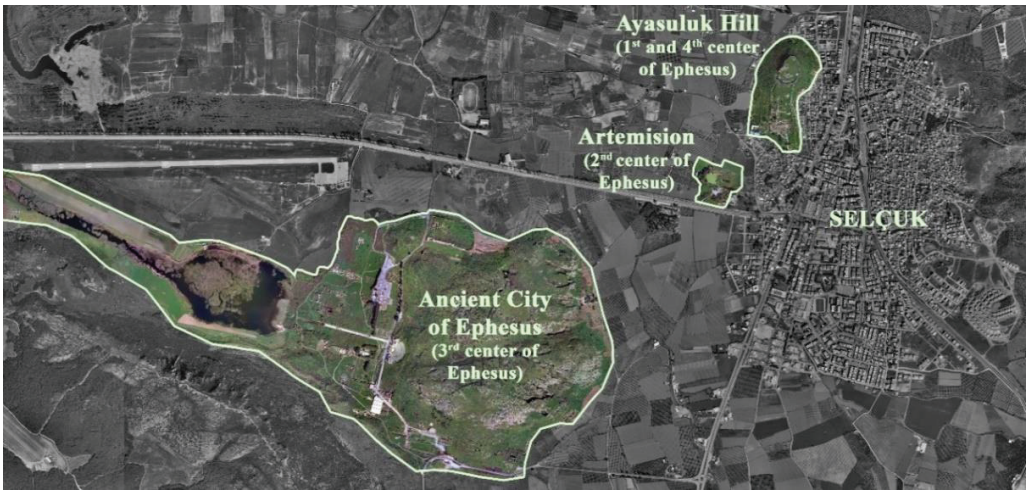


Figure 3.4. Locations of the city centres of Ephesus
(Processed on a satellite image from "İzmir Kent Rehberi" 2016)

The grave of St. Jean, to whom Ayasuluk Hill and the basilica were dedicated, is on the southern slope of the hill. The first church was built in the 5th century AD with a wooden roof covering the grave, a baptistery and a treasure room (or Skeuophylakion) on the north side (Hörmann, Keil, and Sotiriou 1951) (Figure 3.5, 3.6). The church was demolished by the earthquakes occurred in 467-468 AD (Büyükkolancı 2001), and only outer walls of transepts, treasure room and baptistery survived from the first construction period (Figure 3.5). The damaged church was rebuilt by order of Emperor Justinian and designed as a cross-shaped and domed structure (Büyükkolancı 2001; Ladstaetter et al. 2015; Karydis 2016). It was thought that the building was tried to be adapted in an axial plan type with the complex that involved the baptistery and treasure room. In the second construction period, two transepts in the north-south direction, an apse and bema were constructed in the 520s (Karydis 2016) (Figure 3.5). The third construction period, dated to around 550 AD, was a continuation of the second phase. The west aisle, a narthex, an atrium, and a substructure were added to the church in the third phase. The final church reached the dimensions of 110x130 meters and gained a monumental character (Ladstaetter et al. 2015). The structure was covered with six domes that were carried by pillars. Three naves on the west aisle were separated by arched colonnades (Büyükkolancı 1991; Ladstaetter et al. 2015) (Figure 3.7). The entrance to the Church was provided from narthex with three porticos (Büyükkolancı 2001). There was an atrium with a courtyard surrounded by arcades supported by columns in front of the church (Figure 3.5). The atrium was thought to be constructed through the substructure that was built to raise the ground level to the church level (Ladstaetter et al. 2015) (Figure 3.8).

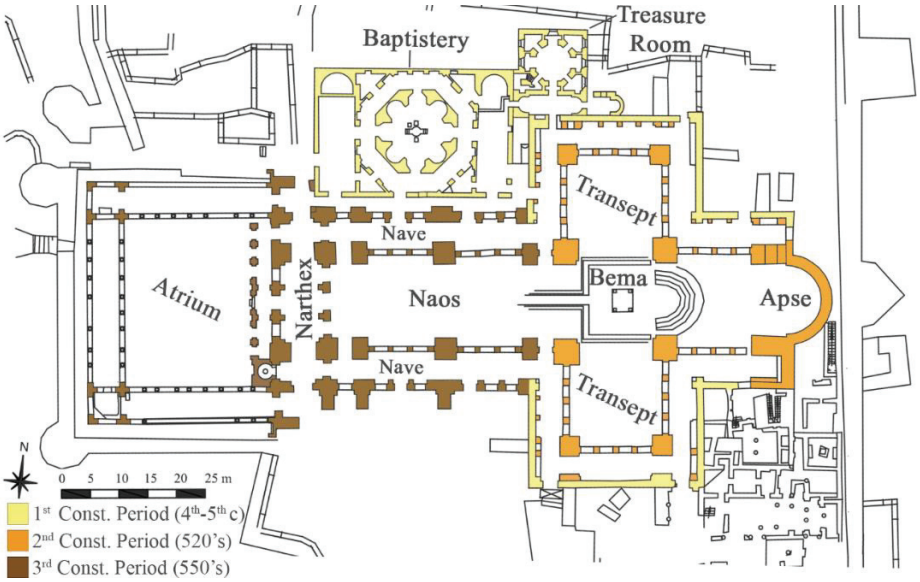


Figure 3.5. Plan of St. Jean Basilica showing the construction phases (Revised from drawing by Ayasuluk Hill and St. Jean Basilica Excavation Archive, 2020)

The Basilica was built in masonry technique and covered with domes. The walls and pillars were the bearing elements that carried arches and domes.

The masonry walls were constructed with brick and stone in alternating bonds or with only brick, while domes and arches were built with brick totally. The bricks of the walls were measured in sizes of 45x30 cm, 35x35 cm, 20x35 cm, and 17-18x35 cm during the field survey. The domes were carried by pillars that were made of cut stone. The cut-stone pillars were considered to continue as bricks on the second floor and joined with the brick arches carried by the stone columns (Büyükkolancı 2001). The bricks used in arches were found in three sizes: measuring 35x50x4.5 cm, 34x34x4.5 cm, and half-size measuring 17x34x4.5 cm (Karydis 2012). As binding material, lime mortar was used in the walls, superstructure, and pillars.

Besides, there were differences between the bonding types of structural elements regarding construction periods. The walls of the treasure room, baptistery, and some parts of transepts that belonged to the first phase were constructed with brick and stone alternating bonds (Figure 3.6). The brick was used alone in the walls of the second and third construction periods, such as the external walls of naves, transepts, narthex, and apse walls (Figure 3.9). Also, the bond type of pillars differed between bema and naos, dated to the second and third construction periods, respectively, as mentioned in the study of Karydis (2016).



Figure 3.6. Baptistery pool and wall structures from 1st period



Figure 3.7. Photo of southern nave with outer brick wall on the left and stone columns and pillars on the right



Figure 3.8. Photo of the exterior walls of substructure and the atrium built on top of it (Source: Büyükkolancı 2018, 24–25)



Figure 3.9. Different wall bonding types from the northern transept (Right side of the wall was a part of 1st phase, and the left side was built in later periods)

3.2. Anaia Church, Kadıkalesi

Kadıkalesi/Anaia is in Davutlar neighbourhood of Kuşadası, Aydın. Kuşadası is located on the west side of Aydın city center on the Aegean Sea coast and opposite the island of Samos. It is a neighbouring town of Selçuk and Söke (Figure 3.2).

Kadıkalesi is a fortress from the Byzantine Period, which was built on a mound measuring 20-25 m high and 250 m in diameter, dominating the sea and Samos Island (Akdeniz 2004). Kadıkalesi involves a monastery complex, Anaia Church on the northeast corner of the fortress. Also, there are structures used for other functions such as masjid, ateliers, and emplacements from World War 1 (Figure 3.10). Kadıkalesi and the closeby environment were listed as 1st-degree archaeological sites on 22.05.2008 with decision number 1531 by Aydın Regional Board for Conservation of Cultural and Natural Assets. Scientific excavations of Kadıkalesi/Anaia have been carried out under the supervision of Prof. Dr. Zeynep Mercangöz since 2001.

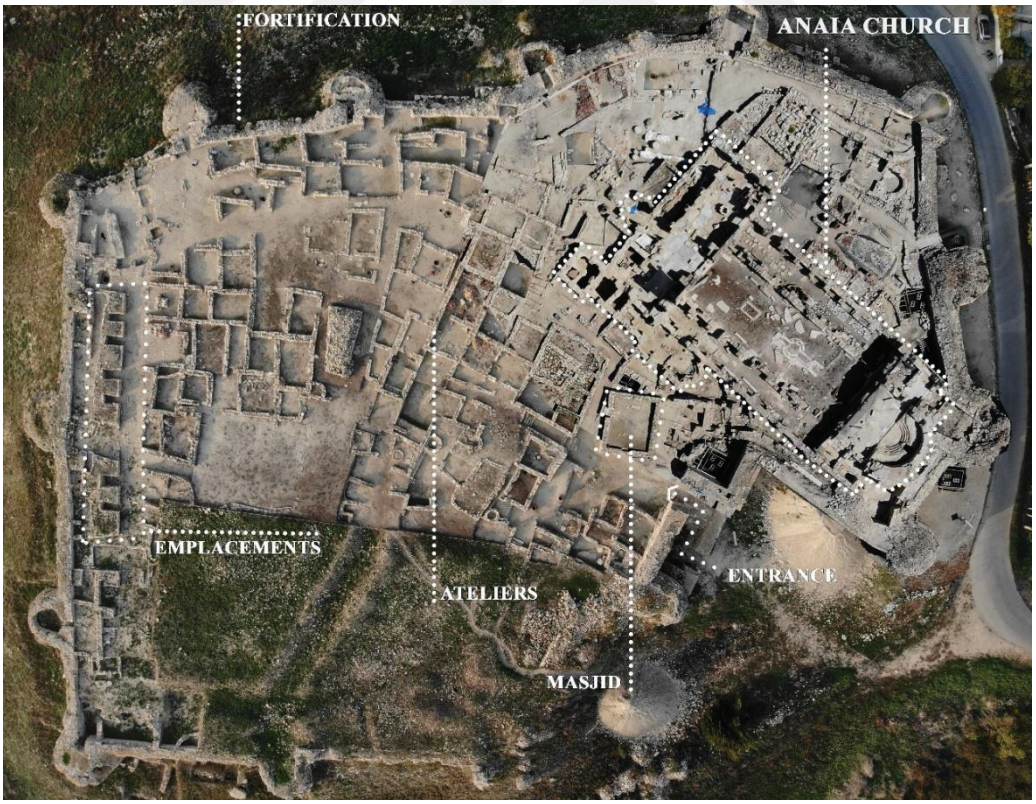


Figure 3.10. Anaia Church and other structures placed within Kadıkalesi (Two aerial photos taken in 2018 and 2021 from Kadıkalesi/Anaia Excavation Archive were overlapped to show the Church without top shelter.)

The ancient settlements in the coastal region from Ephesus to Miletus were dated back to Neolithic Age, about the 8th millennium BC (Yüksel et al. 2011). The Mira principality, which was subordinate to the Hittite state, ruled the region until 1200 BC. Following that, the area was governed by Hellenic colonizations (11th - 6th BC), Persian (6th - 4th BC) and Alexander the Great (334 - 323 BC) dominions, and Roman Empire (2nd BC - 4th AD), respectively (Yüksel et al. 2011). The first settlement in the mound, on which Kadıkalesi was placed, was thought to be established around the 4th millennium BC in the Late Chalcolithic Age, according to the findings (Akdeniz 2007). During that age, Kadıkalesi mound was a peninsula surrounded by the sea and probably used as a harbour (Karadaş et al. 2019). Anaia city was first mentioned in history in a book about the Peloponnesian War in the 5th century BC as "*the stronghold of the Samian emigres*" (Thucydides 1950). However, there is a lack of information about Anaia during the Hellenistic and Roman Periods. In the Byzantine Period, Anaia became a bishopric with the acceptance of Christianity (Foss 1979).

Anaia Church was constructed on the mound in the 5th century and continued to be used during the Byzantine Period with some interventions. In the 13th century, Anaia Church, the monastery complex of the City, became an archbishopric, while the city gained importance and status as a trade centre and port of entry (Foss 1979; Mercangöz 2007; Mimaroğlu 2011). The fortification walls, which would later be called Kadıkalesi during the Ottoman Period, were constructed around the mound to include the Church within its borders during this period to protect the harbour and the city (Mercangöz 2007). When the threats of pirates maximized at the end of the 13th century, the people of Anaia migrated to the interior part from the coast (today's Soğucak, Figure 3.2). Afterwards, Kadıkalesi was conquered by the Aydınoğulları at the beginning of the 14th century. Conversely, Christianity was present in the castle until the middle of the 14th century (Akdeniz 2004; Mercangöz 2007; Mimaroğlu 2011; Onar et al. 2012). The church was thought to be ruined by an earthquake; hence it was abandoned (Mercangöz and Tok 2011). Anaia came under the rule of the Ottoman Empire in the 15th century (Onar et al. 2012). During World War 1, Ottoman soldiers used Kadıkalesi as a positioning area (Mercangöz 2005).

Anaia Church has a three-aisled plan with a dimension of 51.1 by 27.5 meters (Kanmaz 2015) (Figure 3.11, 3.12). The Church was thought to be built first in the Early Byzantine Period, around the 5th century AD (Mercangöz 2013; Kanmaz and Ipekoğlu 2016). In the first construction period, the Church was designed in a three-aisle plan scheme with an apse (Mercangöz, Tok, and Hazinedar Coşkun 2012). Also, it was thought to be constructed with a wooden roof and to have an atrium and a narthex (Kanmaz 2015). Since the Church was located on a mound, a vaulted substructure was constructed under the bema to rise and equalize the ground (Mercangöz, Tok, and Hazinedar Coşkun 2012) (Figure 3.13). A baptistery in the north corner of the Church was revealed during the excavation, and it was dated to the first construction period as well (Hazinedar Coşkun 2021).

The first church was affected and severely damaged by an earthquake in this area (probably occurred in 1040 and 1056 ("AFAD, Tarihsel Depremler" n.d.)) (Mercangöz and Tok 2011). Consequently, the bema and western walls of naos survived, but the Church was rebuilt between 11th-13th centuries, which was regarded as the second construction period (Kanmaz and Ipekoğlu 2016) (Figure 3.11). During the second period, piers supporting survived walls from 1st phase were added, and external walls of aisles and inner narthex were reconstructed (Figure 3.11, 3.14). Entrances to the naves from the narthex were provided from three door openings designed symmetrically on the north and south sides (Mercangöz and Tok 2011). Subsequently, some interventions dated back to 13th-14th centuries were evaluated as the third construction period (Kanmaz 2015). Buttresses were added to the narthex wall, and walls were constructed between naves and naos during the third construction period to strengthen the structure against earthquakes (Figure 3.11, 3.15, 3.16). Besides the measures taken against earthquakes, outer narthex and baptistery were added to the northwest of the Church in same period either (Mercangöz and Tok 2011; Kanmaz 2015) (Figure 3.11). Thereafter, cisterns by division of outer narthex and a southern chapel were built (Figure 3.17). The cisterns and southern chapel were thought to be constructed after the outer narthex, regarding the joints between the walls (Mercangöz and Tok 2011; Kanmaz 2015; Mercangöz 2018). Nevertheless, cisterns and southern chapel were evaluated as a part of the third construction period since they were also dated to the 13th-14th centuries (Kanmaz and Ipekoğlu 2016) (Figure 3.11).

Anaia Church was built in masonry technique with brick-stone bearing walls (Kanmaz 2015). Buttresses supported the walls and also carried arches that were thought to bear the roof (Mercangöz and Tok 2011). Building materials used in the Anaia Church

were brick and stone, and lime mortar as binding material. The walls of the Church had different bonding types that provided to distinguish the construction periods (Figure 3.14, 3.15). The first and second construction periods' walls were built with brick and stone alternating bonds generally, exceptionally, the external wall of the northern nave. The walls and buttresses of the third construction period were made of rough-cut and rubble stone, and bricks were used in joints (Kanmaz 2015) (Figure 3.16). The bricks found in situ and most likely from the walls were measured in variable sizes as 24-26x16x5 cm, 36.5x20x4.5 cm, 34x13x5 cm, 32-33x20x4 cm, 35x15x4 cm. The bonding quality of structural elements from 3rd phase was found to be poorer than that of the other periods regarding the material usage and workmanship (Kanmaz and Ipekoğlu 2016). The arches and vaults which were observed in substructure and narthexes were constructed by using brick materials (Figure 3.13). In addition, remains of domes covering the cistern, which was juxtaposed to the west corner of the Church, were built with bricks and supported by a marble column (Figure 3.17). There were also marble columns probably bearing the arches in naos, southern chapel and substructure. The floor coverings were generally composed of marble. However, there was a brick paving in the middle of the outer narthex from the 3rd phase and in a part of the baptistery from the 1st construction period, in 41x29 cm and 35x35 cm sizes, respectively.

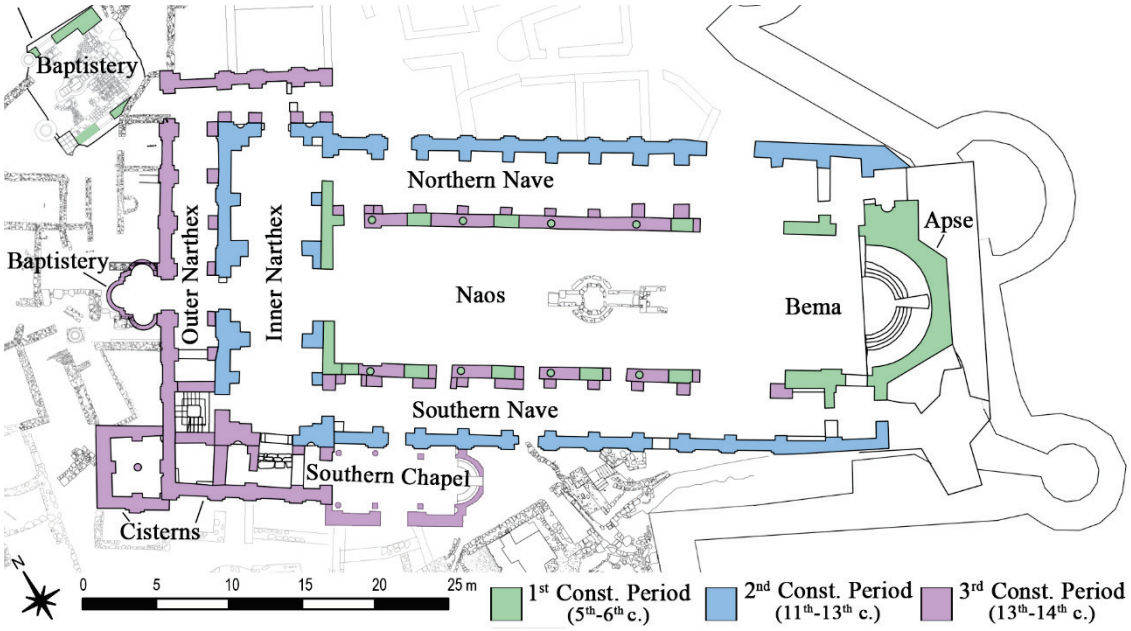


Figure 3.11. Plan of Anaia Church (Revised from the drawing by M. Buğra Kanmaz and Umut Kardaşlar, Kadıkalesi/Anaia Excavation Archive, 2021)

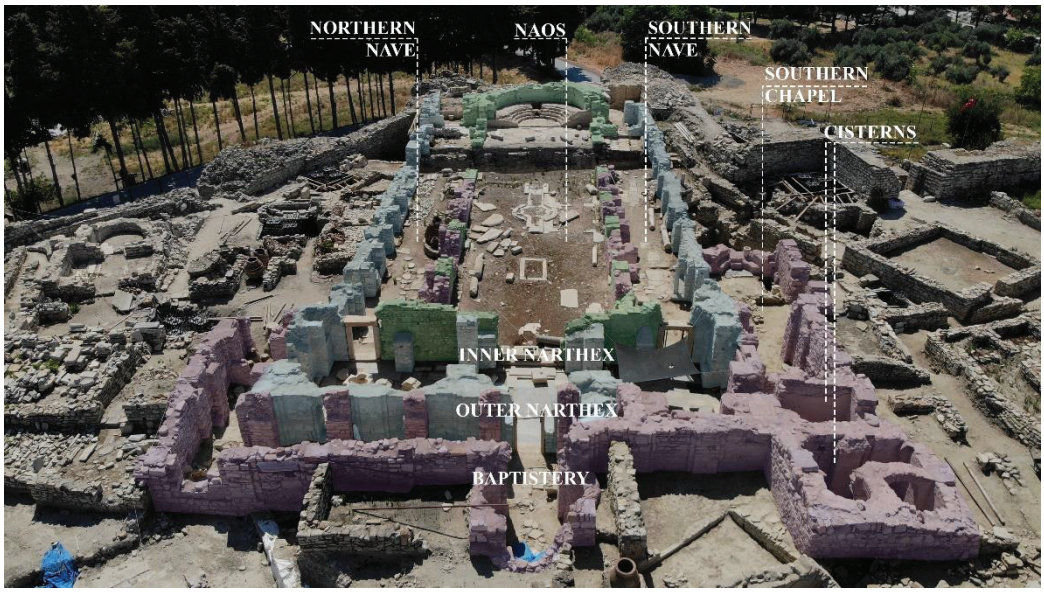


Figure 3.12. Photo of Anaia Church showing the spaces and their construction periods (Colours indicating the periods were expressed in Figure 3.11) (Revised from Kadıkalesi/Anaia Excavation Archive, 2021)



Figure 3.13. Substructure from 1st phase with brick vault and arches

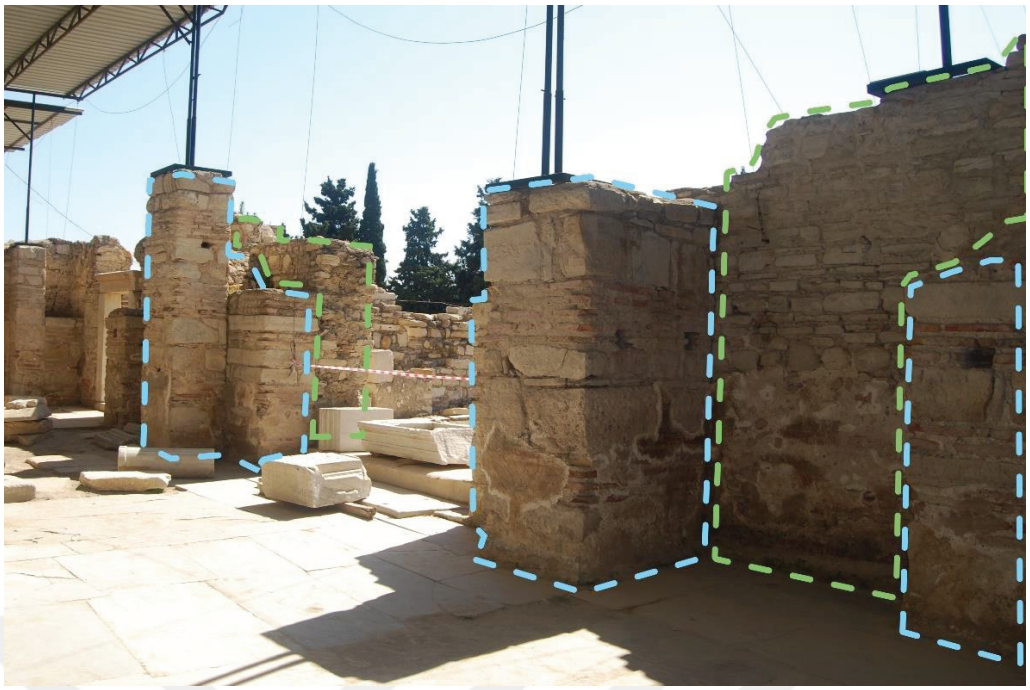


Figure 3.14. Photo of the wall between naos and inner narthex, buttresses from 2nd phase (blue dashed lines) supports the wall from 1st phase (green dashed lines)



Figure 3.15. The wall between naos and southern nave, walls added in 3rd period (purple dashed lines) between piers from 1st period (green dashed lines)



Figure 3.16. A buttress on the northern façade from the 3rd phase



Figure 3.17. Photo of the cistern in the west corner showing the remains of arches and domes

CHAPTER 4

EXPERIMENTAL STUDIES

Characteristics of brick samples collected from two Byzantine churches, St. Jean Basilica, Ayasuluk Hill and Anaia Church, Kadıkalesi, were investigated by standard test methods, scanning electron microscope (SEM) coupled with energy dispersive spectroscopy (EDS), X-ray diffraction (XRD) and Fourier transformed infrared spectroscopy (FTIR), thermogravimetric analysis (TGA), mechanical tests. Sampling procedures, sample definitions and the experimental methods used for the determination of basic physical properties, colourimetry, chemical compositions and microstructural properties, mineralogical compositions, pozzolanic activities, and mechanical properties were described in this chapter.

4.1. Sampling

Brick samples were collected from two Byzantine churches, the Anaia Church in Kadıkalesi, Kuşadası and the St. Jean Basilica in Ayasuluk Hill, Selçuk, with the permission and guidance of the excavation teams in July 2020. Sampling was performed from the upper parts of the building elements where deterioration problems were not observed. Samples were taken as small as possible to avoid damage to the integrity of the monuments. Sampling locations were documented by photographs. The sampling was performed on the basis of architectural spaces and construction period differences in the churches. The colours and sizes of the bricks were considered during the sampling since these properties might be indicators of different periods. The samples were labelled and stored in polythene bags.

Samples were labelled according to the names of the churches and the spaces they had been collected. The first letter of the label indicated the name of the site (A: Ayasuluk, K: Kadıkalesi). The spaces where samples were collected were abbreviated in the second letter (B: Bema, Ba: Baptistery, C: Cistern, G: Gate, I: Inner Narthex, O: Outer Narthex, N: Naos, P: Southern Chapel, R: Treasure Room, S: Substructure, T: Transept). Numbers were used for differentiating samples from the same spaces of churches (Figure 4.1).

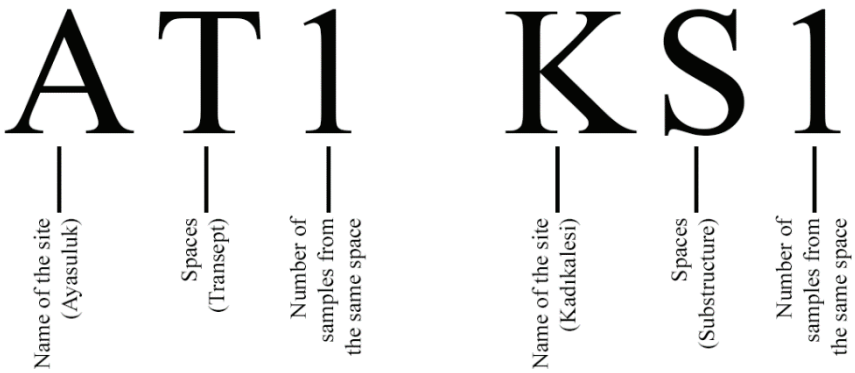


Figure 4.1. Sample labelling method

Thirty samples were collected from both buildings totally, ten samples from St. Jean Basilica in Ayasuluk Hill, and 20 samples from Anaia Church in Kadıkalesi. Both study areas were built during the Byzantine period and had different construction phases.

St. Jean Basilica was constructed in three phases (Büyükkolancı 2001; Karydis 2016). The baptistery, the treasure room (or Skeuophylakion), and outer walls of transepts and east cross arm were considered as the first construction period dated between the middle of 4th century and the beginning of 5th century. The remains of apse wall, columns and wall fragments of transepts and east cross arm were thought to be built during the second phase of the church dated back to the first half of 6th century. The third phase, which was dated to the second half of 6th century, involves the substructure, atrium, and west cross arm of the church (Karydis 2016). The samples collected from St. Jean Basilica were classified according to these construction periods, as three samples from each of the first and third phases and four samples from the second construction period (Figure 4.2, Table 4.1).

Anaia Church was thought to be built in different periods (Mercangöz and Tok 2011; Mercangöz, Tok, and Hazinedar Coşkun 2012). In the study of Kanmaz and İpekoğlu (2016), three construction periods were determined. The naos with apse, the substructure, and the baptistery on the north of the church were constructed during the first phase dated between the 5th-6th centuries. The second phase of the church (11th-13th centuries) comprises the reconstruction of inner narthex and walls of naves, and also addition of buttresses to support the western wall of naos. The outer narthex, baptistery, southern chapel and cisterns were added to the church during the 13th-14th centuries in the third construction period (Mercangöz and Tok 2011; Kanmaz and Ipekoğlu 2016). Nine samples from the first, four from the second, and seven samples from the third construction period of Anaia Church were collected (Figure 4.3, Table 4.2).

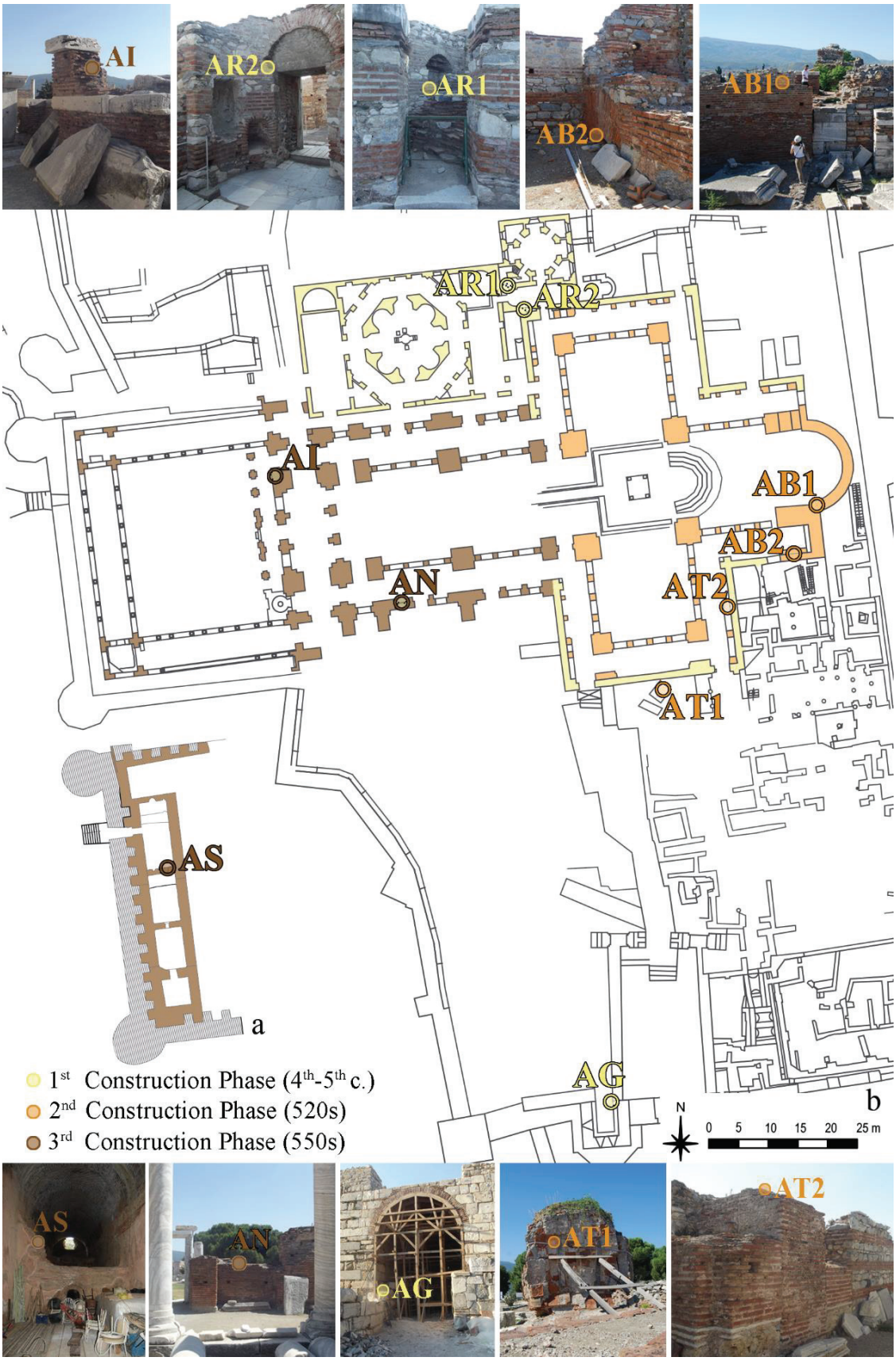
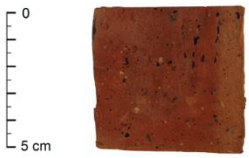
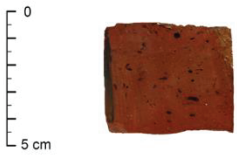
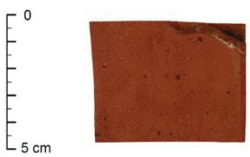
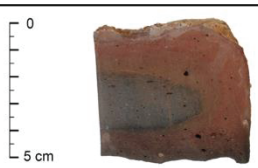


Figure 4.2. a: Substructure plan, b: General plan of St. Jean Basilica, Ayasuluk Hill and photos show where samples were taken (Revised from the drawing from Ayasuluk Hill and St. Jean Basilica Excavation Archive, 2020)

Table 4.1. Brick samples from St. Jean Church, Ayasuluk Hill

Sample			Photos	Location
ST. JEAN BASILICA / AYASULUK	First Construction Phase (4th-5th c.)	AR1		Inside of the niche in the southwesten cell of the treasure room
		AR2		The southern wall of corridor located between treasure room and transept
		AG		The bottom part of the wall of gate tower
	Second Construction Phase (520s)	AB1		The top part of outer apse wall
		AB2		Under the arch in the southern space of the outer apse (The brick was 4 cm thick and 16,5 cm wide.)
		AT1		Dome ruin of the southern transept
		AT2		Top of the eastern wall of southern transept
	Third Construction Phase (550s)	AI		Top of the western wall of the narthex
		AN		Top of the outer wall of the south aisle
		AS		The separating wall of the substructure located under the atrium

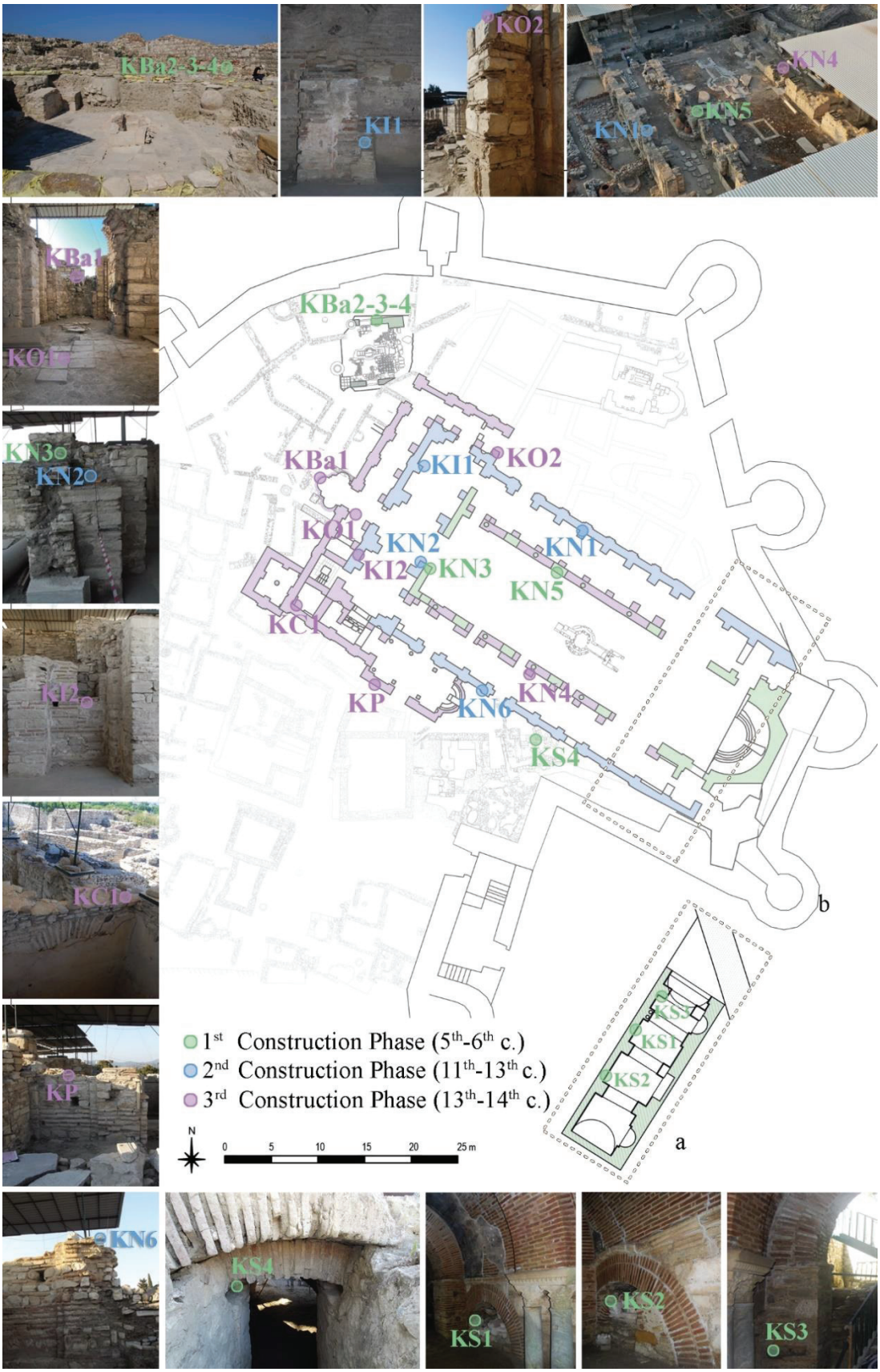
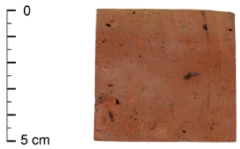
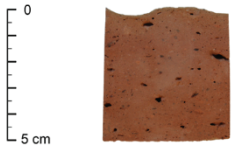
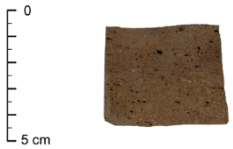
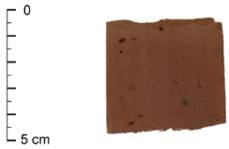
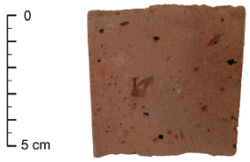
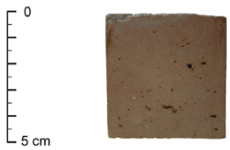
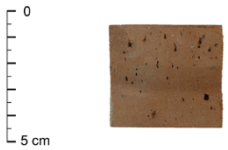
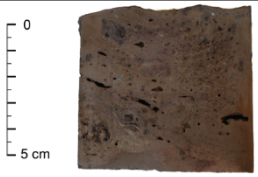


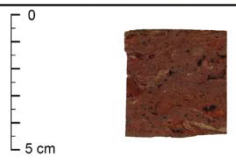
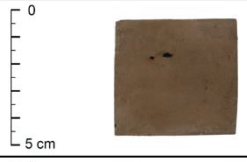
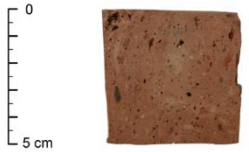
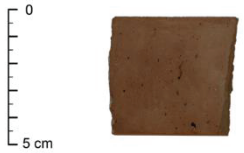
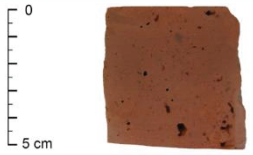
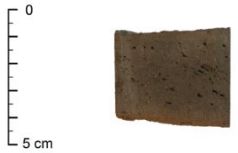
Figure 4.3. a: Substructure plan, b: General plan of Anaia Church, Kadıkalesi and photos show where samples were taken (Revised from the drawings by Buğra Kanmaz and Umut Kardaşlar, Kadıkalesi/Anaia Excavation Archive, 2021)

Table 4.2. Brick samples from Anaia Church, Kadıkalesi

Sample			Photos	Location
ANAIA CHURCH/KADIKALESİ	First Construction Phase (5th-6th c.)	KS1		Rubble waste under the first arch of substructure (Full size of brick was 36,5x20x4,5 cm)
		KS2		Infill wall under the second arch of the substructure (The brick was 4 cm thick and 17,5 cm wide.)
		KS3		The buttress of the substructure
		KS4		The arch in the corridor with the ribbed vault
		KBa2		Finds of baptistery that is located north side of the basilica (Three samples in different colors were collected from the same place to observe differences in firing temperature. The bricks were in the size of 4 cm thick and 17,5 cm wide.)
		KBa3		
		KBa4		
		KN3		The wall that located between inner narthex and naos
		KN5		The upper part of buttress in the northern part of naos

(cont. on next page)

Table 4.2. (cont.)

Sample			Photos	Location
ANAIA CHURCH/KADIKALESİ	Second Construction Phase (11th-13th c.)	KN1		The top of the buttress in the north aisle of the naos (The brick was in the size of 34x13x5 cm.)
		KN2		The top of the buttress that located between inner narthex and naos
		KN6		The top of the buttress in the southern aisle of the naos
		KI1		The remain of buttress in the inner narthex (The brick was 4,5 cm thick and 16 cm wide.)
	Third Construction Phase (13th-14th c.)	KN4		The top of buttress between southern aisle and naos
		KBa1		The wall of baptistery connected with the outer narthex
		KC1		The upper part of the inner cistern wall
		KI2		The wall infill that is located between inner and outer narthex
		KO1		The floor covering of outer narthex in front of the baptistery
		KO2		The top of buttress in outer narthex that connected to the inner narthex
		KP		Outer wall of the southern chapel

4.2. Experimental Studies

Experimental studies were carried out on brick samples to identify their properties as listed below:

- Basic Physical Properties
    - Porosity, Apparent Density, Saturation Coefficient, Pore Interconnectivity
    - Drying Rate
- Mineralogical and Chemical Composition, Microstructural Properties, Thermogravimetric Analyses
- Colour Measurements
- Pozzolanic Activity
- Mechanical Properties
    - Uniaxial Compressive Strength
    - Modulus of Elasticity

4.2.1. Determination of Basic Physical Properties

Standard test methods were used for the determination of the basic physical properties of brick samples (RILEM 1980). For this purpose, two parallel cubic samples of each brick, with sizes ranging between 3 and 6.5 cm due to the thickness of the bricks, were prepared. Samples were dried in an oven at 40°C for at least 24 hours, and their dried weights (M_{dry}) were measured (Figure 4.4). The samples were kept in distilled water for 24 hours at atmospheric pressure in room condition and also under low pressure in a vacuum oven (3608-6CE Vacuum Oven, Lab-Line) (Figure 4.4). The saturated weights of samples at atmospheric pressure (M_{atm}) and low pressure (M_{sat}) were measured. Afterwards, the Archimedes weights (M_{arch}) were measured when samples were totally immersed in distilled water (Figure 4.4). The weight measurements were carried out by a precision balance with the sensitivity of 0.01 g (HF-3000G, A&D). Porosity (P), apparent density (D), saturation coefficient (S) and pore interconnectivity (A_x) were calculated by using weights.

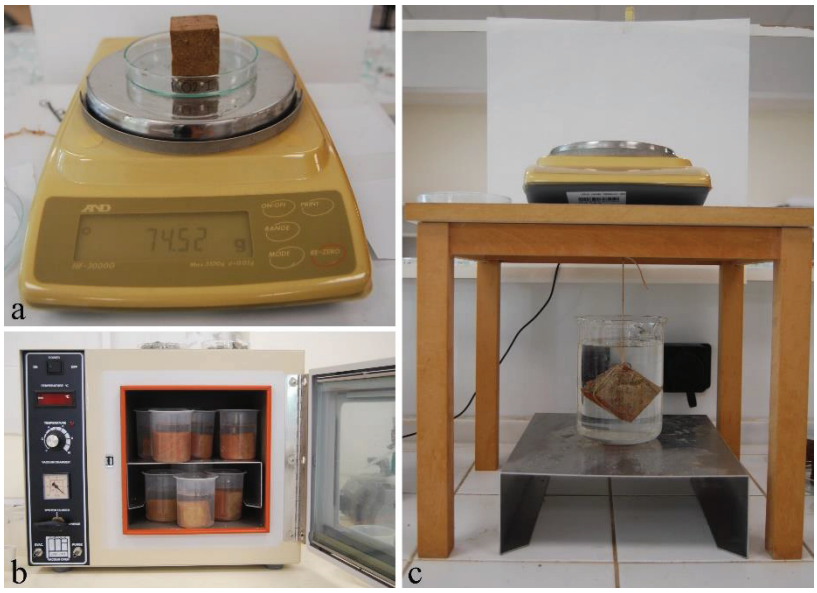


Figure 4.4. a: Weight measurements, b: Samples in vacuum oven, c: Measurements of Archimedes weight

Porosity (P) is the ratio of the volume of pores to bulk volume. It is expressed in percent (%) and calculated by the equation below (4.1) (RILEM 1980).

$$P\ (\%) = [(M_{sat} - M_{dry}) / (M_{sat} - M_{arch})] \times 100 \quad (4.1)$$

The apparent density (D), or bulk density, is defined as the ratio of the mass to the bulk volume of samples and expressed in grams per cubic centimeters (g/cm^3) (4.2) (RILEM 1980).

$$D\ (g/cm^3) = M_{dry} / (M_{sat} - M_{arch}) \quad (4.2)$$

Saturation coefficient (S) is the ratio of water volume in the pores at atmospheric pressure to water volume in the pores at low pressure (RILEM 1980). It is an indicator of the amount of pores open to water absorption. The equation was given below (4.3).

$$S = (M_{atm} - M_{dry}) / (M_{sat} - M_{dry}) \quad (4.3)$$

Pore interconnectivity (A_x) indicates the connection between the pores of the material and the presence of pores that are difficult for water to penetrate under natural conditions (4.4) (Cultrone et al. 2004).

$$A_x = [(M_{sat} - M_{atm}) / M_{sat}] \times 100 \quad (4.4)$$

For determination of drying rates, brick samples prepared in cubic shapes were weighed in dry (M_{dry}) and saturated condition (M_{sat}) that waited within distilled water in a vacuum oven at low pressure (at -25 in. Hg) for 24 hours. Following measurement of saturated weights, they were left to dry in room conditions. The samples were placed as the surfaces were open to evaporation equally (Figure 4.5). The weight losses were followed with measurements at certain time intervals (M_t) such as 15-30-60 minutes, 2-3-4 hours, and 1-2-3-4-6 days. A precision balance with the sensitivity of 0.1 mg (Libror AEX-200G, Shimadzu) was used for all measurements.

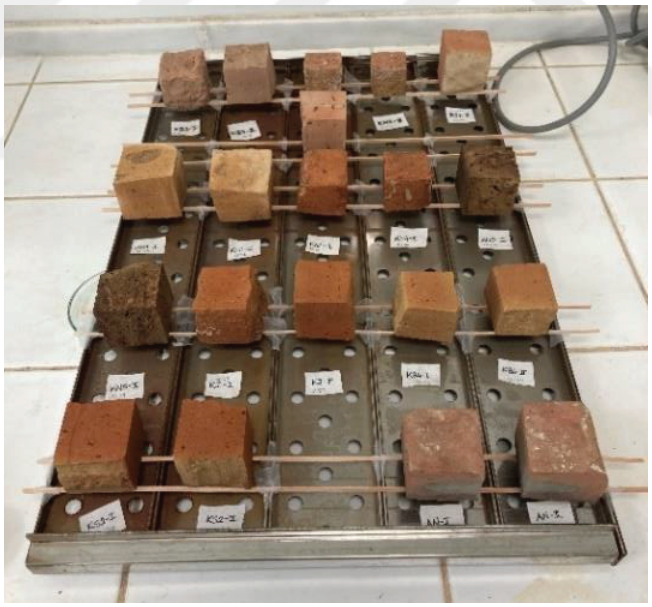


Figure 4.5. Brick samples during drying cycle in room condition for determination of drying rate

The drying rate was calculated as density of flow rate (g) by the equation below (4.5), and the diagrams were prepared to express the results.

$$g\ (kg/m^2.s) = M / A \times t \qquad (4.5)$$

where;

g : Density of flow rate (kg / m^2.s)

A : Total surface of the area of the prismatic test specimen (m^2)

t : Time (second)

M : Moisture content of the sample at a certain time (kg)

$$M = (M_t - M_{dry}) / (M_{sat} - M_{dry}) \qquad (4.6)$$

M_t : Wet weight at a certain time (kg)

M_{sat} : Saturated weight (kg)

M_{dry} : Dry weight (kg)

4.2.2. Determination of Mineralogical and Chemical Compositions, Microstructural Properties, Thermogravimetric Analyses

Mineralogical compositions of brick samples were determined by Fourier Transform Infrared Spectrometry (FT-IR) and X-ray Diffraction (XRD) analyses. For the FT-IR analysis, fine brick powders (<53 μm) were grounded with KBr and pressed into pellets. FT-IR spectra of all samples was obtained by using PerkinElmer Spectrum BX FT-IR spectrometer in wavenumber range from 4000 cm^{-1} to 400 cm^{-1} with the resolution of 4 cm^{-1}. All spectra data were recorded in the absorbance mode and corrected for pure KBr spectrum.

XRD analysis was performed by using a Philips X-Pert Pro X-ray Diffractometer with CuKά radiation on brick powder grounded less than 53 μm. XRD patterns of samples were obtained in the range of 5-60 ^{o}2Theta and with a scan speed of 1,6^o per minute. The Panalytical Highscore Plus software was used to determine XRD data.

Microstructural properties and chemical composition of bricks were determined by Philips XL 30S-FEG Scanning Electron Microscope (SEM) equipped with X-Ray Energy Dispersive System (EDS). Determination of microstructural properties was performed on bricks cut as pieces. Furthermore, chemical analysis was carried out on

samples pressed into pellets. Data were obtained from three different areas (approximately 800 x 800 μm) of samples at 500 magnifications in terms of oxide compositions.

The results of chemical compositions were evaluated with hierarchical cluster and one-way ANOVA analyses. IBM SPSS Statistics software was used for analyses. Hierarchical cluster analysis classifies data and categorizes them into groups by differentiating similarities and dissimilarities. For the analysis, "Average Linkage Method" and "Euclidean Method" were implemented to variables which were major chemical compositions (SiO_2, Al_2O_3, CaO, FeO, MgO, K_2O, Na_2O, TiO_2). The one-way ANOVA analysis is used to determine whether there is a statistically significant difference between the means of independent groups. It was applied for each oxide, and results were given by the means, F-value, and p-value.

Thermogravimetric Analyses (TGA) were conducted on a Perkin Elmer Diamond TG/DTA. Approximately 4 mg of brick powders grounded less than 53 μm were heated in the temperature range of 25-1000°C at a rate of 10°C/min, and the changes in their weight were recorded.

4.2.3. Colour Measurements

The colour of brick materials depends on the mineralogical composition of raw material and firing temperature. Consequently, the determination of the colour is significant for the classification of bricks. Colour of brick samples was examined by using Munsell Soil Colour Chart (Munsell Colour (Firm) 2000). In Munsell colour system, colours are defined with three variables: hue, value, and chroma. The Hue, that represents the colour, consists of five principal hues, which are red (R), yellow (Y), green (G), blue (B), purple (P), and five intermediate hues (YR, GY, BG, PB, RP). The degree of overlapping of colours expresses with four values that 2.5, 5, 7.5, 10 (Figure 4.6). In the system, the value indicates the lightness of the colour. It changes in the range of 0 to 10, in other words, dark to light. The saturation of colour is represented by the chroma in the Munsell colour system. The zero point of the chroma in all hues is the colour grey, and the saturation increases in higher values (Gerharz, Lantermann, and Spennemann 1988) (Figure 4.6).

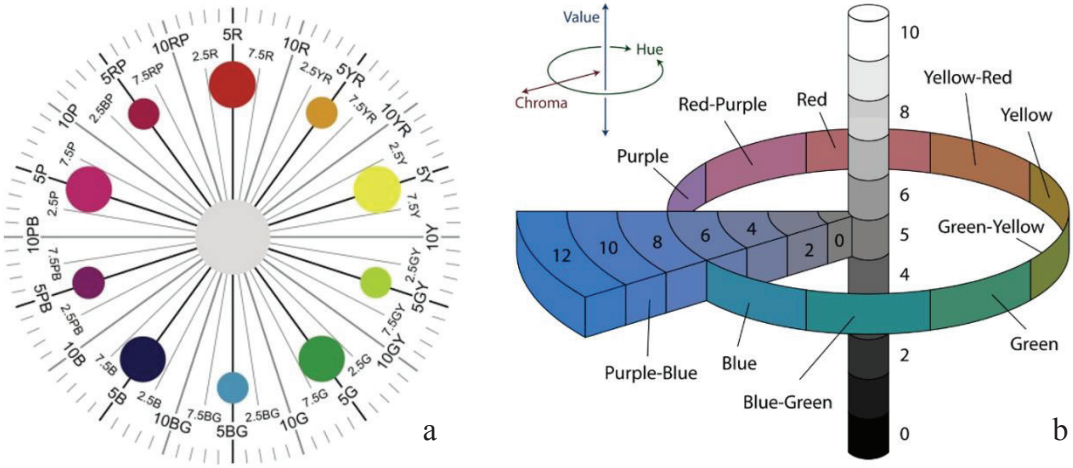


Figure 4.6. a: Munsell Hue scale (Source: Setchell 2012, 103), b: Munsell colour system (Source: Cochrane 2014, 29)

4.2.4. Determination of Pozzolanic Activities

Pozzolanic activity is the ability of materials to react with lime in the presence of water. Pozzolanic activities of bricks were determined by measuring the electrical conductivity differences of saturated calcium hydroxide solution ($Ca(OH)_2$) before and after the addition of finely grounded samples (<53µm) (Luxan, Madruga, and Saavedra 1989) by using pH/conductivity meter (Multiline P3, WTW). Brick powders were added to $Ca(OH)_2$ with the ratio of 1 g/40 ml and stirred with a magnetic mixer for 2 minutes (Figure 4.7). The differences between the electrical conductivity values (ΔEC in mS/cm) of saturated $Ca(OH)_2$ and the solution-brick powder mixture express the pozzolanic activity of bricks. The ΔEC values greater than 1.2 mS/cm indicate good pozzolanicity (Luxan, Madruga, and Saavedra 1989).

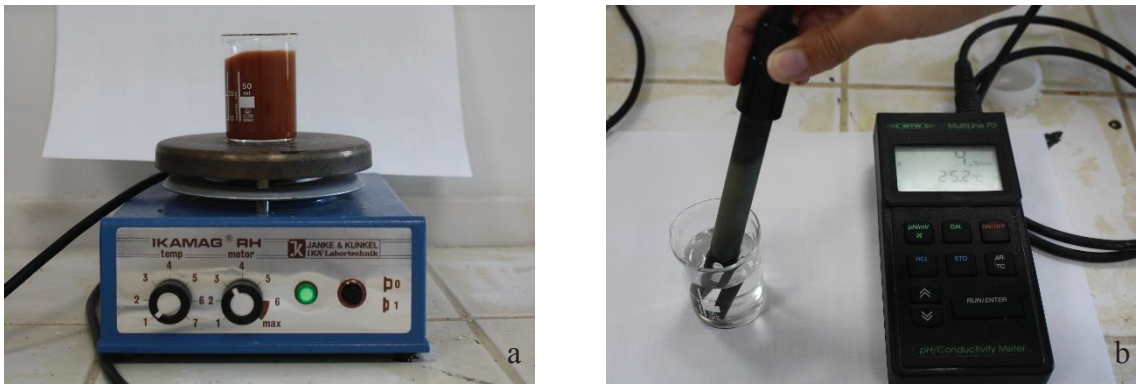


Figure 4.7. a: Mixing $Ca(OH)_2$ and brick powder, b: Measurement of electrical conductivity

4.2.5. Determination of Mechanical Properties

Mechanical properties of brick samples were determined by mechanical tests following the procedure TS EN 772-1+A1. All bricks (30 samples totally) as two parallel samples were tested. Samples were prepared as if the surfaces to which load would be applied were plane and parallel to each other. The surface area of the bricks ranged from 23.7x23.8 cm to 48.5x48.8 cm, and the height ranged from 17.5 to 43.2 cm.

Samples that stayed in distilled water for 24 hours at atmospheric pressure were kept in room condition to ensure they became air-dry condition before testing. Mechanical analyses were conducted using Shimadzu AG-I mechanical test instrument with a capacity of 250 kN (Figure 4.8). Force was applied to samples with 0.5 mm/min speed (Figure 4.8). The test machine was operated by Trapezium2 software, force and stroke were loaded automatically and given as graphics by the software. Mechanical properties of bricks were defined by compressive strength and modulus of elasticity. The equations used for the calculation of compressive strength (σ) and modulus of elasticity (E_{mod}) were given below.

$$\sigma = F/A \tag{4.7}$$

where;

σ : Compressive strength

F : Maximum load (kN)

A : Loaded surface area of sample (mm^2)

$$E_{mod} = (F/A)/(\Delta l/l_o) \quad (4.8)$$

where;

E_{mod} : Modulus of elasticity

F : Maximum load (kN)

A : Loaded surface area of sample (mm^2)

Δl : Change in heigh of sample (mm)

l_o : Initial heigh of sample (mm)

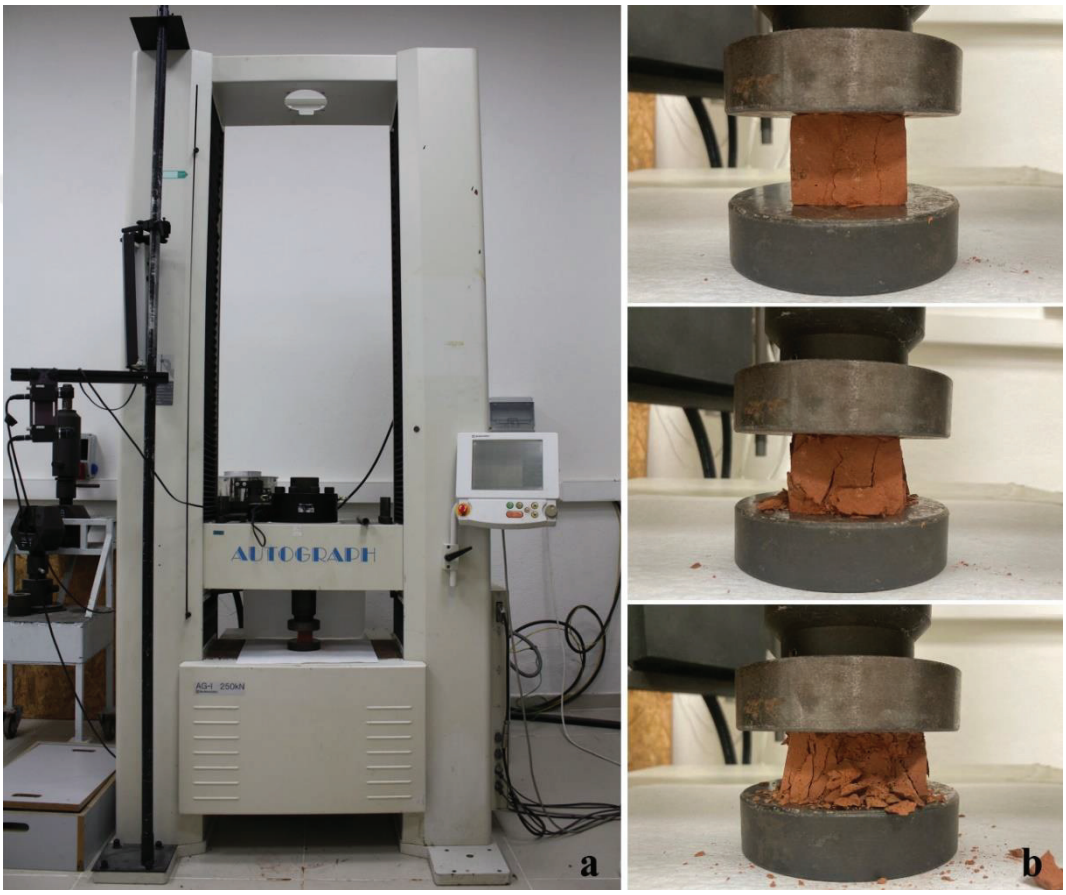


Figure 4.8. a: Photo of Shimadzu AG-I mechanical test instrument, b: Process of loading force to a brick sample

CHAPTER 5

RESULTS AND DISCUSSIONS

Basic physical properties, chemical and mineralogical compositions, microstructural properties, pozzolanic activities and mechanical properties of bricks used in St. Jean Basilica, Ayasuluk Hill and Anaia Church, Kadıkalesi were determined by standard test methods, SEM-EDS, XRD, FTIR, TGA, and mechanical analyses. The results of the experimental studies were given and discussed in this chapter.

5.1. Basic Physical Properties

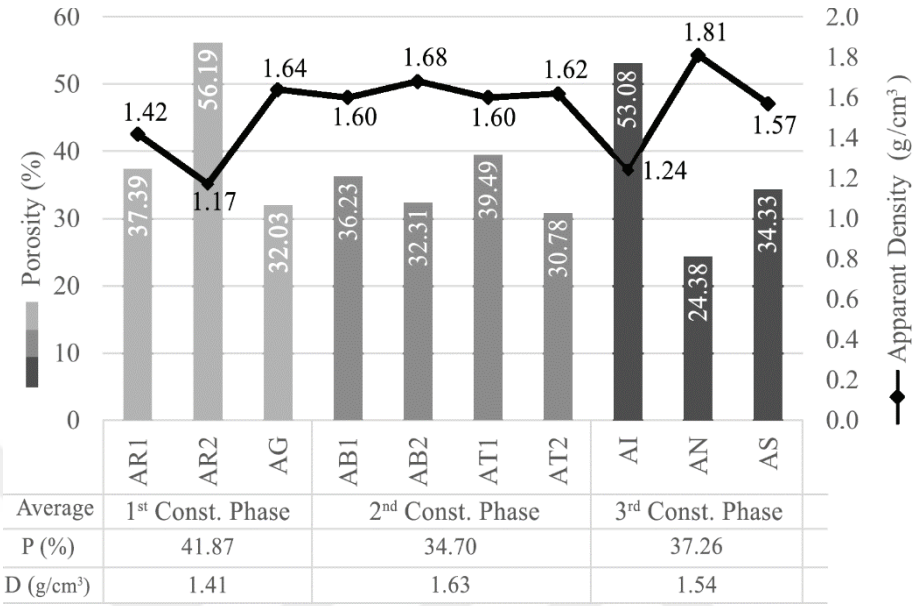
The basic physical properties of bricks were defined by their apparent density values (g/cm3), porosity values (%), and pore characteristics. These properties depend on the mineralogical, textural, and physical changes that occur during the manufacturing process (Cultrone et al. 2004; Karaman, Ersahin, and Gunal 2006; Fernandes, Lourenço, and Castro 2010).

The basic physical properties of brick samples were determined according to RILEM standard test methods (RILEM 1980), and the results were depicted in Figure 5.1, 5.2, and Table 5.2.

In the bricks from St. Jean Basilica, porosity and apparent density values were in the range of 32.03–56.19% and 1.17–1.64 g/cm^3 in samples from the 1st phase, 30.78–39.49% and 1.60–1.68 g/cm^3 in samples from the 2nd phase, and 24.38–53.08% and 1.24–1.81 g/cm^3 in samples from the 3rd phase. The porosity and apparent density of bricks from St. Jean Basilica were found generally in a close range, between 30.78–39.49% and 1.42–1.68 g/cm^3, whereas three samples have porosity and density values different from the average.

The samples AR2 from the 1st phase and AI from the 3rd phase were determined to have higher porosity (56.19% and 53.08%, respectively) and lower density (1.17 g/cm^3 and 1.24 g/cm^3) values than average. Also, AN from the 3rd phase had lower porosity (24.38%) and higher density (1.81 g/cm^3) values (Figure 5.1, Table 5.2). These differences could most likely be explained by the fact that the bricks were exposed to

different firing temperatures due to their variable positions in the kiln because vitrification increases in brick matrices at higher temperatures and, accordingly, the density value increases while the porosity decreases (Weng, Lin, and Chiang 2003).



Average	1st Const. Phase	2nd Const. Phase	3rd Const. Phase
P (%)	41.87	34.70	37.26
D (g/cm³)	1.41	1.63	1.54

Figure 5.1. Porosity (%) and apparent density (g/cm^3) values of St. Jean Basilica samples from different construction periods

The bricks from Anaia Church have porosity and apparent density values ranging between 24.25–51.78% and 1.22–1.73 g/cm^3 in the samples from the 1st phase, 36.33–51.28% and 1.26–1.55 g/cm^3 in the samples from the 2nd phase, and 29.66–50.48% and 1.23–1.67 g/cm^3 in the samples from the 3rd phase (Figure 5.2, Table 5.2). The average density and porosity values of the periods were found to be in similar ranges.

The lowest average of porosity and the highest average of density were found in the 3rd phase. However, KN3 from the 1st construction period indicated the lowest porosity (24.25%) and the highest density (1.73 g/cm^3) value, but it could not be accepted to represent the 1st phase. Besides, there was no similar trend in Anaia Church brick, even among their periods, in terms of porosity and density values. It was thought that the reason for the differences between the bricks is the inability to produce homogeneous bricks due to the shaping and firing methods used in their production.

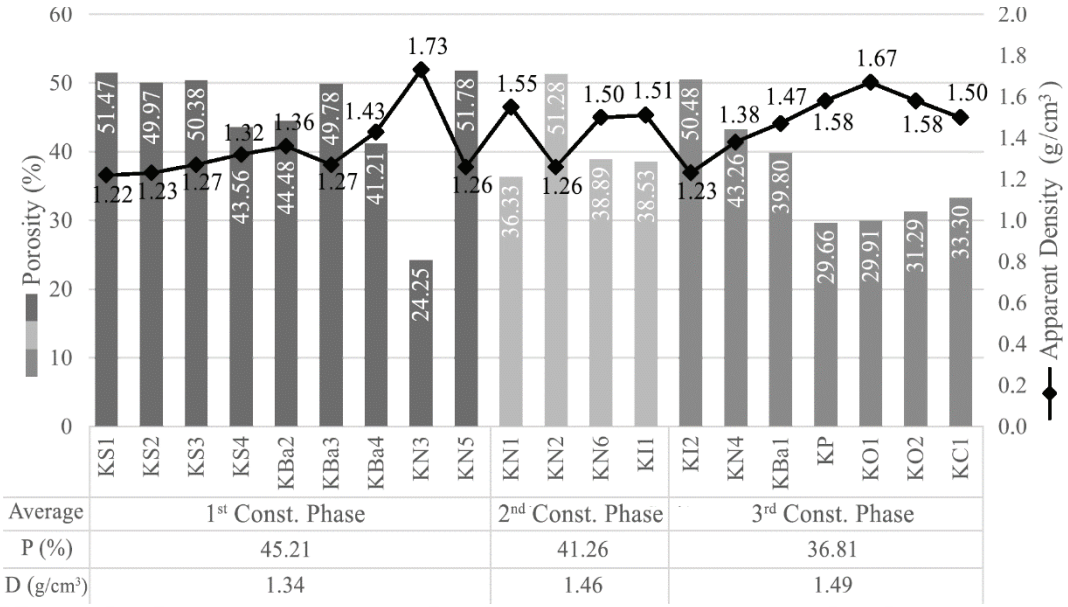


Figure 5.2. Porosity (%) and apparent density (g/cm^3) values of Anaia Church samples from different construction periods

The porosity and apparent density values of bricks from St. Jean Basilica and Anaia Church were in similar ranges with Byzantine bricks from several monuments in Greece (Papayianni and Stefanidou 2000; Stefanidou, Papayianni, and Pachta 2015), from different castle structures in Turkey (Kurugöl and Tekin 2010), from Istanbul (Ulukaya et al. 2017), and from a Monastery in Sicily (Cardiano et al. 2004) (Table 5.1).

Table 5.1. Porosity and apparent density of bricks investigated by recent studies

Location-Reference		**Period of Bricks Samples**	**Apparent Density (g/cm^3)**	**Porosity (%)**
Greece (Stefanidou, Papayianni and Pachta 2015)		Byzantine (7th-14th)	1.46-1.84	-
Greece (Papayianni and Stefanidou 2000)		Byzantine Period	1.38-1.88	14.96-34.87
Castles in Different Cites of Turkey (Kurugöl and Tekin 2010)	Kütahya	Byzantine (8th-14th)	1.33-1.60	32.0-47.4
	Amasra	Byzantine (9th-11th)	1.76-1.81	29.8-33.5
	Trabzon	Byzantine (10th-12th)	1.67-2.05	20.1-34.3
	İstanbul	Byzantine (13th-14th)	1.61-1.83	28.9-36.1
İstanbul/Turkey (Ulukaya, et al. 2017)		Late Byzantine	1.70	31.4-35.3
Monastery of San Filippo di Fragala, Sicily/Italy (Cardiano, et al. 2004)		Byzantine Period	1.52-1.72	31.4-42.6

The saturation coefficient (S) and the pore interconnectivity (A_x) are parameters that vary depending on the total porosity, pore sizes and pore relations. Saturation coefficient value less than 0.80 is an indicator of durability against freezing (ASTM International 2007). The pore interconnectivity depends on microcracks and fissures that occur during the firing process and connect the pores. At higher temperatures, the number of pores that are difficult to reach by water in atmospheric conditions increases in brick structure with the effect of vitrification, resulting in a higher pore interconnectivity value. Bricks with a higher pore interconnectivity value are considered more resistant to deterioration problems caused by salt crystallization and freeze-thaw cycles (Cultrone et al. 2004; Uğurlu Sağın 2017).

The saturation coefficient values of samples from St. Jean Basilica were between 0.71−0.89. The samples with saturation coefficient values less than 0.80 were AG (0.78) from the 1st phase, AB2 (0.79) and AT2 (0.77) from the 2nd phase, and AN (0.71) and AS (0.74) from the 3rd phase. On the other hand, the saturation coefficient values of samples from Anaia Church were between 0.70−0.93, and two samples, one from the 1st phase (KS3) and the other from the 2nd phase (KN6), had the value less than 0.80. In addition, the average of saturation coefficient of 3rd construction period bricks from Anaia Church was found to be higher than the other periods of the church (Table 5.2). Whereas the saturation coefficient values of bricks were in a close range, although there was more sample with a value under 0.80 from St. Jean Basilica bricks than from Anaia Church.

The pore interconnectivity values of samples were found between 2.99−5.51 in the St. Jean Basilica and 1.50−6.47 in the Anaia Church (Table 5.2). The A_x values of bricks used in all construction periods of St. Jean Basilica were found in a similar range. Besides, Anaia Church bricks had higher pore interconnectivity values in the 1st phase, and the values decreased towards 3rd construction phase (Table 5.2). Samples from St. Jean Basilica and from 1st phase of Anaia Church were found to be similar regarding their average pore interconnectivity and higher than samples from 2nd and 3rd phases of Anaia Church.

As a result, it could be evaluated that bricks from St. Jean Basilica and 1st phase of Anaia Church were fired at higher temperatures than bricks from 2nd and 3rd phases of Anaia Church.

Table 5.2. Porosity (P), apparent density (D), saturation coefficient (S), and pore interconnectivity (Ax) values of St. Jean Basilica and Anaia Church bricks

Sample			P (%)	D (g/cm^3)	S	A_x
St. Jean Basilica Ayasuluk Hill, Selçuk	1st Phase (4th-5th c)	AR1	37.39	1.42	0.83	4.73
		AR2	56.19	1.17	0.89	3.50
		AG	32.03	1.64	0.78	3.55
	2nd Phase (520s)	AB1	36.23	1.60	0.81	3.45
		AB2	32.31	1.68	0.79	3.42
		AT1	39.49	1.60	0.83	3.15
		AT2	30.78	1.62	0.77	3.73
	3rd Phase (550s)	AI	53.08	1.24	0.88	3.37
		AN	24.38	1.81	0.71	2.99
		AS	34.33	1.57	0.74	5.51
Anaia Church Kadıkalesi, Kuşadası	1st Phase (5th-6th c.)	KS1	51.47	1.22	0.88	3.28
		KS2	49.97	1.23	0.87	3.62
		KS3	50.38	1.27	0.77	6.47
		KS4	43.56	1.32	0.88	2.91
		KBa2	44.48	1.36	0.85	3.81
		KBa3	49.78	1.27	0.85	4.27
		KBa4	41.21	1.43	0.88	2.64
		KN3	24.25	1.73	0.84	2.08
		KN5	51.78	1.26	0.81	5.53
	2nd Phase (11th-13th c.)	KN1	36.33	1.55	0.92	1.53
		KN2	51.28	1.26	0.88	3.25
		KN6	38.89	1.50	0.70	6.09
		KI1	38.53	1.51	0.89	2.11
	3rd Phase (13th-14th c.)	KI2	50.48	1.23	0.87	3.68
		KN4	43.26	1.38	0.93	1.50
		KBa1	39.80	1.47	0.91	1.84
		KP	29.66	1.58	0.89	1.60
		KO1	29.91	1.67	0.89	1.75
		KO2	31.29	1.58	0.91	1.51
		KC1	33.30	1.50	0.91	1.59

Drying rates of bricks were determined by following decreases in the saturated weights of samples over time. The results were given as graphs regarding flow rate versus time (Figure 5.3, 5.4). The drying rate of bricks depends on the pore size distribution in their structure. The larger pores (>2 μm) in the structure of the bricks induce faster drying (Elert et al. 2003). The results of drying tests indicated that 50% of the absorbed water was evaporated within the first 30 minutes in all samples, which demonstrated that the structure of the bricks mainly consisted of large-sized pores (>2 μm). The pressure on the pore surface caused by the freeze-thaw and salt crystallization reduces in larger pores (Elert et al. 2003; Uğurlu Sağın 2017). The higher amount of large-sized pores in the examined bricks may be accepted as an indicator of their durability to deteriorations caused by freeze-thaw and soluble salts.

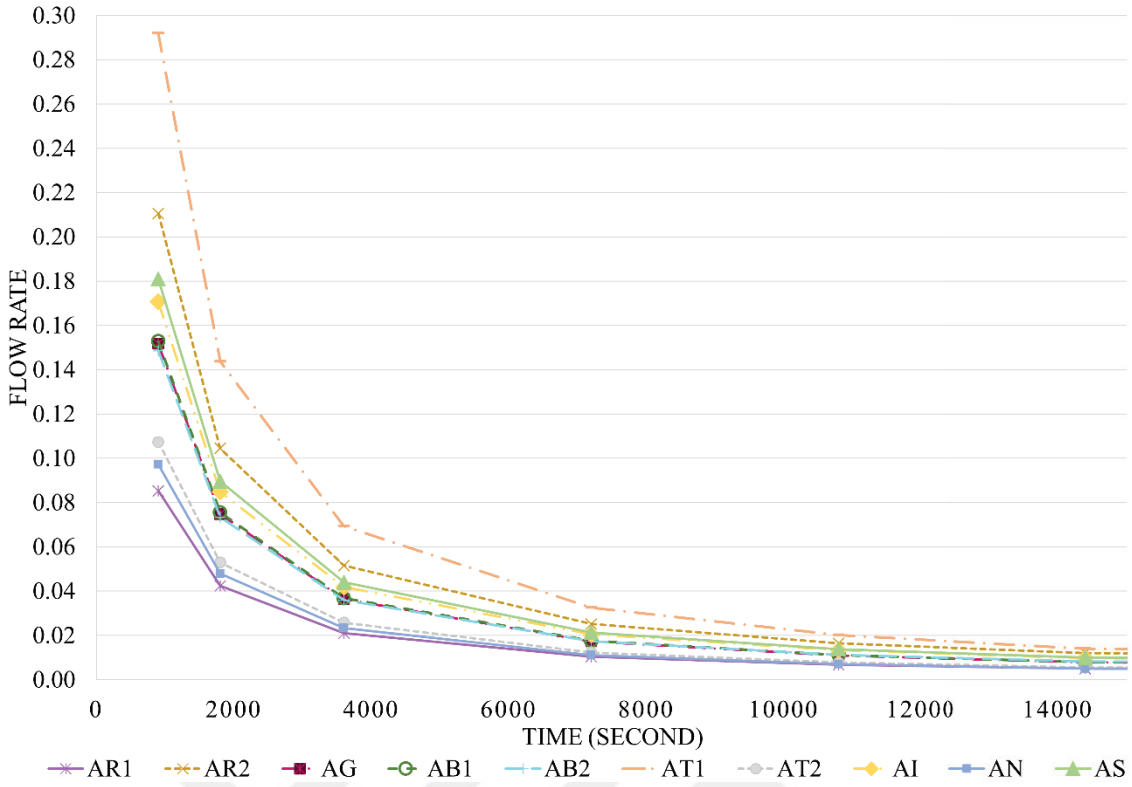


Figure 5.3. Drying rates of bricks from St. Jean Basilica, Ayasuluk Hill

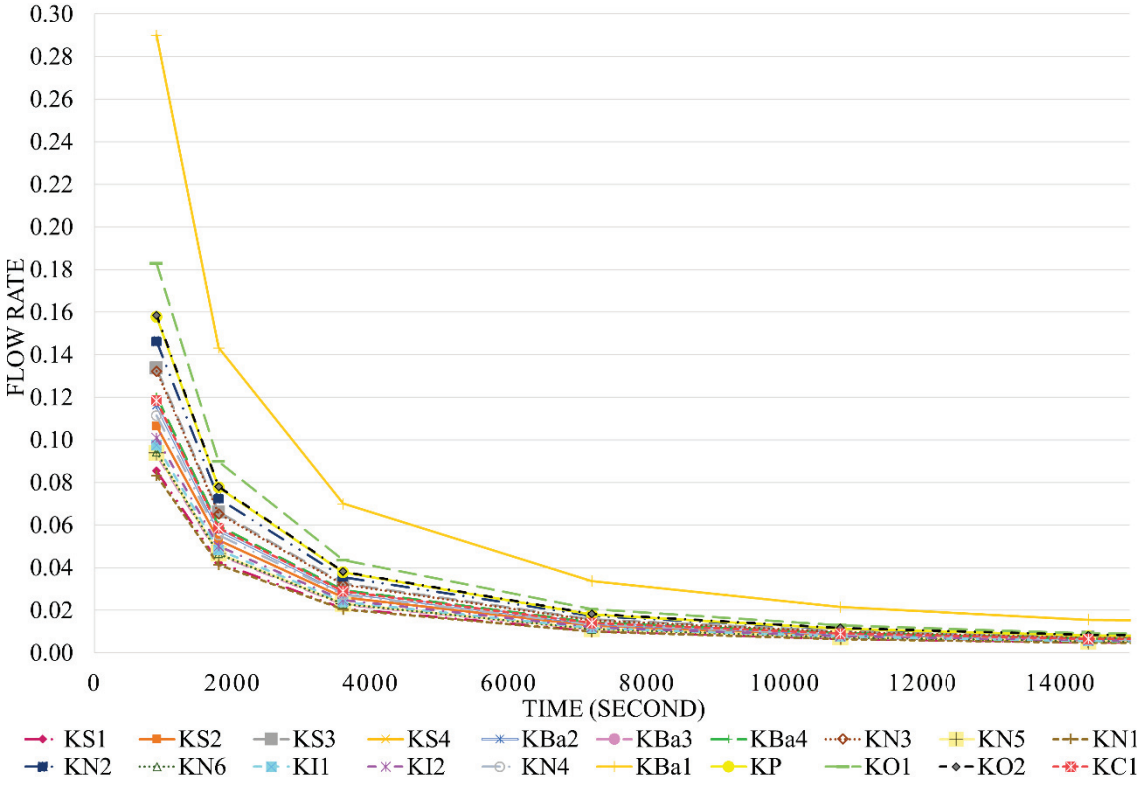


Figure 5.4. Drying rates of bricks from Anaia Church, Kadıkalesi

5.2. Chemical Compositions

The chemical compositions of bricks were investigated by SEM-EDS analysis. Chemical compositions provide information about the possible raw material sources of bricks since the firing process does not alter the chemical compositions (Cultrone et al. 2001; Mommsen 2001).

Generally, historic bricks were produced by using raw materials mainly composed of SiO_2, Al_2O_3, CaO, FeO, MgO, K_2O, Na_2O, and TiO_2 (Fernandes, Lourenço, and Castro 2010). Among these major oxides, SiO_2 and Al_2O_3 were present in brick matrices in high percentages since they are the basic elements of clays (Fernandes, Lourenço, and Castro 2010). Further the SiO_2/Al_2O_3 was used to estimate the ratio of quartz over clay minerals (Monteiro and Vieira 2004; Budak Ünaler 2013; Pérez-Monserrat et al. 2021).

Also, CaO content of clays was accepted as a decisive feature for determination of clay type (Riccardi, Messiga, and Duminuco 1999; Elert et al. 2003; Bartz and Chorowska 2016; Taranto et al. 2019). The clays were classified basically into two groups as calcareous (or Ca-rich) clays which have CaO content above 6%, and non-calcareous (or Ca-poor) clays, which have CaO below 6% (Maniatis and Tite 1981; Moropoulou, Bakolas, and Bisbikou 1995; Taranto et al. 2019). However, some studies indicated that the carbonates of calcareous clays could be originated from CaO and MgO (Monteiro and Vieira 2004; Trindade et al. 2009, 2010). The presence of Fe_2O_3 in clay provides the reddish colour of bricks (Monteiro and Vieira 2004; Pavia 2006; Fernandes, Lourenço, and Castro 2010). The alkaline oxides (K_2O and Na_2O) were determined to improve vitrification since they acted as fluxes (Mirti and Davit 2001; Monteiro and Vieira 2004).

SEM-EDS analyses revealed that bricks from St. Jean Basilica contained high amounts of SiO_2 (47.44−52.32%), Al_2O_3 (18.98−24.80%), FeO (8.44−12.05%) and MgO (3.20−12.16%), and low amounts of CaO (1.42−5.40%), K_2O (2.72−4.49%), Na_2O (0.69−2.77%) and TiO_2 (0.44−0.94%). Bricks of Anaia Church composed of high amounts of SiO_2 (43.61−55.57%), Al_2O_3 (15.19−25.28%), and CaO (8.59−26.33%), moderate FeO (5.29−8.98%) and low amount of MgO (1.98−7.95%), K_2O (2.77−4.50%), Na_2O (0.50−1.60%), and TiO_2 (0.46−0.87%) (Table 5.3). According to these results, the clays of Anaia Church bricks can be classified as Ca-rich or calcareous since bricks have CaO percent more than 6% and the clays of St. Jean Basilica bricks as Ca-poor or non-calcareous by the fact that they contained CaO under 6%.

Table 5.3. Chemical compositions (%) of brick samples determined by SEM-EDS

Sample			SiO_2	Al_2O_3	CaO	FeO	MgO	K_2O	Na_2O	TiO_2
St. Jean Basilica Ayasuluk Hill, Selçuk	1st Phase (4th-5th c.)	AR1	47.44 ±0.47	18.98 ±0.30	3.64 ±0.08	11.70 ±0.56	11.07 ±0.17	3.66 ±0.17	2.77 ±0.18	0.74 ±0.13
		AR2	48.79 ±0.60	20.06 ±0.22	3.24 ±0.15	11.94 ±0.68	10.58 ±0.14	3.29 ±0.15	1.25 ±0.14	0.84 ±0.10
		AG	51.99 ±0.23	24.80 ±0.31	2.35 ±0.11	11.01 ±0.26	3.20 ±0.29	4.44 ±0.07	1.29 ±0.12	0.91 ±0.11
	2nd Phase (520s)	AB1	51.34 ±0.33	20.70 ±0.27	1.48 ±0.10	11.29 ±0.36	10.82 ±0.36	2.79 ±0.18	0.84 ±0.07	0.74 ±0.08
		AB2	50.43 ±1.19	21.67 ±0.83	2.59 ±0.10	11.77 ±0.34	8.10 ±0.07	3.14 ±0.12	1.49 ±0.10	0.83 ±0.06
		AT1	49.79 ±0.52	18.49 ±0.29	5.40 ±0.31	11.05 ±0.43	10.46 ±0.28	3.26 ±0.02	0.69 ±0.09	0.87 ±0.26
		AT2	52.32 ±0.63	22.39 ±0.18	1.42 ±0.07	11.03 ±0.15	7.79 ±0.48	3.34 ±0.19	0.99 ±0.07	0.73 ±0.23
	3rd Phase (550s)	AI	47.49 ±0.49	19.48 ±0.31	3.36 ±0.05	11.99 ±0.25	12.16 ±0.10	3.35 ±0.27	1.23 ±0.13	0.94 ±0.32
		AN-a	50.34 ±0.12	20.69 ±0.14	4.04 ±0.16	11.48 ±0.29	8.93 ±0.07	2.72 ±0.12	0.95 ±0.23	0.85 ±0.11
		AN-b	51.97 ±0.54	21.10 ±0.48	1.61 ±0.17	12.05 ±0.19	8.92 ±0.08	2.75 ±0.12	1.15 ±0.22	0.44 ±0.17
		AS	49.31 ±0.21	21.43 ±0.75	4.78 ±0.45	8.44 ±0.12	8.91 ±0.12	4.49 ±0.06	2.07 ±0.18	0.56 ±0.19
Anaia Church Kadıkalesi, Kuşadası	1st Phase (5th-6th c.)	KS1	46.97 ±0.20	23.61 ±0.28	12.21 ±0.19	8.81 ±0.51	2.74 ±0.13	3.81 ±0.07	1.16 ±0.25	0.69 ±0.06
		KS2	47.61 ±0.27	24.19 ±0.22	10.68 ±0.15	8.96 ±0.32	2.55 ±0.04	4.14 ±0.18	1.17 ±0.07	0.71 ±0.11
		KS3	52.93 ±0.22	20.34 ±0.35	12.26 ±0.24	6.9 ±0.23	2.24 ±0.08	3.3 ±0.10	1.29 ±0.07	0.74 ±0.11
		KS4	49.47 ±0.56	23.89 ±0.23	9.52 ±0.10	8.44 ±0.14	2.49 ±0.05	4.5 ±0.09	1.08 ±0.09	0.62 ±0.23
		KBa2	49.19 ±0.47	24.47 ±0.66	8.59 ±0.22	8.98 ±0.46	2.19 ±0.19	4.18 ±0.15	1.54 ±0.16	0.86 ±0.05
		KBa3	48.28 ±0.72	22.92 ±0.40	11.44 ±0.18	8.39 ±0.15	3.61 ±0.15	3.38 ±0.08	1.27 ±0.14	0.71 ±0.12
		KBa4	44.94 ±0.47	17.06 ±0.11	22.16 ±0.32	5.93 ±0.12	4.87 ±0.22	3.56 ±0.12	0.81 ±0.12	0.66 ±0.07
		KN3	43.81 ±0.29	15.22 ±0.33	26.33 ±0.28	5.85 ±0.09	4.11 ±0.17	3.49 ±0.05	0.55 ±0.02	0.65 ±0.17
		KN5	47.99 ±0.24	22.19 ±0.52	13.76 ±0.18	8.4 ±0.19	2.56 ±0.23	2.77 ±0.14	1.60 ±0.10	0.73 ±0.06
	2nd Phase (11th-13th c.)	KN1	45.03 ±1.43	15.19 ±0.10	24.96 ±0.71	5.74 ±0.44	4.88 ±0.33	2.97 ±0.02	0.78 ±0.05	0.46 ±0.08
		KN2	48.86 ±0.19	25.28 ±0.33	9.70 ±0.33	8.55 ±0.14	2.21 ±0.02	3.46 ±0.03	1.40 ±0.10	0.55 ±0.20
		KN6	55.57 ±0.51	19.58 ±0.53	9.64 ±0.16	7.75 ±0.23	1.98 ±0.19	3.61 ±0.02	1.24 ±0.05	0.63 ±0.17
		KI1	43.87 ±0.99	15.99 ±0.75	23.64 ±0.35	5.29 ±0.11	5.29 ±0.13	4.18 ±0.12	1.11 ±0.03	0.63 ±0.09
	3rd Phase (13th-14th c.)	KI2	48.75 ±0.46	23.46 ±0.43	11.22 ±0.13	8.39 ±0.37	2.64 ±0.22	3.66 ±0.09	1.10 ±0.11	0.78 ±0.06
		KN4	48.67 ±0.39	23.87 ±0.17	10.45 ±0.33	8.47 ±0.35	2.39 ±0.03	4.10 ±0.10	1.17 ±0.05	0.87 ±0.07
		KBa1	43.61 ±0.51	17.11 ±0.20	21.54 ±0.20	7.16 ±0.24	5.82 ±0.13	3.25 ±0.11	0.74 ±0.13	0.77 ±0.09
		KP	44.64 ±0.44	16.74 ±0.50	19.78 ±0.11	6.04 ±0.28	7.95 ±0.22	3.22 ±0.18	0.93 ±0.11	0.69 ±0.08
		KO1	43.76 ±0.39	16.61 ±0.31	22.33 ±0.53	6.11 ±0.31	5.15 ±0.29	4.29 ±0.11	1.00 ±0.16	0.74 ±0.08
		KO2	43.80 ±0.34	16.36 ±0.12	23.82 ±0.61	6.39 ±0.25	4.91 ±0.26	3.48 ±0.08	0.50 ±0.20	0.73 ±0.10
		KC1	43.93 ±0.34	18.06 ±1.00	21.32 ±0.18	6.38 ±0.46	4.75 ±0.34	3.95 ±0.29	0.91 ±0.06	0.70 ±0.17

The chemical compositions of bricks from St. Jean Basilica were in a similar range with Hagia Sophia Bricks from Byzantine Period (Taranto et al. 2019) (Table 5.4). Also, the composition of Anaia bricks with CaO content between 8.6–13.8% was similar to Roman bricks from Nysa (Uğurlu Sağın 2017), Byzantine bricks from Kütahya and Trabzon fortifications (Kurugöl and Tekin 2010), Monastery of San Filippo di Fragala, Sicily (Cardiano et al. 2004), and Hagia Sophia (Taranto et al. 2019). As well, the group of Anaia bricks with the highest CaO percentage (19.78−26.33%) was observed in a similar range with Era Bath bricks from Roman Period (Oguz, Turker, and Kockal 2014) and bricks of a monument from Byzantium in İstanbul (Ulukaya et al. 2017) (Table 5.4).

Table 5.4. Chemical compositions of bricks investigated by recent studies

Period	Location-Reference		Chemical Composition (%)									
			Method	SiO_2	Al_2O_3	CaO	Fe_2O_3	MgO	Na_2O	K_2O	TiO_2	Other
Roman	Nysa, Aydın/Turkey (Uğurlu Sağın 2017)		XRF	48.0-50.3	18.4-22.5	4.5-10.4	6.2-8.3	3.2-5.1	0.5-0.8	2.9-3.9	0.9-1.0	-
	Era Bath, Myra/Turkey (Oguz, Turker and Kockal 2014)		SEM-EDS	45.5	16	22.8	6.9	4.3	1.8	2.4	-	-
Byzantine	Hagia Sophia, İstanbul/Turkey (Taranto, et al. 2019)		XRF	39.0-64.1	11.7-19.9	1.3-19.0	7.1-12.6	2.4-9.1	0.8-1.7	1.1-3.2	0.6-1.4	0.2-2.8
	Castles/Turkey (Kurugöl and Tekin 2010)	Kütahya	ICP	49.1-50.4	15.3-19.3	7.8-9.7	5.3-6.4	4.1-5.6	0.6-0.8	3.2-3.6	0.7-0.8	0.2-0.3
		Trabzon		56.7-60.2	13.1-13.3	7.0-9.1	6.5-8.0	2.4-3.3	0.8-1.3	1.2-1.3	0.9-1.0	0.5-0.6
	İstanbul/Turkey (Ulukaya,et al. 2017)		XRF	48.4	14	23.1	7.7	2.4	1.1	2	-	-
	Monastery of San Filippo di Fragala, Sicily/Italy (Cardiano, et al. 2004)		ICP & INAA	50-60	15-19	1-12	5-8	1-2	~1	3-4	<1	-

Chemical compositions of bricks can also give information about the provenance of raw material sources used for their production. Major oxide compositions of investigated bricks showed that they could be distinguished from each other by their CaO and FeO contents. CaO contents of bricks were observed to be set in three groups regardless of construction periods. Bricks of St. Jean Basilica comprised CaO ranging between 1.42–5.40%. A group of Anaia Church bricks (KS1, KS2, KS3, KS4, KBa2, KBa3, KN5, KN2, KN6, KI2, KN4) contained CaO in the range of 8.59−13.76%, while the rest of them (KBa4, KN3, KN1, KI1, KBa1, KP, KO1, KO2, KC1) had CaO content ranging between 19.78−26.33%. Besides, FeO percentages of St. Jean Basilica bricks (8.44–12.05%) were found to be higher than Anaia bricks (5.26–8.98%).

Moreover, multivariate statistical analysis was implemented in order to classify the brick samples into homogenous groups which have similar chemical compositions and to distinguish them from those which are significantly different. For this purpose, Hierarchical Cluster Analysis and one-way ANOVA were employed by using IBM SPSS Statistics software program.

First, all bricks were analysed by hierarchical cluster analysis based on their major oxide percentages. SiO_2, Al_2O_3, CaO, FeO, MgO, K_2O, Na_2O, and TiO_2 were processed together for evaluation of bricks according to the statistically significant similarities and differences of their compositions. The results revealed three main clusters (Figure 5.5). Samples from Anaia Church constituted Cluster 1 (KN4, KI2, KS2, KBa3, KS1, KS4, KBa2, KN2, KN5, KS3, KN6) and Cluster 3 (KN3, KN1, KI1, KO2, KBa4, KO1, KC1, KBa1, KP), while Cluster 2 was comprised of all samples from St. Jean Basilica.

Furthermore, to determine oxides that were decisive for the division of the clusters and to support cluster analysis, one-way ANOVA was applied to oxides one by one. ANOVA test provided the mean of oxides for each cluster, the F value and the p-value that indicate the differences between variables. It is assumed that there are significant differences between groups if the F has a higher value and the p-value is less than the 0.05 significance level.

According to results of ANOVA tests, oxides which have p-value under 0.05 were found as SiO_2, Al_2O_3, CaO, FeO, MgO and Na_2O (Table 5.5). Furthermore, the highest F value was determined in CaO (374.6) and FeO (117.7). These results revealed that the clusters generated by hierarchical cluster analysis were robust. The significant differences between clusters originated from CaO and FeO mainly, and respectively MgO, Al_2O_3, SiO_2, Na_2O. However, the mean values demonstrated that Na_2O provided a distinction just between Cluster 1-2 and Cluster 3. Also, it was observed that K_2O and TiO_2 were not distinctive oxides between the clusters (Table 5.5).

Consequently, multivariate statistical analyses revealed that bricks of St. Jean Basilica were produced with clay extracted from the same source for three construction periods, whereas Anaia Church bricks were manufactured from two different raw clay sources for centuries.

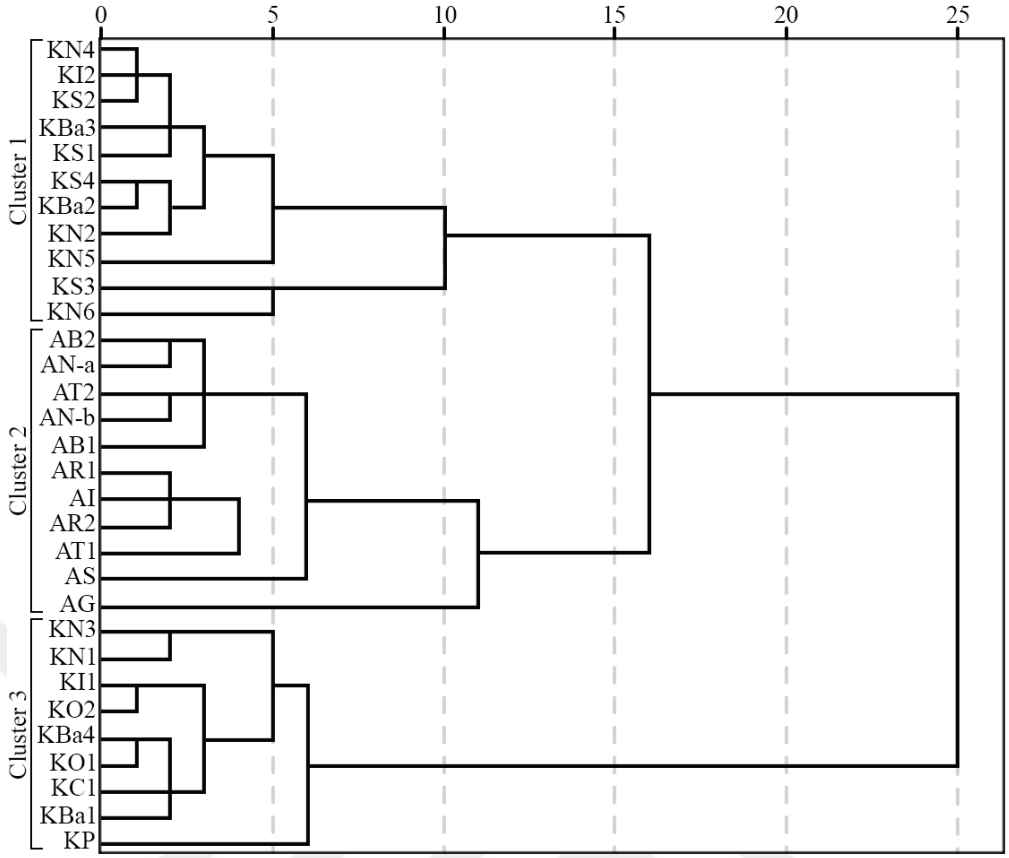


Figure 5.5. Dendrogram of Hierarchical Cluster Analysis

Table 5.5. Mean, F and P values obtained by ANOVA test (P-value is represented with *** if it was lower than 0.01, ** if it was lower than 0.05, and * if it was lower than 0.1)

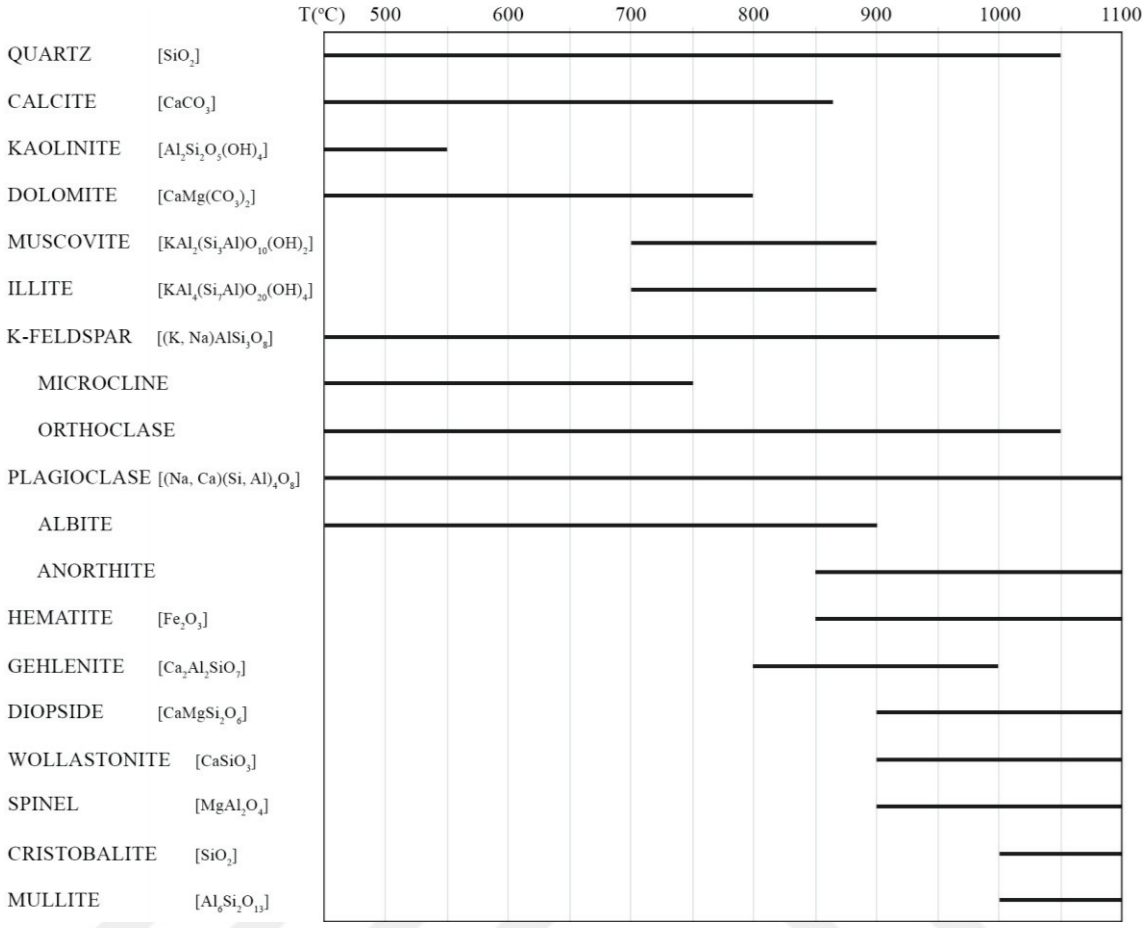
Values / Oxides	Mean			F	P-value
	Cluster 1	Cluster 2	Cluster 3		
CaO	10.9%	3.1%	22.9%	374.6	***<0.001
FeO	8.4%	11.2%	6.1%	117.7	***<0.001
MgO	2.5%	9.2%	5.3%	49.9	***<0.001
Al_2O_3	23.1%	20.9%	16.5%	45.3	***<0.001
SiO_2	49.5%	50.1%	44.1%	29.8	***<0.001
Na_2O	1.3%	1.3%	0.8%	5.2	**0.012
TiO_2	0.7%	0.8%	0.7%	1.7	0.205
K_2O	3.7%	3.4%	3.6%	1.1	0.34

5.3. Mineralogical Compositions

The mineralogical composition of bricks was determined using X-ray Diffractometer (XRD) and Fourier Transform Infrared Spectrometry (FTIR). XRD and FTIR methods were used in combination in order to obtain adequate accuracy in mineralogical compositions. Mineralogical compositions were also used to estimate the firing temperatures of bricks.

Firing temperatures lead to mineralogical modifications in raw materials of bricks (Table 5.6). One of the early reactions observed due to temperature is the decomposition of kaolinite ($Al_2Si_2O_5(OH)_4$) at 550°C (Cultrone et al. 2001; El Ouahabi et al. 2015). In bricks made of calcareous clays, dolomite ($CaMg(CO_3)_2$) disappears at 800°C (Cultrone et al. 2001; Rat'ko et al. 2011), while calcite ($CaCO_3$) can be observed above 800°C and begins to decompose around 870°C (Cultrone et al. 2001; Uğurlu Sağın 2017). With the decomposition of these minerals, new mineral phases occur at higher temperatures. Gehlenite ($Ca_2Al_2SiO_7$) appears at 800°C as a result of a reaction between calcite and illite, and it is observed up to 1000°C (Cultrone et al. 2001; Cardiano et al. 2004). Diopside ($CaMgSi_2O_6$) is found in calcareous bricks between 900 to 1050°C (Cardiano et al. 2004). On the other hand, hematite (Fe_2O_3), an indicator of firing temperature in non-calcareous bricks, forms at 850°C (Bartz and Chorowska 2016; Cardiano et al. 2004; Uğurlu Sağın and Böke 2013). Feldspars, both plagioclase and K-feldspars, are stable up to higher temperatures. K-feldspars are observed to increase in quantity at 900°C and to disappear above 1000°C (Pavia 2006; El Ouahabi et al. 2015). Plagioclase feldspars (such as albite, anorthite, etc.) can be found in brick matrices below 1100°C (El Ouahabi et al. 2015; Scatigno et al. 2018). Albite ($NaAlSi_3O_8$) begins to change phase above 900°C (Riccardi, Messiga, and Duminuco 1999; Tekin and Kurugöl 2011); whereas anorthite ($CaAl_2Si_2O_8$) forms at 850°C (Cardiano et al. 2004; Uğurlu Sağın 2017). High-temperature mineral phases, wollastonite ($CaSiO_3$) (Cultrone et al. 2004; Pavia 2006; Uğurlu Sağın and Böke 2013) and spinel ($MgAl_2O_4$) (Pavia 2006; El Ouahabi et al. 2015) begin to form at temperatures around 900-1000°C. Quartz (SiO_2), which is found in raw clays, exists up to 1050°C. The modification of quartz to cristobalite (SiO_2) begins to be observed at temperatures around 1000°C (El Ouahabi et al. 2015). Muscovite/illite forms at 700°C, begins to decompose above 900°C and completely transforms into mullite ($Al_6Si_2O_{13}$) above 1000°C (El Ouahabi et al. 2015; Uğurlu Sağın 2017; Scatigno et al. 2018).

Table 5.6. Temperature thresholds of mineralogical transformations



XRD analyses were conducted on powdered brick samples and scanned between 5-60 2θ° with Cu Kα radiation. The diffraction patterns were depicted in Table 5.6–5.9.

According to XRD results, St. Jean Basilica bricks mainly consisted of quartz, albite, coesite, hematite and spinel (Figure 5.6, 5.7). Albite, hematite and spinel were the minerals formed in the bricks structure with the effect of firing. Coesite (SiO_2) is a formation of quartz that occurs at high pressure and a temperature range of 500-800°C (Worrall 1986). It was considered that the presence of coesite in the samples originated from the raw clay as a natural formation that occurred by geological movements because the pressing under high pressure was not implemented as a shaping method in Byzantium. Also, muscovite, calcite, anorthite, and diopside were detected in some of the St. Jean Basilica samples as a result of firing. Calcite was determined in three bricks with the highest CaO percentage (AT1: 5.40%, AN: 4.04%, and AS: 4.78%) among St. Jean Basilica bricks; also, anorthite was only present in AT1.

The main mineral phases detected on the XRD patterns of Anaia Church bricks were quartz, calcite and muscovite. In addition, albite, anorthite, hematite, magnetite, gehlenite, dolomite and diopside were determined in some samples (Figure 5.8–5.10). Magnetite (Fe_3O_4) is an iron oxide that occurs due to the firing kiln atmosphere. It is formed by the reduction of hematite as a result of the loss of oxygen in the kiln (Gredmaier, Banks, and Pearce 2011; Tarhan and Işık 2020). Dolomite and calcite were the carbonates that existed in Anaia Church bricks since they contained CaO in high percentages. In addition, iron oxides, such as hematite and magnetite, were detected only in the bricks of Cluster 1 (CaO: <20%) among the Anaia Church samples, most probably because of the higher percentages of carbonates in Cluster 3 (CaO: >20%) preventing the formation of iron oxides (Cultrone, Sidraba, and Sebastián 2005; Pavia 2006).

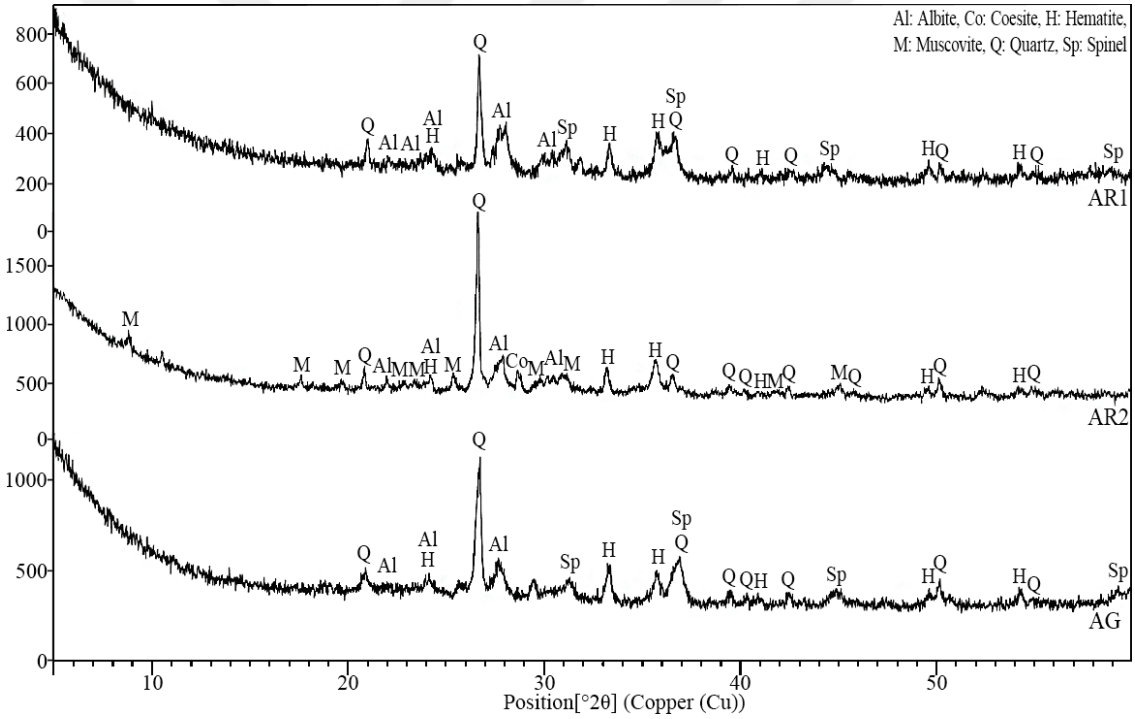


Figure 5.6. XRD spectra of bricks from 1st phase (AR1, AR2, AG) of St. Jean Basilica

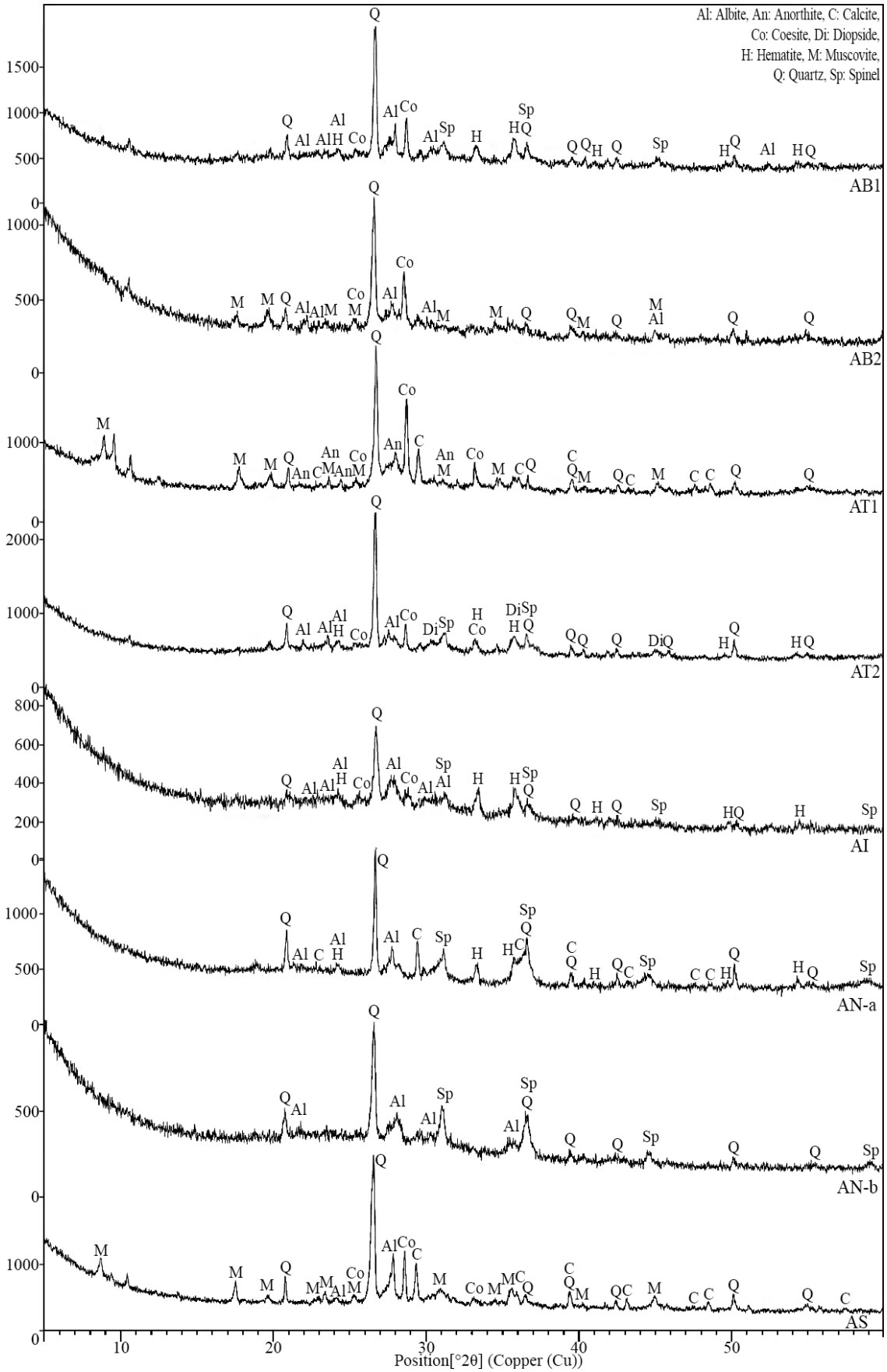


Figure 5.7. XRD spectrum of bricks from 2nd phase (AB1, AB2, AT1, AT2) and 3rd phase (AI, AN, AS) of St. Jean Basilica

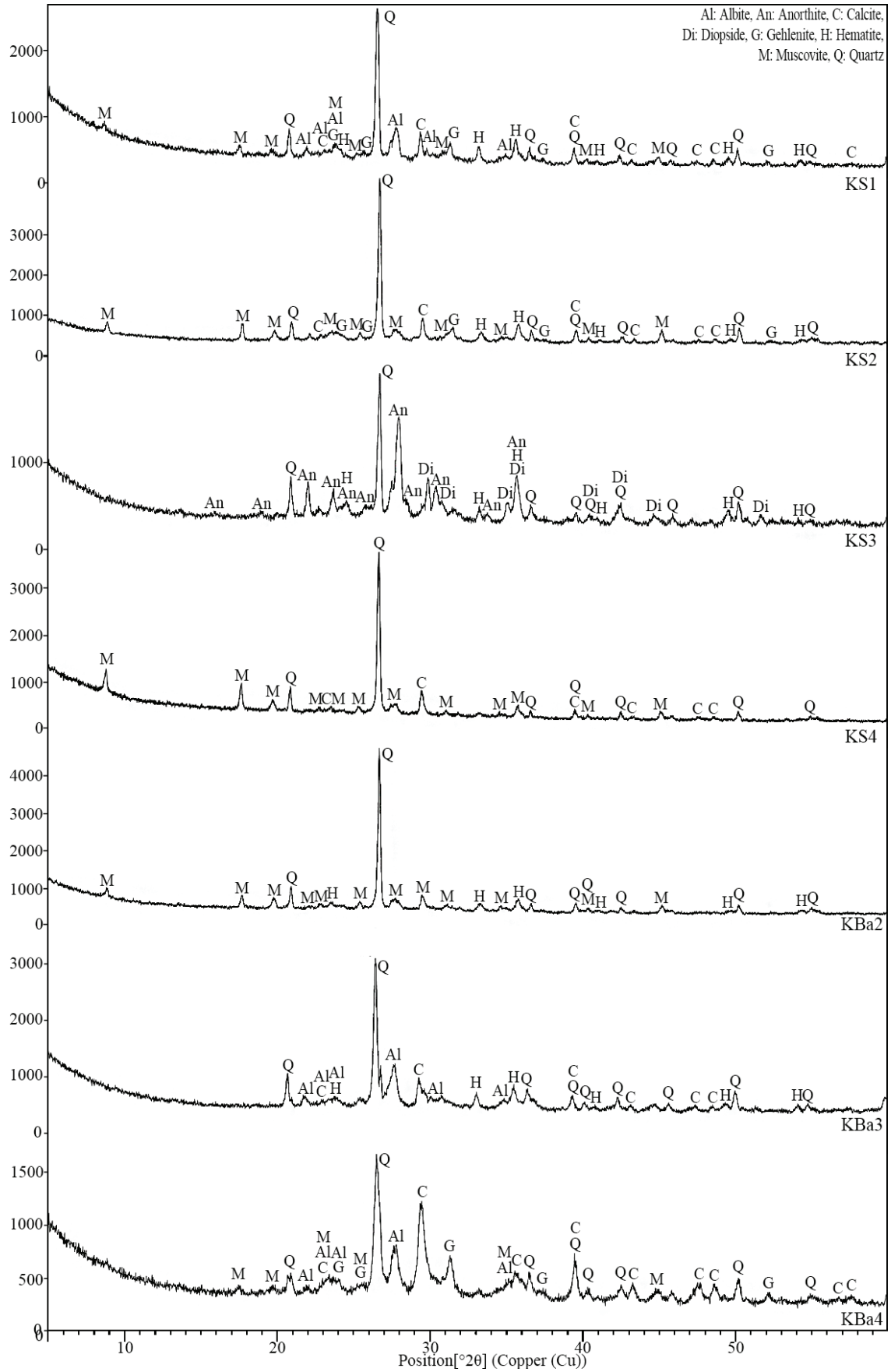


Figure 5.8. XRD spectrum of bricks from 1st phase (KS1, KS2, KS3, KS4, KBa2, KBa3, KBa4) of Anaia Church

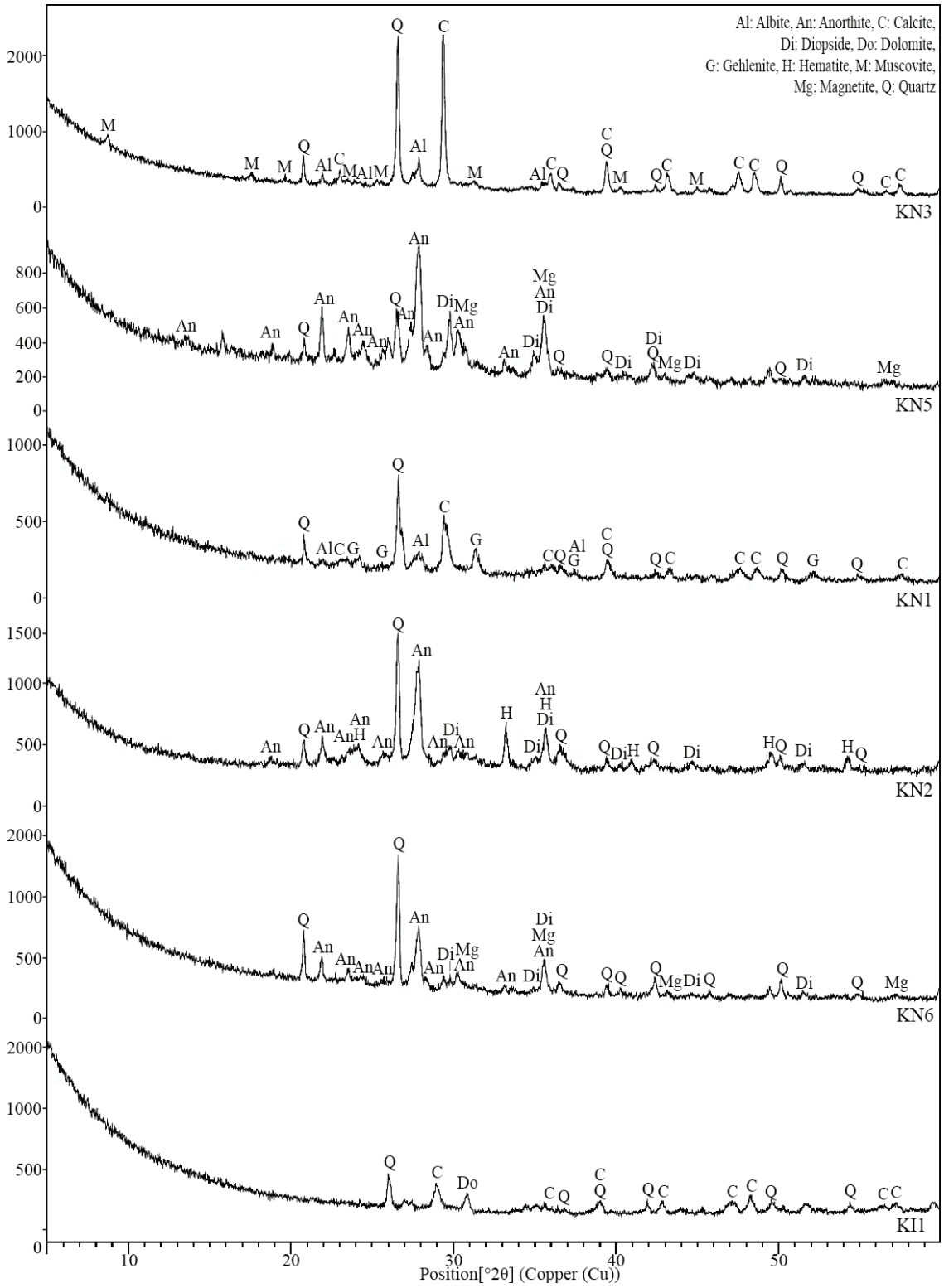


Figure 5.9. XRD spectrum of bricks from 1st phase (KN3, KN5) and 2nd phase (KN1, KN2, KN6, KI1) of Anaia Church

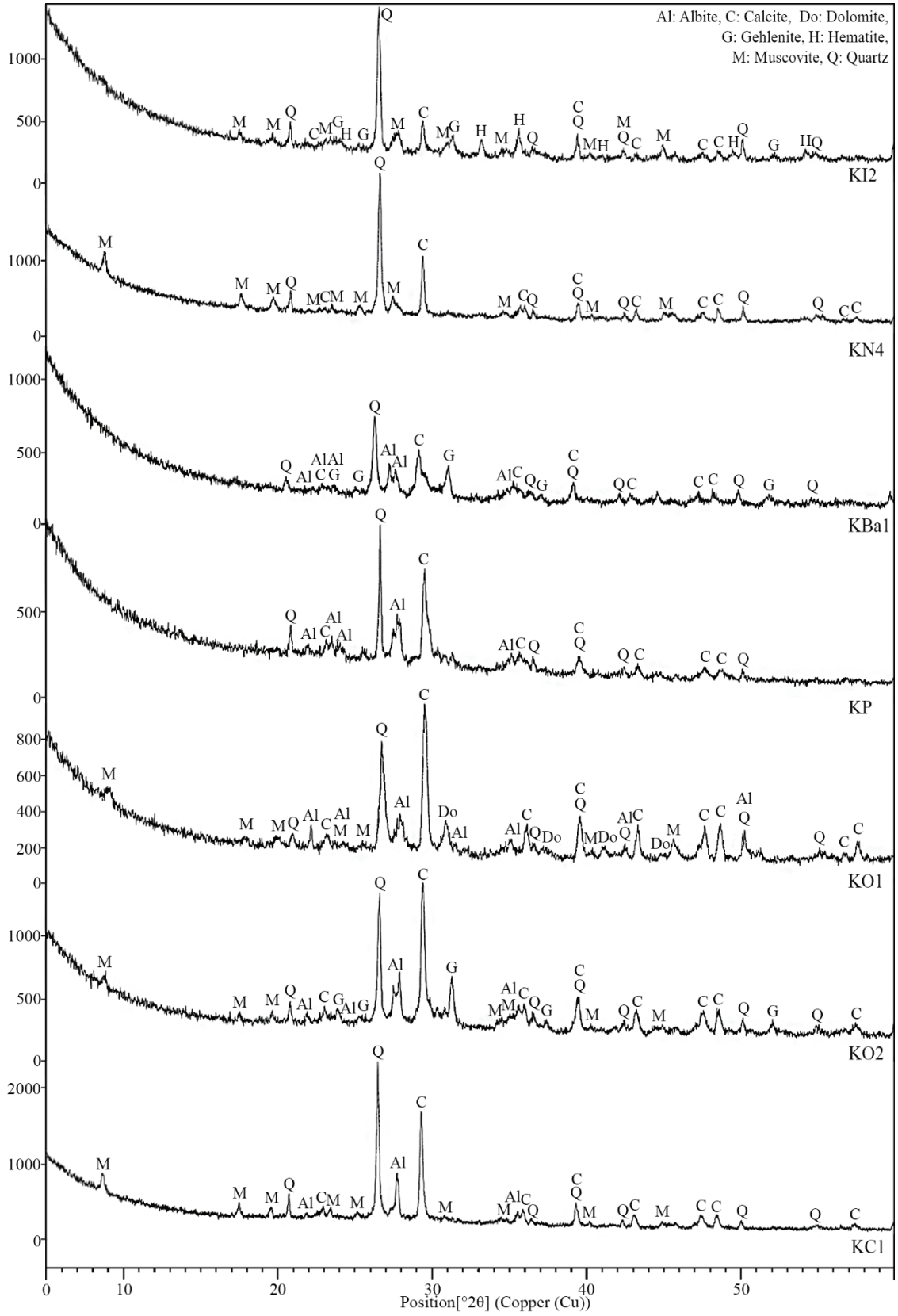


Figure 5.10. XRD spectrum of bricks from 3rd phase (KI2, KN4, KBa1, KP, KO1, KO2, KC1) of Anaia Church

FTIR spectra of powdered form of each sample were obtained in the wavenumber range from 4000 cm^{-1} to 400 cm^{-1}. The FTIR spectra of samples and the functional groups according to the vibrational wave numbers were depicted in Table 5.7, Figure 5.11–5.14.

The peaks of O-H stretching at 3422−3448 cm^{-1} and H-O-H bending at 1630−1645 cm^{-1} observed in all samples indicated absorbed water (Gadsden 1975; Uğurlu Sağın 2017; Şerifaki 2017; Kumar Mishra, Mishra, and Anshumali 2021). Quartz was detected in different absorption regions of spectra of samples. The characteristic peak of Si-O stretching mode at 1020−1084 cm^{-1} (Maritan et al. 2006; Dhanapandian, Gnanavel, and Ramkumar 2009; Uğurlu Sağın 2017), doublet peaks at 796−798 cm^{-1} and 774−779 cm^{-1} (Gadsden 1975; De Benedetto et al. 2002), peaks at 691−695 cm^{-1}, 503−514 cm^{-1} (Gadsden 1975), and peak of Si-O-Si symmetric bending at 456−485 cm^{-1} (Uğurlu Sağın 2017) were attributed to quartz. The absorption bands in the region 2514−2517 cm^{-1} and 1793−1797 cm^{-1} that are associated with calcite (Gadsden 1975) were observed in some samples from Kadıkalesi (as KBa4, KN3, KN1, KBa1, KO1, KO2, KP, KC1) (Figure 5.13, 5.14). As the other signs of calcite, the peaks at 1384−1385 cm^{-1}, 874−877 cm^{-1} and 713−720 cm^{-1} (Gadsden 1975; Maritan et al. 2006) were detected generally in samples from Anaia Church, while the peaks of $(CO_3)^{-2}$ stretching mode of calcite at 1430−1455 cm^{-1} (Uğurlu Sağın 2017; Şerifaki 2017) were detected in the majority of samples (Figure 5.11–5.14). The shoulder observed at 884−890 cm^{-1} in the samples, namely AR2, AB1, AI, and weak absorption peak of AR1, AI, and KBa3 at 728−731 cm^{-1} may be attributed to the dolomite. The presence of a band at 647−649 cm^{-1} in the bricks (AR1, AB1, AB2, AS, KBa1, KO1, KC1) was due to albite (Gadsden 1975). The peaks that occurred in the region 621-622 cm^{-1}, 573−584 cm^{-1} and 530−540 cm^{-1} are assigned to anorthite (Gadsden 1975). The peaks in this region were observed in samples of Anaia Church, namely KS3, KN5, KN2, and KN6. In the samples, the presence of FeO as hematite may be explained by peaks at 556−558 cm^{-1} (Gadsden 1975) and also peaks around 540 cm^{-1} and 580 cm^{-1} (Dhanapandian, Gnanavel, and Ramkumar 2009; Kumar Mishra, Mishra, and Anshumali 2021), however, these last couple of regions overlap with anorthite vibrations.

Table 5.7. Functional groups and their vibrational wavenumbers (cm^{-1}) determined in FTIR spectra of brick samples

Vibrational Wavenumbers (cm^{-1})			3422-3448	2514-2517	1793-1797	1630-1648	1430-1455 1384-1385	1020-1084	874-877	884-890	796-798	774-779	728-731	713-720	691-695	647-649	621-622	573-584	530-540	580	556-558	503-514	456-485
Peak characteristics									shoulder	shoulder	dublet						triplet					shoulder	
Samples \ Minerals			O-H stretching of absorbed water	Calcite	Calcite	H-O-H bending of absorbed water	$(CO3)^{2-}$ stretching of Calcite	Si-O stretching of Quartz	Calcite	Dolomite	Symmetrical stretching of Quartz	Si-O stretching of Quartz	Dolomite	Calcite	Quartz	Albite	Anorthite	Si-O-Al stretching of Anorthite		Hematite	Hematite	Quartz	Si-O-Si bending of Quartz
St. Jean Basilica, Ayasuluk	1st Phase (4th-5th)	AR1	3429			1639	1384	1073			797	778	730			648				579		508	466
		AR2	3423			1638		1043		884		779			691							503	473
		AG	3437			1639	1451	1081			797	778			695					580			464
	2nd Phase (520s)	AB1	3423			1639		1080		885	796	779			695	649							471
		AB2	3431			1648		1023			796					647							460
		AT1	3431			1637	1438	1022	877			778			693								469
		AT2	3422			1639		1076			797	779			691								465
	3rd Phase (550s)	AI	3429			1641		1062		890	798	778	731									509	470
		AN-a	3427			1640	1438	1081			797	779			693								465
		AN-b	3434			1642		1079			797	778			693								468
		AS	3438			1640	1438, 1385	1040	877			779		717	695	649							474
Anaia Church, Kadikalesi	1st Phase (5th-6th c.)	KS1	3425			1638	1432	1038			796	778		714	695						556		485
		KS2	3438			1637	1438	1038				778			693						557		484
		KS3	3437			1639		1078			797	778			695		621	584	536			511	461
		KS4	3432			1643	1446	1036	877		797	779		717	695						556		482
		KBa2	3427			1642	1441	1046			797	779		720							558		484
		KBa3	3429			1645	1455	1084			798	778	729		695					578		514	462
		KBa4	3423	2516	1793	1637	1433	1027	874		796			713	693								464
		KN3	3422	2514	1795	1636	1430	1030	875			777		713									472
		KN5	3445			1634		1045									621	573	538				465
	2nd Phase (11th-13th c.)	KN1	3423	2515	1794	1636	1434	1022	874		796			713	694								465
		KN2	3448			1636		1038				774			692		622	574	540				466
		KN6	3460			1630	1434	1076			796	777			694		622	575	539				466
		KI1	3422	2517		1638	1427	1029	875		800			713									473
	3rd Phase (13th-14th c.)	KI2	3424			1639	1438	1050			796	778		713	694						558		483
		KN4	3423			1638	1438	1038	876		797	778		713	695						557		472
		KBa1	3423	2514	1794	1637	1449	1026	875		797	779		714	695	648							472
		KO1	3424	2516	1797	1630	1438	1035	876			778		713		647			530				474
		KO2	3423	2515		1639	1438	1025	876			778		714									456
		KP	3424	2517		1639	1438	1020	875			776		714									456
		KC1	3434	2514	1796	1638	1434	1037	876			778		713		648							479

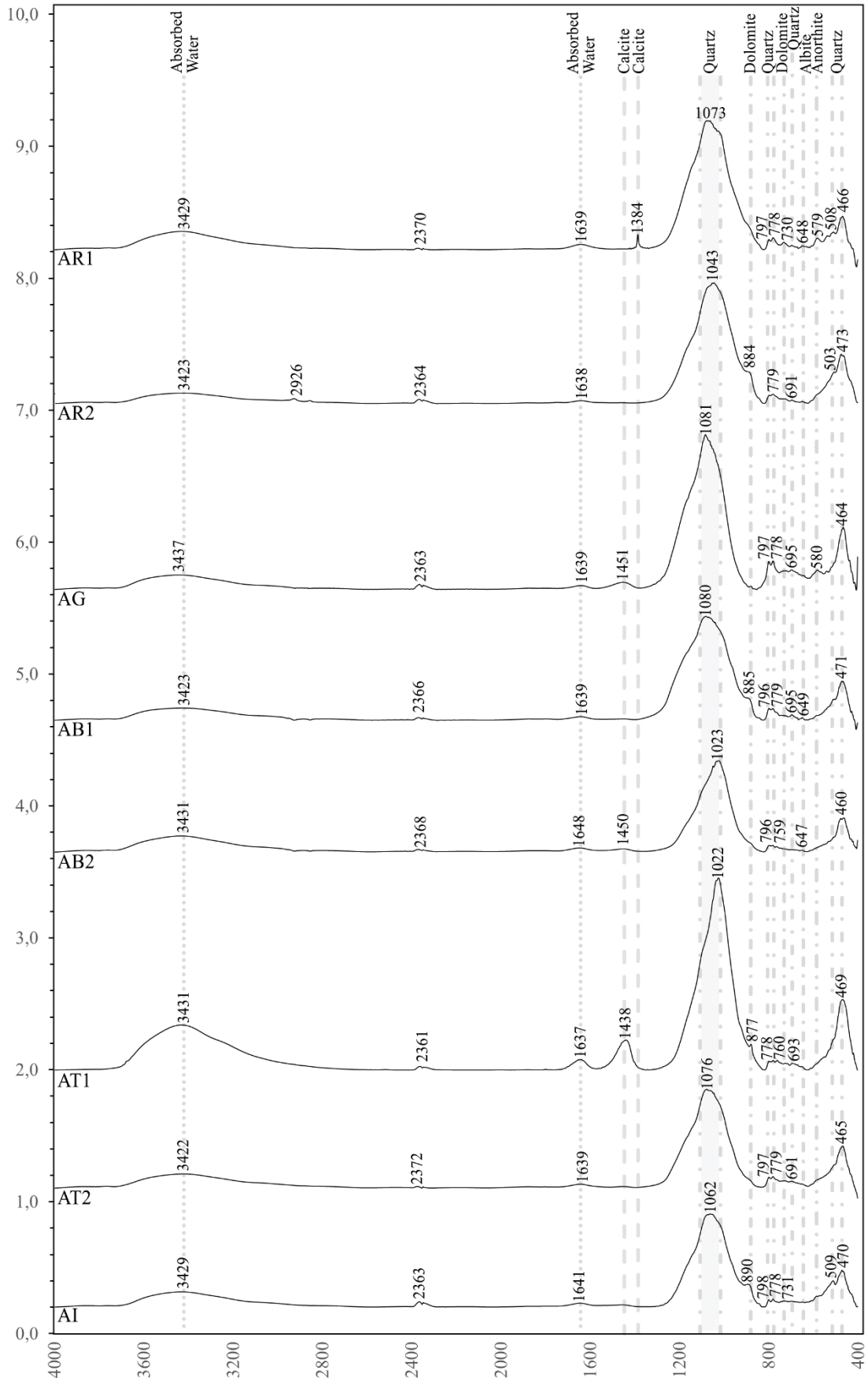


Figure 5.11. FTIR spectra of brick samples from 1st (AR1, AR2, AG), 2nd (AB1, AB2, AT1, AT2) and 3rd (AI) periods of St. Jean Basilica

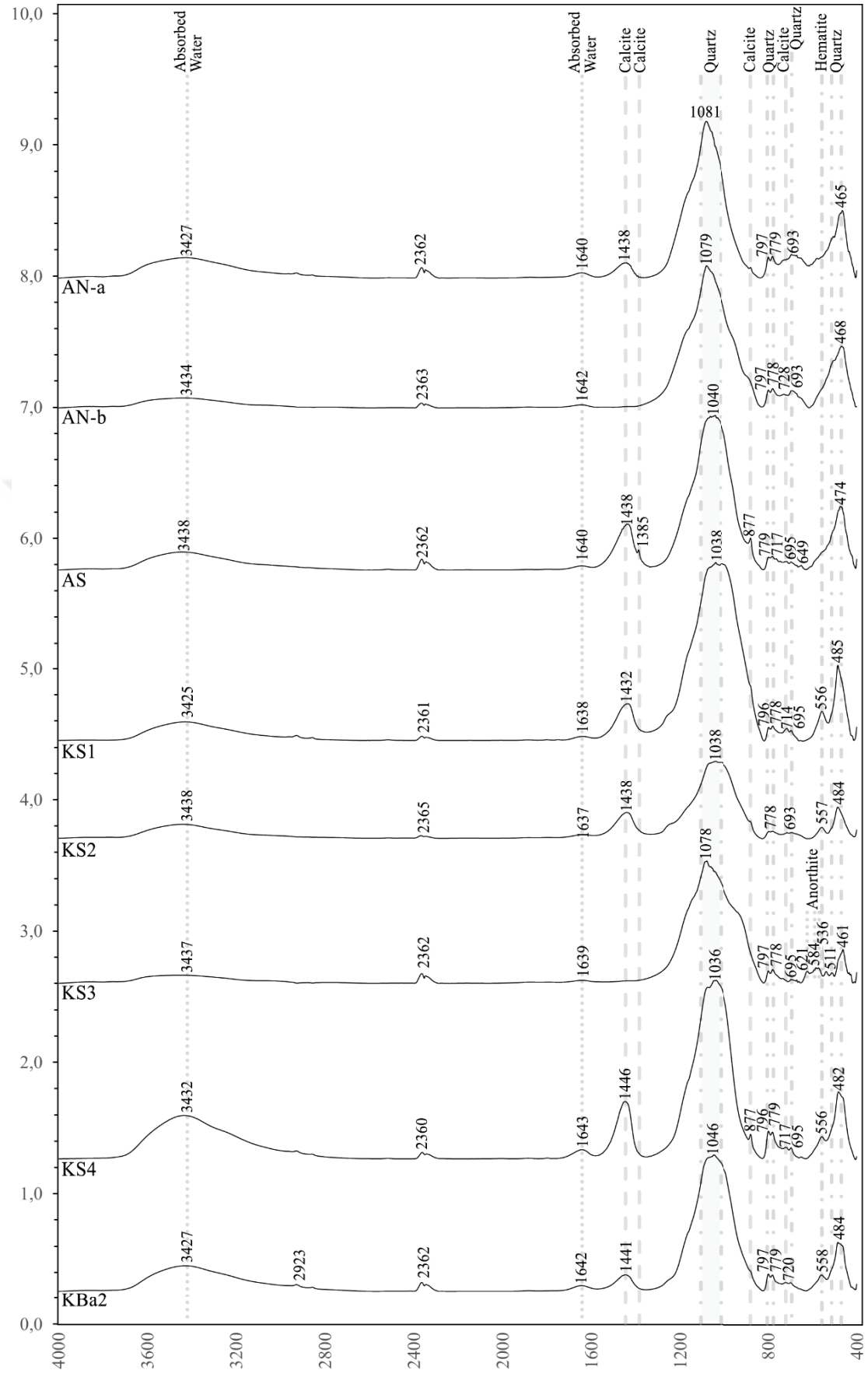


Figure 5.12. FTIR spectra of brick samples from 3rd period (AN, AS) of St. Jean Basilica and 1st period (KS1, KS2, KS3, KS4, KBa2) of Anaia Church

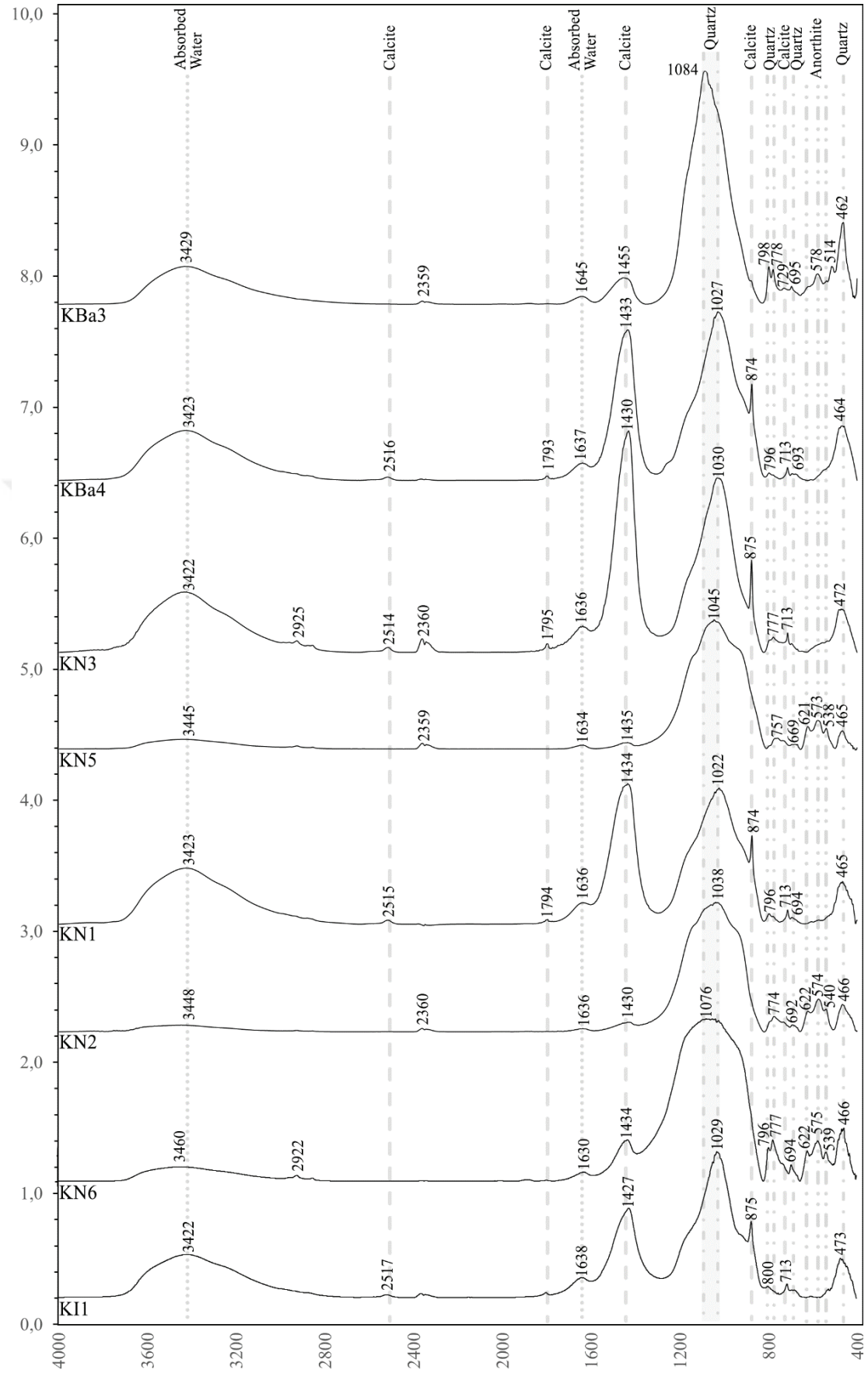


Figure 5.13. FTIR spectra of brick samples from 1st (KBa3, KBa4, KN3, KN5) and 2nd (KN1, KN2, KN6, KI1) period of Anaia Church

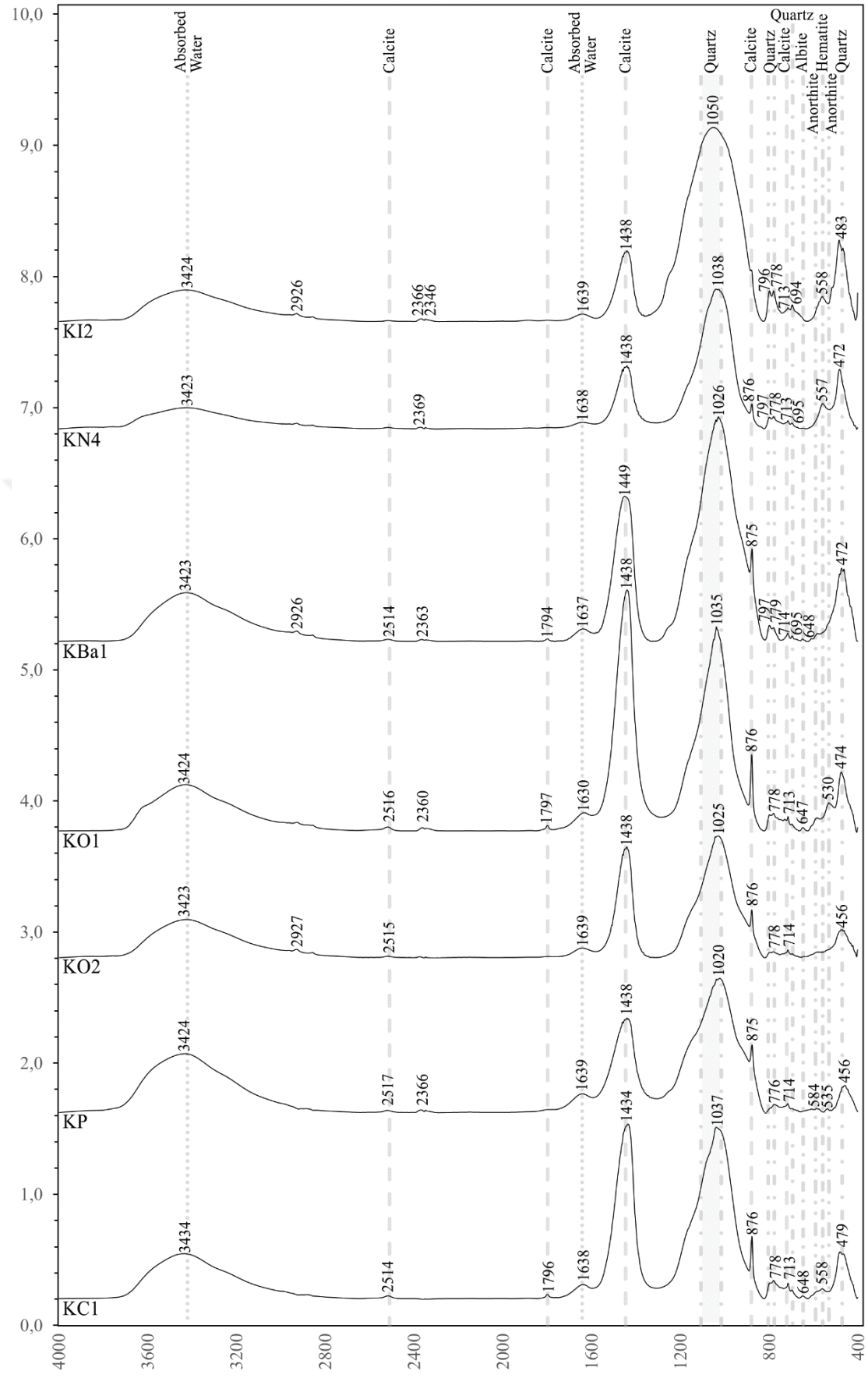


Figure 5.14. FTIR spectra of brick samples from 3rd period (KI2, KN4, KBa1, KO1, KO2, KP, KC1) of Anaia Church

Results of mineralogical analyses were evaluated to predict the firing temperatures for each brick sample (Table 5.8). The lowest firing temperature was thought to be applied to KI1 and KP bricks from Anaia Church because none of the minerals formed in bricks by temperature rises was detected in those. Therefore, they were estimated to be fired under 700°C, regarding the absence of muscovite.

Two bricks from St. Jean Basilica (AB2 and AS) and five bricks from Anaia Church (KS4, KN3, KN4, KO1, and KC1) contained muscovite, so it could be stated that their firing temperatures were higher than 700°C. The presence of albite and calcite (also dolomite in KO1), and the absence of gehlenite or hematite/anorthite, demonstrated that the temperature did not reach 800 °C.

Furthermore, gehlenite was the distinctive mineral for firing temperatures of the samples KBa4, KN1, KBa1 and KO2. The existence of gehlenite indicated that the firing temperatures of these bricks exceeded 800°C. Also, it could be inferred that the bricks were not fired over 850°C due to the absence of hematite or anorthite and the presence of calcite, albite, and muscovite.

The formation of hematite in AR2, KS1, KS2, KBa2, KBa3, KI2 and anorthite in AT1 pointed out the firing temperatures were over 850°C. Calcite which decomposes at 870°C, was determined in these samples, apart from AR2 and KBa2, so the firing temperatures were estimated to be around 850°C and 870°C. On the contrary, AR2 and KBa2, in which muscovite was observed, were thought to be fired between 850°C and 900°C.

The highest firing temperature was evaluated as around 900°C for six of St. Jean Basilica bricks (AR1, AG, AB1, AT2, AI, AN) containing spinel, and for four of Anaia Church bricks (KS3, KN5, KN2, KN6) containing diopside.

A strict difference between the construction periods in terms of firing temperatures did not exist both for St. Jean Basilica and Anaia Church. Just, the firing temperatures of any bricks from the third phase of Anaia Church did not reach 900°C even though it occurred in earlier bricks of the church. Moreover, it was observed that the bricks of Cluster 1 (Anaia Church, CaO: <20%) and Cluster 2 (St. Jean Basilica) were fired between 700–900°C, while the bricks in Cluster 3 (Anaia Church, CaO: >20%) were not fired at temperatures over 800°C. Overall, the bricks from St. Jean Basilica were determined to be fired at higher temperatures than those from Anaia Church, in general.

Table 5.8. Mineralogical compositions and estimated firing temperatures of bricks (Q: Quartz, C: Calcite, Al: Albite, H: Hematite, Co: Coesite, Sp: Spinel, M: Muscovite, G: Gehlenite, An: Anorthite, Di: Diopside, Mg: Magnetite, Do: Dolomite)

Sample			Q	C	Al	H	Co	Sp	M	G	An	Di	Mg	Do	°C
St. Jean Basilica, Ayasuluk Hill	1st Phase (4th-5th c.)	AR1	X		X	X		X							~900
		AR2	X		X	X	X		X						850<x<900
		AG	X		X	X		X							~900
	2nd Phase (520s)	AB1	X		X	X	X	X							~900
		AB2	X		X		X		X						700<x<800
		AT1	X	X			X		X		X				~850–870
		AT2	X		X	X	X	X				X			~900
	3rd Phase (550s)	AI	X		X	X	X	X							~900
		AN-a	X	X	X	X		X							~900
		AN-b	X		X			X							~900
		AS	X	X	X		X		X						700<x<800
Anaia Church, Kadıkalesi	1st Phase (5th-6th c.)	KS1	X	X	X	X			X	X					~850–870
		KS2	X	X		X			X	X					~850–870
		KS3	X			X					X	X			~900
		KS4	X	X					X						700<x<800
		KBa2	X			X			X						850<x<900
		KBa3	X	X	X	X									~850–870
		KBa4	X	X	X				X	X					800<x<850
		KN3	X	X	X				X						700<x<800
		KN5	X								X	X	X		~900
	2nd Phase (11th-13th c.)	KN1	X	X	X					X					800<x<850
		KN2	X			X					X	X			~900
		KN6	X								X	X	X		~900
		KI1	X	X										X	<700
	3rd Phase (13th-14th c.)	KI2	X	X		X			X	X					~850–870
		KN4	X	X					X						700<x<800
		KBa1	X	X	X					X					800<x<850
		KP	X	X	X										<700
		KO1	X	X	X				X					X	700<x<800
		KO2	X	X	X				X	X					800<x<850
		KC1	X	X	X				X						700<x<800

5.4. Thermogravimetric Analyses

Weight losses of samples in certain temperature ranges were determined by thermogravimetric analyses (TGA). Results of TGA were used to support mineralogical studies in the estimation of firing temperatures. Fifteen samples were selected for TGA, considering their construction periods and mineralogical compositions. The weight losses depending on temperature changes were recorded, and thermograms were depicted in Table 5.9, Figure 5.15 and Figure 5.16.

In the bricks from St. Jean Basilica, the weight losses between 25-1000°C were in the range of 1.03–4.43% (Table 5.9). The highest losses (% 0.83–2.59) occurred between 200-400°C. Also, a decrease in the temperature range of 550-650°C was observed in AB2 (0.66%), AI (0.28%) and AN-a (1.24%) (Figure 5.15).

The total weight losses of Anaia Church samples were measured between 1.30-16.91% (Table 5.9). Most of the weight losses were at around 700°C in KN3 (10.72%), KN1 (7.57%), KI1 (7.96%), KO1 (14.07%) and KC1 (9.60%) samples. The weight of KS4 and KI2 reduced gradually by 5.77% and 4.31%, respectively, up to 550°C, and dropped by 3.02% and 2.01%, respectively, between 550-680°C (Figure 5.16).

Table 5.9. Weight losses (%) in particular temperature ranges (°C)

% wt	25-100°C	100-200°C	200-400°C	400-600°C	600-800°C	800-1000°C	Total
AR1	0.13	0.66	2.59	0.43	0.51	-0.37	3.95
AR2	0.04	0.47	1.55	0.46	-0.05	-0.08	2.38
AB2	0.56	0.58	1.23	0.98	0.58	0.50	4.43
AI	0.08	0.38	0.83	0.15	-0.04	-0.38	1.03
AN-a	0.59	0.79	1.48	0.82	0.90	-0.18	4.40
AN-b	0.09	0.52	1.12	0.35	-0.36	-0.66	1.06
KS3	0.05	0.26	0.83	0.28	0.04	-0.15	1.30
KS4	0.91	1.61	2.21	1.50	2.15	-0.89	7.49
KN3	0.83	1.34	2.03	1.17	9.65	-1.12	13.90
KN1	0.47	0.79	0.81	1.49	6.61	-0.29	9.88
KN6	0.11	0.31	1.11	0.64	0.35	-0.05	2.48
KI1	1.43	1.68	2.30	1.39	7.25	-0.65	13.38
KI2	0.35	0.81	2.42	0.98	1.53	-0.59	5.51
KO1	0.29	0.44	1.46	1.94	12.88	-0.10	16.91
KC1	0.92	1.52	2.34	3.04	7.89	0.00	15.71

The changes in thermograms indicated decompositions occurred during firing (Figure 5.15, 5.16). The weight losses between 25−400°C were associated with the loss of water from the brick structure; where the losses between 25 and 100°C were due to the physically absorbed water, and the losses below 400°C were due to the dehydration of bound water (Paama, Pitkãnen, and Perämäki 2000; Cardiano et al. 2004; Drebushchak et al. 2005; Singh and Sharma 2016). Samples showed decreases between 0.04–0.59% for St. Jean Basilica and 0.05–1.43% for Anaia Church, attributed to removing absorbed water from room temperature to 100°C. Also, dehydration caused weight losses of 1.21–3.25% in St. Jean Basilica bricks and 1.08–3.98% in Anaia Church bricks in the range of 100−400°C.

Dehydroxylation appears with a weight reduction between 400−600°C (Cardiano et al. 2004; Drebushchak et al. 2005; Stubňa and Podoba 2013; Singh and Sharma 2016). Besides, oxidation of organic materials contributed to the weight losses between 200−600°C (Ramachandran et al. 2002; Singh and Sharma 2016; Kumar Mishra, Mishra, and Anshumali 2021). Between 400−600°C, a decrease between 0.15% and 0.98% occurred in St. Jean bricks and 0.28−3.04% in Anaia Church bricks. Nevertheless, the weight losses at these temperatures cannot be attributed to organic materials because no organic compounds were detected in the FTIR analysis of any of the bricks.

The weight losses in AB2 (0.66%), AI (0.28%), AN-a (1.24%), KS4 (5.77%) and KI2 (4.31%) at about 600°C may indicate the quartz transformation (Ion et al. 2011).

Furthermore, carbonates decompose at about 700–800°C, and the reductions at around 700°C in KN3 (10.72%), KN1 (7.57%), KI1 (7.96%), KO1 (14.07%), and KC1 (9.60%) samples can be associated with decomposition of carbonates, especially calcite (Paama, Pitkãnen, and Perämäki 2000; Cardiano et al. 2004; Drebushchak et al. 2005; Stubňa and Podoba 2013; Singh and Sharma 2016).

The firing temperatures of bricks were also evaluated in relation to the weight losses determined by thermogravimetric analysis. It is known that the total weight losses are lower in bricks produced at higher firing temperatures (Kumar Mishra, Mishra, and Anshumali 2021). The total weight losses of the samples were arranged, from most to least, as KO1, KC1, KN3, KI1, KN1, KS4, KI2, AB2, AN-a, AR1, KN6, AR2, KS3, AN-b, and AI. Thus, it could be suggested that this arrangement may also be similar to the firing temperatures of samples.

In addition, the decomposition of calcite is an irreversible process, so the weight reduction between 700–800°C suggests that the firing temperature did not exceed 800°C,

roughly (Drebushchak et al. 2005; Stubňa and Podoba 2013). As a result of thermogravimetric analyses, it was presumed that KO1, KC1, KN3, KI1, and KN1 were the bricks having the highest carbonate content and fired under 800°C. In addition, the bricks fired at the highest temperatures were AI, KS3, AR2, and KN6.

The findings of thermogravimetric analyses supported the mineralogical composition analyses and estimated firing temperatures.

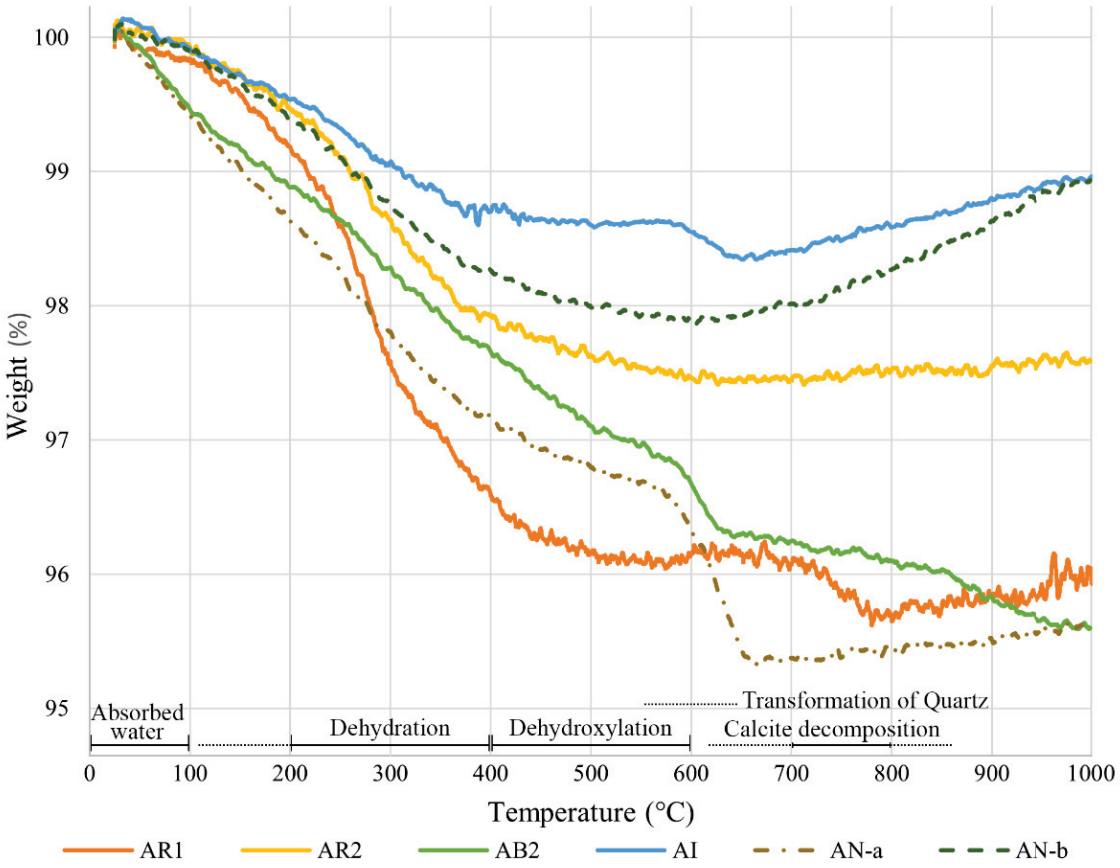


Figure 5.15. TGA graphs of St. Jean Basilica bricks

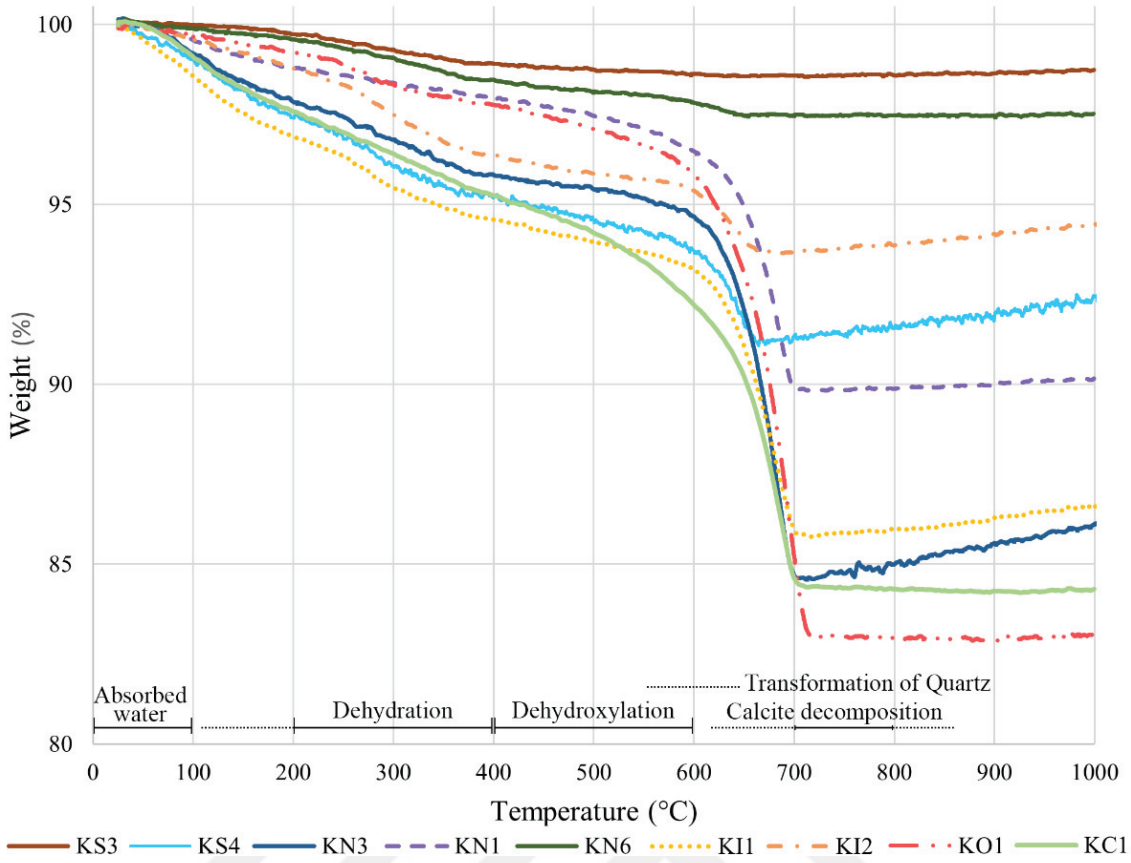


Figure 5.16. TGA graphs of Anaia Church bricks

5.5. Colour Identification

The colours of bricks depend on the firing process (kiln atmosphere, firing temperature), and the chemical and mineralogical compositions of the raw material. Hence, the colour of bricks is an indicator of their raw materials and production technologies, apart from their physical appearance.

Ca and Fe content of the raw material cause variations in brick colours from yellow/beige to red (Cultrone, Sidraba, and Sebastián 2005; Valanciene, Siauciunas, and Baltusnikaite 2010; Scatigno et al. 2018). The reddish colour of brick occurs with the presence of Fe, which is mostly found in the form of hematite (Fe_2O_3) in the oxidizing kiln atmosphere (Pavia 2006; Scatigno et al. 2018). On the other hand, the presence of carbonates results in a yellowish colour of the brick matrix since they have the ability to inhibit the formation of iron oxides, the reason for the reddish colour (Cultrone, Sidraba, and Sebastián 2005; Pavia 2006).

The firing temperature of bricks affects their value. As the temperature rises, colour of Ca-rich bricks was observed to become lighter due to the mineralogical changes likely formation of diopside (Cultrone, Sidraba, and Sebastián 2005; Rathossi and Pontikes 2010). On the contrary, bricks with a high amount of Fe and a low amount of Ca were found to become darker shades of red with temperature increment (Pavia 2006; Rathossi and Pontikes 2010; Karaman, Günal, and Gökalp 2012). In addition, the formation of a black core in the center of bricks is due to the prevention of sulphur release and the reduction of iron oxides from hematite to magnetite when the brick was fired in a kiln atmosphere deficient in oxygen (Pavia 2006; Gredmaier, Banks, and Pearce 2011; Tarhan and Işık 2020). The burning of organic matter present in clay was observed to cause the formation of black core, as well (Davey 1961; Pavia 2006).

The Munsell Soil Colour Chart (Munsell Colour (Firm) 2000) was used to determine the colours of the studied brick samples, and results were given as colour codes (in terms of hue, value, and chroma, Figure 4.6), images, and the name of the colours (Table 5.10).

The results revealed that the hue of bricks changed between 10R-10YR, in the red and yellow-red colour range. The bricks from St. Jean Basilica showed a small range of hue (10R-5YR) in the red part of the Munsell hue scale, while the hue of bricks from the Anaia Church showed a wider range between 10R-10YR. The value, which indicates the lightness, was determined to be between 4 and 8. The value of bricks from Anaia Church was found to be higher than those of St. Jean Basilica; that means the colours of Anaia church bricks were lighter than St. Jean Basilica's. The chroma representing the saturation of colour was determined higher in the bricks from St. Jean Basilica than from Anaia Church. Accordingly, the colours of St. Jean Basilica bricks are red, while Anaia Church bricks are in brown-beige colours.

One of the samples from St. Jean Basilica, which was labelled as AN, has a colour transition from reddish colours to grey towards the core. In Table 5.10, the red colour of the shell was defined as AN-a, and the colour of the black core was defined as AN-b.

Table 5.10. Colour of bricks determined by using Munsell Soil Colour Chart

Sample			Hue	Value	Chroma	Color-code	Color Images	Color Name
St. Jean Basilica, Ayasuluk Hill, Selçuk	1st Phase (4th-5th c.)	AR1	2.5YR	5	6	2.5YR/5/6		Red
		AR2	2.5YR	5	8	2.5YR/5/8		Red
		AG	2.5YR	5	8	2.5YR/5/8		Red
	2nd Phase (520s)	AB1	2.5YR	6	8	2.5YR/6/8		Light Red
		AB2	2.5YR	5	6	2.5YR/5/6		Red
		AT1	5YR	4	6	5YR/4/6		Yellowish Red
		AT2	2.5YR	5	8	2.5YR/5/8		Red
	3rd Phase (550s)	AI	2.5YR	6	8	2.5YR/6/8		Light Red
		AN-a	10R	5	6	10R/5/6		Red
		AN-b	2.5Y	5	1	2.5Y/5/1		Gray
		AS	2.5YR	6	8	2.5YR/6/8		Light Red
Anaia Church, Kadıkalesi, Kuşadası	1st Phase (5th-6th c.)	KS1	2.5YR	7	6	2.5YR/7/6		Light Red
		KS2	2.5YR	6	8	2.5YR/6/8		Light Red
		KS3	7.5YR	6	6	7.5YR/6/6		Reddish Yellow
		KS4	2.5YR	7	8	2.5YR/7/8		Light Red
		KBa2	2.5YR	6	6	2.5YR/6/6		Light Red
		KBa3	2.5YR	7	4	2.5YR/7/4		Light Reddish Brown
		KBa4	7.5YR	8	4	7.5YR/8/4		Pink
		KN3	5YR	8	4	5YR/8/4		Pink
		KN5	7.5YR	6	4	7.5YR/6/4		Light Brown
	2nd Phase (11th-13th c.)	KN1	5YR	8	4	5YR/8/4		Pink
		KN2	10R	6	6	10R/6/6		Light Red
		KN6	7.5YR	6	3	7.5YR/6/3		Light Brown
		KI1	10YR	8	3	10YR/8/3		Very Pale Brown
	3rd Phase (13th-14th c.)	KI2	2.5YR	6	6	2.5YR/6/6		Light Red
		KN4	2.5YR	7	6	2.5YR/7/6		Light Red
		KBa1	7.5YR	8	4	7.5YR/8/4		Pink
		KP	5YR	8	4	5YR/8/4		Pink
		KO1	7.5YR	7	4	7.5YR/7/4		Pink
		KO2	5YR	8	4	5YR/8/4		Pink
		KC1	5YR	8	4	5YR/8/4		Pink

The colour characteristics of the bricks were differentiated based on chemical classifications rather than the construction periods. Reddish colour of bricks from St. Jean Basilica originated from their iron oxide content found between 8.44–12.05%. The firing temperature did not contribute to the redness of St. Jean Basilica bricks, probably since the firing temperatures were in close range (Table 5.11). The sample AN, taken from the 3rd phase of St. Jean Basilica, was observed to have a black core, and it was probably caused by a reducing kiln atmosphere, which did not contain sufficient oxygen.

Bricks from Anaia Church had brown-beige colours due to their high calcium content, which was found between 8.59−26.33%. The bricks in Cluster 3, with a calcium content of over 20%, could easily be distinguished from those of Cluster 1 (Table 5.11). They had the highest value (7-8), lowest chroma (3-4) and the colour named as pink according to Munsell Colour Chart (Table 5.10). Thus, it could be stated that the increment in CaO content resulted in a lighter colour, as observed in Anaia Church bricks.

Colours in Ca-rich bricks were expected to lighten as firing temperatures increased. However, the bricks of Cluster 1 became darker towards higher temperatures because of the formation of hematite (KS3, KN2, KBa2, KBa3, KS2, KI2, KS1) and magnetite (KN5 and KN6). For the bricks belonging to Cluster 3, their colours were observed to be very similar due to the proximity of the firing temperatures of the bricks (Table 5.11).

Table 5.11. The colour classification of bricks based on clusters and firing temperatures

Sample		Colours	Estimated Firing Temp.
Cluster 1 (Ca-rich (<20%))	KN6		~900°C
	KS3		~900°C
	KN2		~900°C
	KN5		~900°C
	KBa2		850<x<900°C
	KBa3		~850–870°C
	KS2		~850–870°C
	KI2		~850–870°C
	KS1		~850–870°C
	KN4		700<x<800°C
	KS4		700<x<800°C
Cluster 2 (Ca-poor)	AN		~900°C
	AT2		~900°C
	AG		~900°C
	AB1		~900°C
	AR1		~900°C
	AI		~900°C
	AR2		850<x<900°C
	AT1		~850–870°C
	AB2		700<x<800°C
	AS		700<x<800°C
Cluster 3 (Ca-rich (>20%))	KO2		~800°C
	KN1		~800°C
	KBa1		~800°C
	KBa4		~800°C
	KN3		700<x<800°C
	KO1		700<x<800°C
	KC1		700<x<800°C
	KP		<700°C
	KI1		<700°C

5.6. Pozzolanic Activities

Pozzolanic activity is the ability of materials to react with lime in the presence of water. The raw material of fired bricks may contain amorphous clay minerals composed of reactive silica and/or alumina that can react with lime depending on their clay content and firing temperatures (TSE (Turkish Standards Institution) 2012). The amorphous phase of clay decomposes due to firing at high temperatures (over 900°C); accordingly, pozzolanic activity is lost (Baronio and Binda 1997; Böke, Akkurt, and Ipekoğlu 2004; Böke et al. 2006; Tekin and Kurugöl 2011; Navrátilová and Rovnaníková 2016).

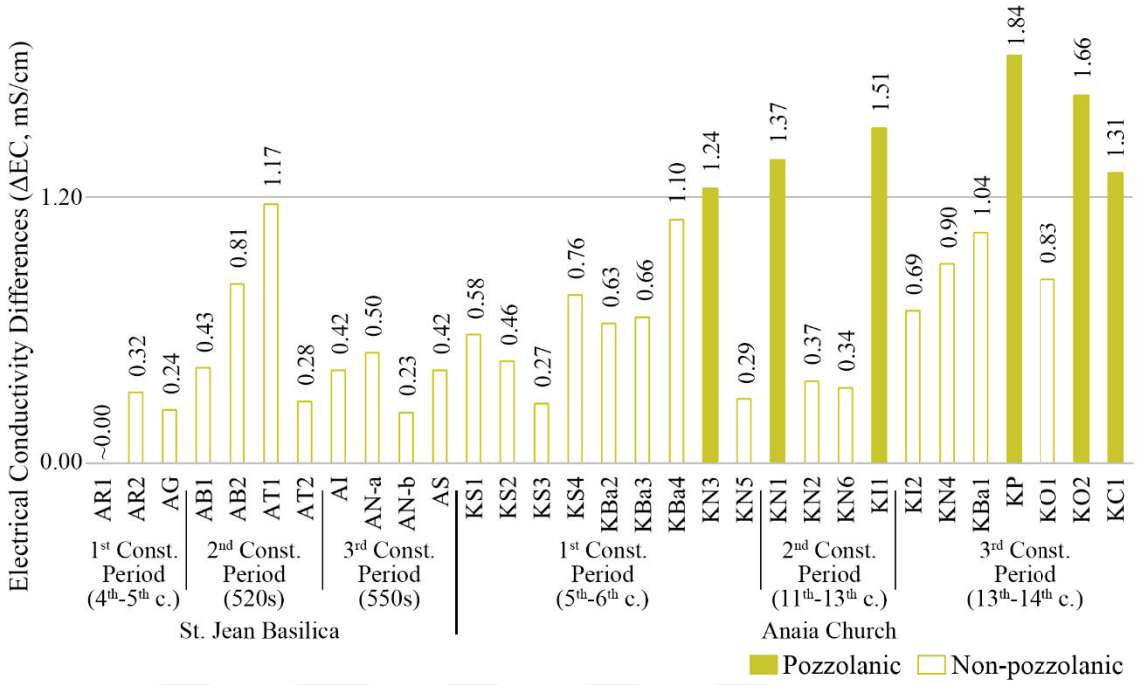
Pozzolanic activities of bricks were determined by the electrical conductivity method (Luxan, Madruga, and Saavedra 1989). In this method, the differences in electrical conductivity values before and after the addition of powdered bricks to saturated $Ca(OH)_2$ solution were measured. The bricks were accepted as good or reactive pozzolans if the electrical conductivity difference was greater than 1.2 mS/cm (Luxan, Madruga, and Saavedra 1989) (Table 5.12).

The electrical conductivity differences were between 0.23−1.17 mS/cm in samples from St. Jean Basilica (Table 5.12). The lowest values (up to 0.32 mS/cm) were calculated in the samples belonging to 4^{th}-5^{th} century (1^{st} construction period). The AT1 sample from 2^{nd} construction period has the highest value, 1.17 mS/cm. The results revealed that building bricks from St. Jean Basilica did not possess pozzolanic properties (Table 5.12).

The bricks from Anaia Church generated electrical conductivity differences between 0.27−1.84 mS/cm (Table 5.12). Samples from the 1^{st} (KS3 and KN5) and 2^{nd} (KN2 and KN6) phases exhibited the lowest values within the Anaia Church bricks. Although conductivity differences were mostly under the 1.20 mS/cm, six bricks (KN3, KN1, KI1, KP, KO1, KC1) presented pozzolanic properties (Table 5.12).

Overall, the majority of bricks were found to be non-pozzolanic. The highest firing temperatures resulted in the lowest electrical conductivity differences, as observed in the AR1, AN, AG, AT2, KS3, KN5, KN6 and KN2. The bricks accepted to have pozzolanic properties were manufactured with Ca-rich clays at temperatures under 800°C. However, their electrical conductivity differences were negligible as they were only slightly above 1.20 mS/cm.

Table 5.12. Electrical conductivity differences and pozzolanic classification of bricks



The non-pozzolanicity of brick samples was thought to be caused by the raw material of bricks not containing enough amorphous clay mineral for pozzolanic activity. Similarly, the historical building bricks from Roman, Byzantine and Ottoman Periods investigated in recent studies were also found non-pozzolanic (Aslan Özkaya and Böke 2009; Uğurlu Sağın and Böke 2013; Oguz, Turker, and Kockal 2014; Gürhan, Uğurlu Sağın, and Böke 2017; Uğurlu Sağın 2017).

5.7. Microstructural Properties

Microstructural properties of brick were determined in order to examine vitrification degrees and pore characteristics (size, shapes, etc.). Microstructure of bricks fired at low temperatures is distinguished by a flaky structure with stratified phyllosilicates, scattered particles, and angular pores between granules (Maniatis and Tite 1981; Cultrone et al. 2004; Cultrone, Sidraba, and Sebastián 2005; Pavia 2006). Between 800 and 870°C, a textural change arises in carbonated bricks; the decomposition of carbonates (dolomite and calcite) leads to an increase in porosity by releasing H_2O and CO_2 (Elert et al. 2003; Cultrone et al. 2004; Buchner et al. 2021). Nevertheless, glassy phases are not observed until 900°C. Above this temperature, sharp-edged structures of

phyllosilicates deform and become smoothed while vitrification increases (Cultrone et al. 2004; Pavia 2006). Although angular-shaped pores still exist in the brick matrix at 900°C, higher temperatures lead to the formation of ellipsoidal pores without interconnections (Cultrone et al. 2001; Benavente et al. 2006).

The microstructural properties were investigated by SEM-EDS analyses performed on eight brick samples which were chosen according to their chemical classifications (Cluster 1–3, Table 5.5) and estimated firing temperatures (Table 5.8). The bricks produced between 700−800°C (KN4, AB2, and KO1) did not display any vitreous phase. They had crystalline structure and lamellar phyllosilicates without any deformation (Figure 5.17). Small-sized pores in irregular and angular shapes were observed between particles of the bricks. At this temperature range, the bricks with different chemical contents showed similar microstructural characteristics (Figure 5.17).

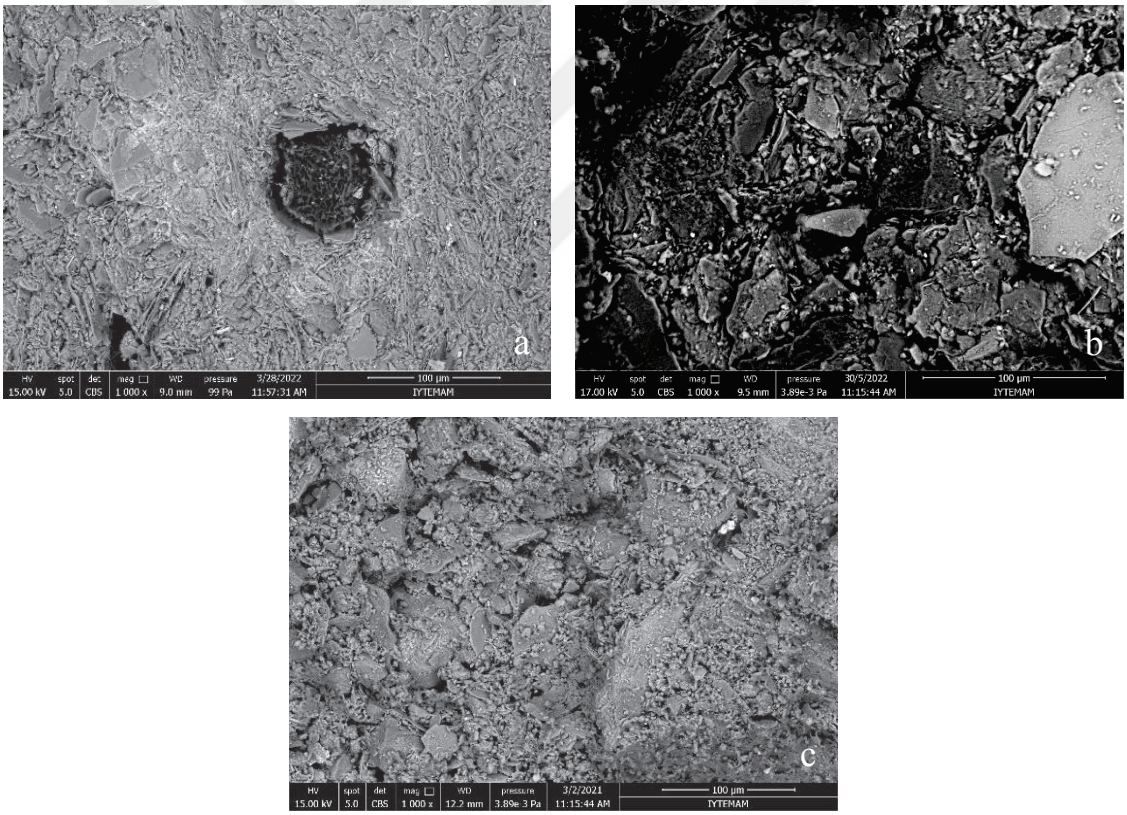


Figure 5.17. SEM (BSE) images of bricks (x1000), a: KN4 (Cluster 1, 700–800°C), b: AB2 (Cluster 2, 700–800°C), c: KO1 (Cluster 3, 700–800°C)

In the bricks produced between 800–870°C firing temperatures, no vitreous phase was detected, and significant changes in pore properties were not observed (Figure 5.18). Besides, the porosity between particles of KS2 (850–870°C) increased compared to KN4 (700–800°C), probably due to the decomposition of calcite which begins above 800°C. The other sample (AT1), fired between 850 and 870°C, exhibited a tendency for phyllosilicates to join together (Figure 5.18). Furthermore, the low CaO percentage and lack of carbonates in AT1 might result in no change in porosity at this temperature compared to the Cluster 2 sample fired between 700 and 800°C (AB2, Figure 5.17). Thus, AT1 had a more compact structure than KS2 and KBa4, which was also confirmed by their total porosity and density values (Table 5.2). A crystalline phase (probably calcite crystals) and flaky structures still existed in KBa4, and its matrix was more like KO1. This was probably due to the higher CaO content in Cluster 3, and the firing temperature of KBa4 did not reach 870°C, at which calcite decomposes.

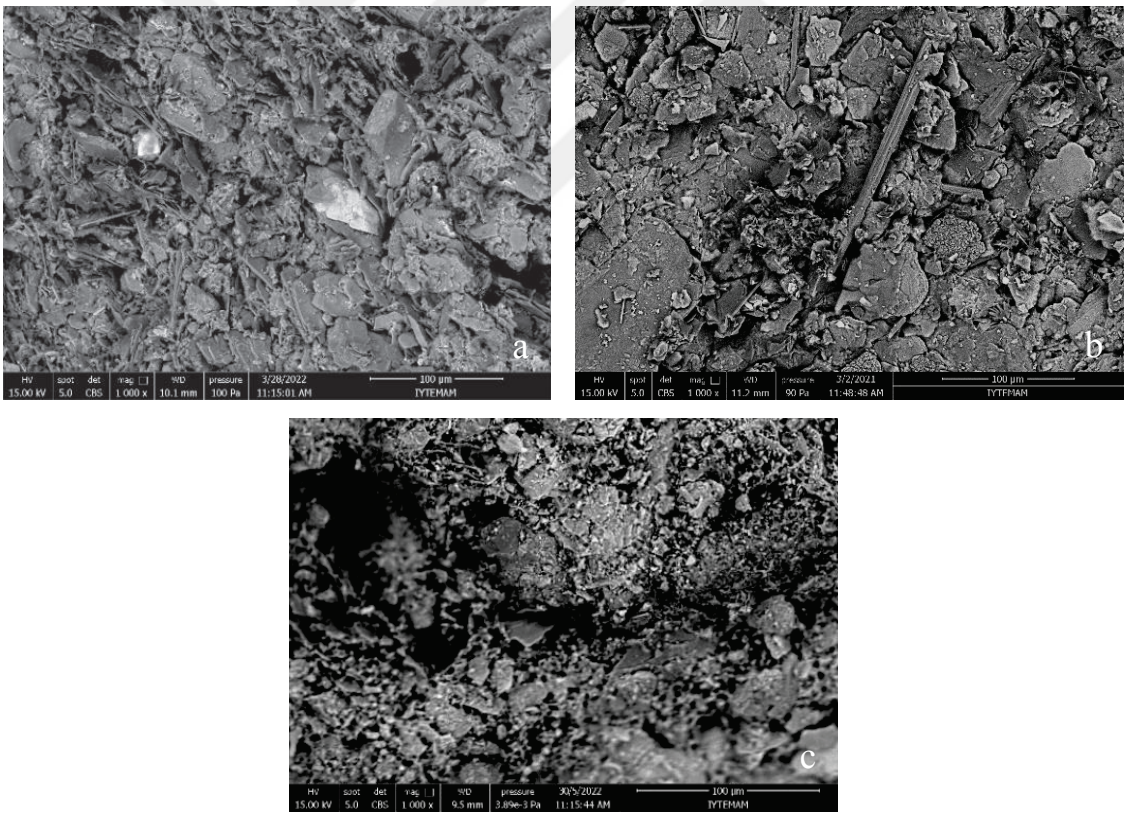


Figure 5.18. SEM (BSE) images of bricks (x1000), a: KS2 (Cluster 1, 850–870°C), b: AT1 (Cluster 2, 850–870°C), c: KBa4 (Cluster 3, 800–850°C)

In the SEM images of KS3 and AN, thought to be fired around 900°C, glassy phases were distinguished clearly (Figure 5.19). KS3 had an initial vitreous stage and crystalline phase. Although its pores were smoothed and larger than the bricks fired at lower temperatures, there were still pores with irregular and partially angular forms. These features might be due to the firing temperature of KS3 not exceeding 900°C. In contrast, AN demonstrated continuous vitrification and larger ellipsoid pores formed by merging the micropores with the effect of melting. Accordingly, it could be stated that AN was fired at a temperature above 900°C. At this temperature, the crystallized matrix presented within the sample could be originated from spinel, which was also detected by XRD analysis (Figure 5.7, Figure 5.19).

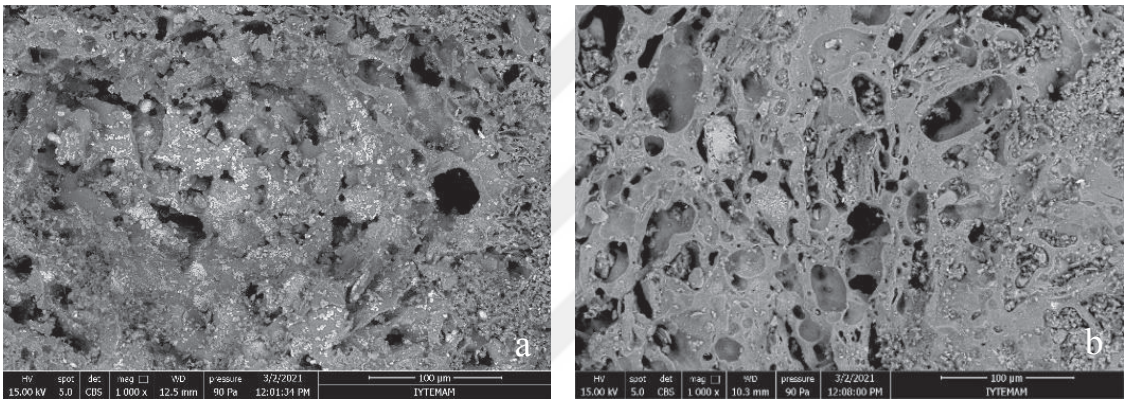


Figure 5.19. SEM (BSE) images of bricks (x1000), a: KS3 (Cluster 1, ~900°C), b: AN (Cluster 2, ~900°C)

In the matrix of Anaia Church bricks, brick fragments (or grog) included in the clay mixture were observed visually. The grog particles were also detected in the SEM observations of the brick sample from Anaia Church. EDX analyses of the grog and main bricks matrix revealed that both bricks contained high amounts of SiO_2, Al_2O_3, FeO, and CaO, while the grog was also found to include manganese in small quantities (Figure 5.20).

The brick additives might be included in raw materials because of their advantages for plastic clay mixture during the drying process in terms of permeability (Vieira and Monteiro 2007).

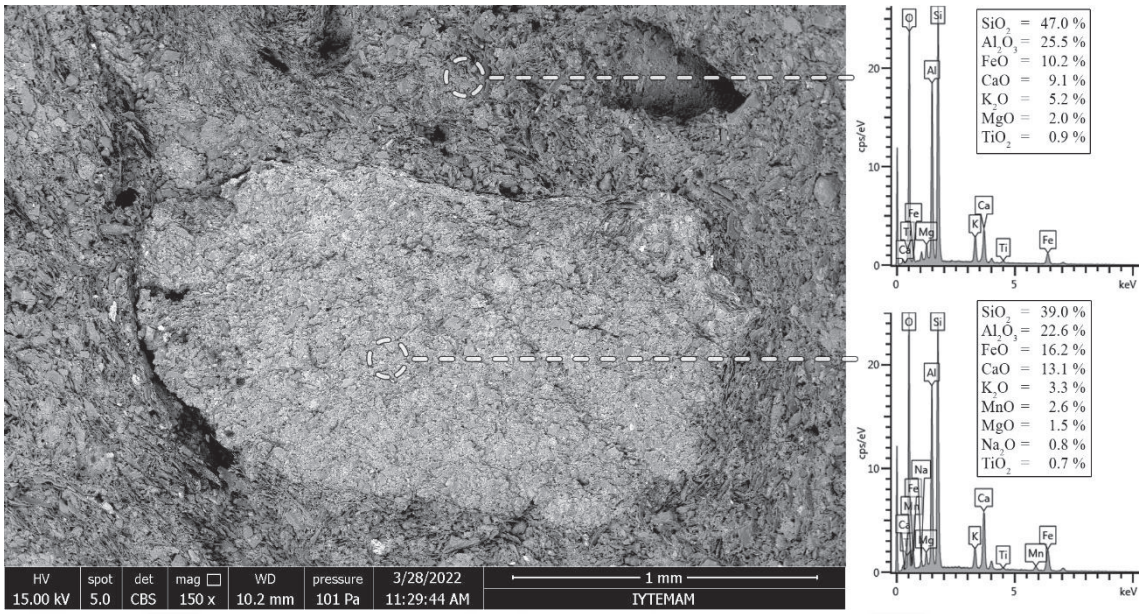


Figure 5.20. SEM image (150x) and EDX results of grog in the brick matrix (KS2)

5.8. Mechanical Properties

Mechanical properties of samples were determined by compression tests. The behaviours of bricks under loading were observed (Figure 5.21–5.23). In the first stage, vertical fissures and cracks occurred near the corners of the bricks and between the pores. With continued loading, the surface of bricks began to split from the cracks. Also, the inner parts lost rigidity and became fragmented at the last stage.

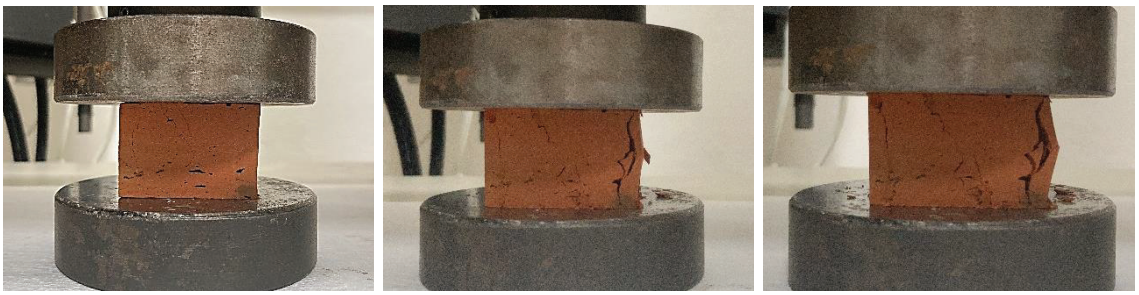


Figure 5.21. The behaviour of AR2 during the mechanical test



Figure 5.22. The behaviour of AN during the mechanical test



Figure 5.23. The behaviour of KN5 during the mechanical test

The uniaxial compressive strength and modulus of elasticity of bricks were used to describe their mechanical properties. Compressive strength is the maximum load the material can resist without deformation, and the modulus of elasticity shows the ability to withstand deformation under external pressures.

The uniaxial compressive strength values of bricks were between 4.16–46.10 MPa for St. Jean Basilica and 3.98–24.50 MPa for Anaia Church (Table 5.13). With regard to the construction periods, St. Jean Basilica bricks had compressive strength in the range of 4.49–39.11 MPa in the 1st phase, 4.16–19.01 MPa in the 2nd phase, 4.60–46.10 MPa in the 3rd phase, while the value of Anaia Church bricks was ranging between 3.98–24.50 MPa in the 1st phase, 10.98–16.38 MPa in the 2nd phase, 4.77-23.44 MPa in the 3rd phase. The uniaxial compressive strength values of bricks changed in a similar range, independent of construction periods, but fluctuations were observed in the values.

The majority of the St. Jean Basilica bricks had compressive strengths in the range of 4.16–9.74 MPa, although the values of four samples were found well above average, which were AT2 (18.36 MPa), AB1 (19.01 MPa), AG (39.11 MPa) and AN (46.10 MPa)

samples. It could be related to the firing temperatures of those bricks being higher than others (~900°C) (Table 5.8).

Besides, compressive strengths were more homogenous among Anaia Church bricks, with an average of 11.60 MPa. The lowest strengths were performed by KS4 and KO1 with values of 3.98 and 4.77 MPa, respectively. The highest values were observed in KP (23.44 MPa) and KN3 (24.50 MPa), although they were estimated to be fired at lower temperatures than others (Table 5.8, Table 5.13).

The modulus of elasticity values were determined ranging between 90.02–1320.18 MPa in bricks from St. Jean Basilica and 89.00–865.39 MPa in bricks from Anaia Church. The highest value was measured in AN among St. Jean Basilica bricks and KP for Anaia Church bricks, while AB2 and KO1 had the lowest modulus of elasticity values in their own groups (Table 5.13).

The strength of bricks is related to porosity values; durability increases with the reduction of porosity (RILEM 1980; Borrelli 1999). However, the uniaxial compressive strength and modulus of elasticity values of investigated bricks were not parallel to the porosity values. It was observed that some samples, likely KS3, KN5, KN2, and KI2, with high porosity percentages were stronger than some with lower porosity, such as AB2, AT1, AS, KS4, and KO1 (Table 5.2, Table 5.13). Similar results were determined in Byzantine bricks from İstanbul by Kahya (1992).

The dissimilarities between mechanical properties and porosity values of bricks were due to their nonhomogeneous structure caused by the mixing and shaping process during their production. The distribution and size of the particles in the clay and the cracks and fissures in the structure of the bricks reduced the strength (Kahya 1992; İspir 2010).

Additionally, the strength was influenced by raw material properties rather than porosity and firing temperature. The carbonates were found to contribute to mechanical properties at lower temperatures since they act as fluxes and promote the degree of vitrification (Elert et al. 2003). The Ca-richest bricks (Cluster 3) fired below 850°C (KN3, KP, KO2, KBa4) showed durability as much as bricks from other clusters, which were fired at about 900°C (KN6 from Cluster 1, and AN, AG, AB1, AT2 from Cluster 2).

Table 5.13. Uniaxial compressive strength and modulus of elasticity values of bricks with porosity percentages

Sample			Uniaxial Compressive Strength (MPa)	Modulus of Elasticity (MPa)
St. Jean Basilica, Ayasuluk Hill	1st Phase (4th-5th c.)	AR1	9.74 ± 2.72	224.33 ± 139.21
		AR2	4.49 ± 1.22	90.02 ± 23.26
		AG	39.11 ± 0.52	972.24 ± 32.55
	2nd Phase (520s)	AB1	19.01 ± 1.19	395.57 ± 118.59
		AB2	5.40 ± 0.71	72.59 ± 11.25
		AT1	4.16 ± 0.36	93.42 ± 11.78
		AT2	18.36 ± 1.02	372.55 ± 99.75
	3rd Phase (550s)	AI	5.80 ± 0.28	98.11 ± 27.54
		AN	46.10 ± 13.13	1320.18 ± 233.15
		AS	4.60 ± 0.14	125.05 ± 73.87
Anaia Church, Kadıkalesi	1st Phase (5th-6th c.)	KS1	7.98 ± 0.71	139.07 ± 49.15
		KS2	5.77 ± 0.77	142.77 ± 2.14
		KS3	11.17 ± 2.78	263.27 ± 34.92
		KS4	3.98 ± 0.64	94.81 ± 15.25
		KBa2	7.26 ± 0.84	190.27 ± 36.39
		KBa3	7.90 ± 0.25	325.71 ± 18.73
		KBa4	14.69 ± 0.64	435.63 ± 63.59
		KN3	24.50 ± 3.25	771.09 ± 146.38
		KN5	9.32 ± 1.28	242.33 ± 30.36
	2nd Phase (11th-13th c.)	KN1	12.88 ± 0.07	405.30 ± 46.13
		KN2	10.98 ± 2.81	321.21 ± 149.76
		KN6	16.38 ± 5.20	485.74 ± 310.28
		KI1	11.50 ± 1.40	449.99 ± 75.99
	3rd Phase (13th-14th c.)	KI2	9.27 ± 0.35	239.39 ± 28.92
		KN4	5.93 ± 0.88	142.60 ± 9.39
		KBa1	12.62 ± 4.48	173.35 ± 53.42
		KP	23.44 ± 4.19	865.39 ± 247.49
		KO1	4.77 ± 1.52	89.00 ± 6.14
		KO2	19.87 ± 5.07	588.50 ± 237.75
		KC1	11.85 ± 0.92	299.78 ± 49.56

CHAPTER 6

CONCLUSIONS

St. Jean Basilica and Anaia Church, important religious centers of the Byzantine period in Western Anatolia, were built in similar centuries and could be regarded as outstanding examples of monumental brick structures.

The characteristics of bricks from St. Jean Basilica and Anaia Church were determined to reveal the production technologies of Byzantium in different centuries and to provide knowledge for future conservation works of the churches. In this regard, basic physical properties, chemical and mineralogical compositions, thermal properties, colours, pozzolanic activities, microstructural and mechanical properties of brick samples were investigated. The results were evaluated by comparison between the buildings and their different construction periods.

The bricks of St. Jean Basilica contained high amounts of SiO_2, Al_2O_3, FeO, and MgO and were mainly composed of quartz, albite, coesite, hematite, and spinel minerals. The raw material of St. Jean Basilica bricks was found as Ca-poor clay (1.4–5.4 %), and it was determined that they were obtained from a single source for centuries. Also, the bricks were fired at low firing temperatures, between 700–900°C, in all construction periods.

The Anaia Church bricks were determined to contain high amounts of SiO_2, Al_2O_3, and CaO and mainly consisted of quartz, calcite, and muscovite. Two clay sources were used for their production throughout the three construction periods (5^{th}–14^{th} centuries). Both were Ca-rich sources which could be differentiated by the CaO percentages (8.6–13.8% and 19.78–26.33%). The firing temperatures of the Anaia Church bricks ranged from temperatures just below 700°C to 900°C. Besides, the bricks used in the 3^{rd} construction period (13^{th}–14^{th} centuries) were produced at lower temperatures than the bricks of the first two periods (5^{th}–6^{th} and 11^{th}–13^{th} centuries).

The bricks of both monuments were highly porous and low-dense materials. The physical properties of bricks did not differ according to the construction periods in both investigated buildings. Nevertheless, the chemical content of clays affected the porosity and apparent density in calcareous bricks; higher calcium oxide content resulted in lower porosity and higher density values. The bricks fired at higher temperatures demonstrated

higher pore interconnectivity and lower saturation coefficient, although the differences were not major. In this regard, those bricks were evaluated to have more pores through which water cannot reach under natural conditions and to be more resistant to deterioration problems caused by salt crystallisation and freeze-thaw cycles.

The colour was a physical property of the bricks affected by their chemical and mineralogical contents, as well. The St. Jean Basilica bricks had a reddish colour, and the Anaia Church bricks had brown-beige colour. The absence of carbonates and the presence of iron oxides were the reasons for red colours of St. Jean Basilica bricks. The lighter colour of Anaia Church bricks was due to the high amounts of carbonates.

Most of the bricks did not possess pozzolanic properties. Despite being fired at low temperatures, the reason for the non-pozzolanicity of bricks was that their raw materials did not contain a sufficient amount of clay minerals to produce pozzolanic amorphous substances.

The microstructure of bricks differed regarding their chemical content and firing temperatures. The structure of bricks fired between 700−870°C from both churches were lamellar and crystallized with irregular and angular pores. An increase in the porosity occurred between 800 and 870°C in Ca-rich bricks due to the decomposition of carbonates. In the bricks fired at about 900°C, vitreous phases were observed, and their pores were smoother and enlarged by coalescing micropores compared to the bricks fired at lower temperatures.

The mechanical strength of the bricks from St. Jean's Basilica and Anaia Church varied in a wide range and could not be correlated to the construction periods. Higher firing temperatures and high calcium contents increased the mechanical strength of bricks.

The properties of Byzantine bricks determined in the scope of this study should be considered during the future conservation studies of St. Jean Basilica and Anaia Church. The new bricks must be physically, mineralogically and mechanically compatible with the original bricks.

The intervention bricks must be produced with the Ca-poor clay for St. Jean Basilica, while Ca-rich clay sources should be used for new bricks of Anaia Church. In this study, the determination of the properties of historical bricks from two Byzantine churches provided information about their raw material characteristics but not about an exact identification of the provenance of clay sources. In further studies, the possible clay sources should be investigated.

Furthermore, traditional moulding should be used as the shaping method, and their firing temperatures should not exceed 900°C. The intervention bricks should be specially manufactured taking into consideration all these features determined by this study for the conservation of the monuments.

REFERENCES

Adam, Jean-Pierre. 2005. *Roman Building: Materials and Techniques*. Routledge.

"AFAD, Tarihsel Depremler." n.d. Accessed June 9, 2022. https://deprem.afad.gov.tr/tarihseldepremler.

Akdeniz, Engin. 2004. "Kuşadası Kadıkalesi Kazısında Bulunan Bir Hitit Heykelciği." *OLBA*, 21–59.

Akdeniz, Engin. 2007. "Kadıkalesi Kazısı Miken Buluntuları-Mycenaean Finds from the Excavation." *Arkeoloji Dergisi IX*, 35–69.

Aslan Özkaya, Özlem, and Hasan Böke. 2009. "Properties of Roman Bricks and Mortars Used in Serapis Temple in the City of Pergamon." *Materials Characterization* 60 (9): 995–1000. https://doi.org/10.1016/j.matchar.2009.04.003.

ASTM International. 2007. *ASTM C67-07 Standard Test Methods for Sampling and Testing Brick and Structural Clay Tile*. West Conshohocken.

Bakırer, Ömür. 1981. *Selçuklu Öncesi ve Selçuklu Dönemi Anadolu Mimarisinde Tuğla Kullanımı*. Ankara: Middle East Technical University.

Ballato, Paolo, Giuseppe Cruciani, Maria Chiara Dalconi, Bruno Fabbri, and Michele Macchiarola. 2005. "Mineralogical Study of Historical Bricks from the Great Palace of the Byzantine Emperors in Istanbul Based on Powder X-Ray Diffraction Data." *European Journal of Mineralogy* 17 (5): 777–84. https://doi.org/10.1127/0935-1221/2005/0017-0777.

Baranaydın, Fırat. 2016. "Ayasuluk Tepesi Korinth Başlıkları." Unpublished MSc Thesis, Dokuz Eylül University.

Baronio, Giulia, and Luigia Binda. 1997. "Study of the Pozzolanicity of Some Bricks and Clays." *Construction and Building Materials* 11 (1): 41–46.

Bartz, W., and M. Chorowska. 2016. "Mineralogy and Technology of Bricks Used for the Construction of the XII Century Ducal Castle on the Island of Ostrów Tumski,

Wrocław (SW Poland).” *Geoscience Records* 2 (1): 4–16. https://doi.org/10.1515/georec-2016-0002.

Bean, G. E. 1979. *Aegean Turkey*. London: Ernst Benn Limited.

Benavente, David, L. Linares-Fernández, Giuseppe Cultrone, and Eduardo Sebastián. 2006. “Influence of Microstructure on the Resistance to Salt Crystallisation Damage in Brick.” *Materials and Structures/Materiaux et Constructions* 39 (1): 105–13. https://doi.org/10.1617/s11527-005-9037-0.

Benedetto, G E De, R Laviano, L Sabbatini, and P G Zambonin. 2002. “Infrared Spectroscopy in the Mineralogical Characterization of Ancient Pottery.” *Journal of Cultural Heritage* 3: 177–86.

Böke, Hasan, Sedat Akkurt, and Başak Ipekoğlu. 2004. “Investigation of the Pozzolanic Properties of Bricks Used in Horasan Mortars and Plasters in Historic Buildings.” *Key Engineering Materials* 264–268: 2399–2402. https://doi.org/10.4028/www.scientific.net/kem.264-268.2399.

Böke, Hasan, Sedat Akkurt, Başak Ipekoğlu, and Elif Uğurlu. 2006. “Characteristics of Brick Used as Aggregate in Historic Brick-Lime Mortars and Plasters.” *Cement and Concrete Research* 36 (6): 1115–22. https://doi.org/10.1016/j.cemconres.2006.03.011.

Borrelli, Ernesto. 1999. “Vol 1: Porosity.” In *ARC Laboratory Handbook: Conservation of Architectural Heritage, Historic Structures and Materials*. Vol. 1. Rome: ICCROM. www.iccrom.org/pdf/ICCROM_14_ARCLabHandbook02_en.pdf.

Buchner, Thomas, Thomas Kiefer, Wolfgang Gaggl, Luis Zelaya-Lainez, and Josef Füssl. 2021. “Automated Morphometrical Characterization of Material Phases of Fired Clay Bricks Based on Scanning Electron Microscopy, Energy Dispersive X-Ray Spectroscopy and Powder X-Ray Diffraction.” *Construction and Building Materials* 288 (June): 122909. https://doi.org/10.1016/J.CONBUILDMAT.2021.122909.

Budak Ünaler, Meral. 2013. “‘Fine-Sgraffito Ware’, ‘Aegean Ware’ from Anaia: An Analytical Approach.” Unpublished MSc Thesis, Izmir Institute of Technology.

Büyükkolancı, Mustafa. 1991. “Efes St. Jean Kilisesi.” *Ege Mimarlık* 2: 9.

Büyükkolancı, Mustafa. 2001. *St. Jean Hayatı ve Anıtı*. Efes 2000 Vakfı Yayınları.

Büyükkolancı, Mustafa. 2008. "Selçuk Ayasuluk Tepesi (Eski Efes) Appasas Mı?" In *Batı Anadolu ve Doğu Akdeniz Geç Tunç Çağı Kültürleri Üzerine Yeni Araştırmaları*, 41–55. Ankara.

Büyükkolancı, Mustafa. 2016. "UNESCO Dünya Kültür Mirası Efes: Üç Dönem Bölge Başkenti ve Mermer Ustalığının Merkezi." In *Kömürcüoğlu Taş Heykel Kolonisi 6*.

Büyükkolancı, Mustafa. 2018. "Efes'te Hıristiyanlık, Aziz Yuhanna ve Kilisesi." *Arkhe* 5: 18–23.

Calliari, Irene, Ernesto Canal, Silvia Cavazzoni, and Lorenzo Lazzarini. 2001. "Roman Bricks from the Lagoon of Venice: A Chemical Characterization with Methods of Multivariate Analysis." *Journal of Cultural Heritage* 2: 23–29.

Cardiano, Paola, Salvatore Ioppolo, Concetta De Stefano, Antonello Pettignano, Sergio Sergi, and Pasquale Piraino. 2004. "Study and Characterization of the Ancient Bricks of Monastery of 'San Filippo Di Fragalà' in Frazzanò (Sicily)." *Analytica Chimica Acta* 519 (1): 103–11. https://doi.org/10.1016/j.aca.2004.05.042.

Çizer, Özlem. 2004. "Investigation of Lime Mortar Characteristics for Conservation of the Ottoman Baths in Seferihisar-Urla Region." Unpublished MSc Thesis, Izmir Institute of Technology.

Cochrane, Sally. 2014. "The Munsell Colour System: A Scientific Compromise from the World of Art." *Studies in History and Philosophy of Science*, 26–41.

Cultrone, Giuseppe, Carlos Rodriguez-Navarro, Eduardo Sebastian, Olga Cazalla, and Maria Jose De La Torre. 2001. "Carbonate and Silicate Phase Reactions during Ceramic Firing." *European Journal of Mineralogy* 13 (3): 621–34. https://doi.org/10.1127/0935-1221/2001/0013-0621.

Cultrone, Giuseppe, Eduardo Sebastián, Kerstin Elert, Maria José de la Torre, Olga Cazalla, and Carlos Rodriguez-Navarro. 2004. "Influence of Mineralogy and Firing Temperature on the Porosity of Bricks." *Journal of the European Ceramic Society* 24 (3): 547–64. https://doi.org/10.1016/S0955-2219(03)00249-8.

Cultrone, Giuseppe, Inese Sidraba, and Eduardo Sebastián. 2005. "Mineralogical and Physical Characterization of the Bricks Used in the Construction of the 'Triangul

Bastion', Riga (Latvia)." *Applied Clay Science* 28: 297–308. https://doi.org/10.1016/j.clay.2004.02.005.

Davey, Norman. 1961. *A History of Building Materials*. London: Phoenix House Publication.

Dhanapandian, Swaminathan, Balasubramani Gnanavel, and Thirunavukkarasu Ramkumar. 2009. "Utilization of Granite and Marble Sawing Powder Wastes as Brick Materials." *Carpathian Journal of Earth and Environmental Sciences* 4 (2): 147–60.

Drebushchak, V. A., L. N. Mylnikova, T. N. Drebushchak, and V. V. Boldyrev. 2005. "The Investigation of Ancient Pottery: Application of Thermal Analysis." *Journal of Thermal Analysis and Calorimetry* 82 (3): 617–26. https://doi.org/10.1007/S10973-005-0942-9.

Elert, Kerstin, Giuseppe Cultrone, Carlos Rodriguez-Navarro, and Eduardo Sebastián Pardo. 2003. "Durability of Bricks Used in the Conservation of Historic Buildings - Influence of Composition and Microstructure." *Journal of Cultural Heritage* 4 (2): 91–99. https://doi.org/10.1016/S1296-2074(03)00020-7.

"Ephesus - UNESCO World Heritage Centre." 2015. 2015. https://whc.unesco.org/en/list/1018/.

Eroğlu, Murat, and Ali Akın Akyol. 2017. "Antik Yapı Malzemesi Olarak Tuğla ve Kiremit: Boğsak Adası Bizans Yerleşimi Örneklemi." *Sanat ve Tasarım Dergisi*, 141–62. https://doi.org/10.18603/sanatvetasarim.370745.

Eyice, Semavi. 1963. *Son Devir Bizans Mimarisi*. İstanbul: İstanbul Üniversitesi Edebiyat Fakültesi Yayınları.

Fernandes, Francisco M., Paulo B. Lourenço, and Fernando Castro. 2010. "Ancient Clay Bricks: Manufacture and Properties." *Materials, Technologies and Practice in Historic Heritage Structures*, 29–48. https://doi.org/10.1007/978-90-481-2684-2_3.

Foss, Clive. 1979. *Ephesus After Antiquity: A Late Antique, Byzantine and Turkish City*. Cambridge University Press.

Gadsden, J. A. 1975. *Infrared Spectra of Minerals and Related Inorganic Compounds*.

Butterworths.

Gerharz, Rudolf Richard, Renate Lantermann, and Dirk Spennemann. 1988. “Munsell Colour Charts: A Necessity for Archaeologists?” *Australian Historical Archaeology*, 88–95.

Gredmaier, L., C. J. Banks, and R. B. Pearce. 2011. “Calcium and Sulphur Distribution in Fired Clay Brick in the Presence of a Black Reduction Core Using Micro X-Ray Fluorescence Mapping.” *Construction and Building Materials* 25 (12): 4477–86. https://doi.org/10.1016/j.conbuildmat.2011.03.054.

Gürhan, Fatma, Elif Uğurlu Sağın, and Hasan Böke. 2017. “Aydın Eski Hamam Sıva Özellikleri.” In *Uluslararası Katılımlı 6. Tarihi Yapıların Korunması ve Güçlendirilmesi Sempozyumu*, 227–36. Trabzon.

Hazinedar Coşkun, Tümay. 2021. “Kuşadası, Kadıkalesi Kazısı’nın 2017-2020 Sezonlarına Ait Bizans Cam Örnekleri.” *Sanat Tarihi Dergisi* 30 (2): 1019–37.

Helen, Tapio. 1975. *Organization of Roman Brick Production in the First and Second Centuries A.D.: An Interpretation of Roman Brick Stamps*. Annales Academiae Scientiarum Fennicae. Dissertationes Humanarum-Litterarum. Helsinki: Suomalainen Tiedeakatemia.

Hörmann, H., J. Keil, and G. A. Sotiriou. 1951. *Die Johanneskirche (Forschungen in Ephesos IV. 3)*. Vienna.

Ion, Rodica Mariana, Irina Dumitriu, Radu Claudiu Fierascu, Mihaela Lucia Ion, Simona Florentina Pop, Constantin Radovici, Raluca Ioana Bunghez, and V. I.R. Niculescu. 2011. “Thermal and Mineralogical Investigations of Historical Ceramic: A Case Study.” *Journal of Thermal Analysis and Calorimetry* 104 (2): 487–93. https://doi.org/10.1007/s10973-011-1517-6.

İspir, Medine. 2010. “A Comprehensive Experimental Research on the Behaviour of Historical Brick Masonry Walls of 19th Century Buildings.” Unpublished PhD Thesis, Istanbul Technical University.

“İzmir Kent Rehberi.” 2016. İzmir Büyükşehir Belediyesi Coğrafi Bilgi Sistemleri Şube Müdürlüğü. 2016. https://kentrehberi.izmir.bel.tr/izmirkentrehberi.

Jeffreys, E., J. Haldon, and R. Cormack. 2008. *The Oxford Handbook of Byzantine Studies*. Oxford University Press.

Kahya, Yegan. 1992. "İstanbul Bizans Mimarisinde Kullanılan Tuğlaların Fiziksel ve Mekanik Özellikleri." Unpublished PhD Thesis, Istanbul Technical University.

Kanmaz, Mehmet Buğra. 2015. "Evaluation of Conservation Problems of Anaia Byzantine Church, Kadıkalesi, Kuşadası." Unpublished MSc Thesis, Izmir Institute of Technology.

Kanmaz, Mehmet Buğra, and Başak Ipekoğlu. 2016. "Antik Kentlerde Deprem Sonrası Yapılan Onarımlar: Anaia Bizans Kilisesi." In *Kargir Yapılarda Koruma ve Onarım Semineri VIII Bildiri Kitabı*, 189–205.

Karadaş, Aylin, Rifat İlhan, Ertuğ Öner, Serdar Vardar, and Senem Yıldız. 2019. "Kadıkalesi'nin (Antik Anaia) Paleocoğrafya ve Jeoarkeolojisi (Kuşadası-Aydın)." In *35. Arkeometri Sonuçları Toplantısı*, 527–45.

Karaman, Sedat, Sabit Ersahin, and Hikmet Gunal. 2006. "Firing Temperature and Firing Time Influence on Mechanical and Physical Properties of Clay Bricks." *Journal of Scientific and Industrial Research* 65 (2): 153–59.

Karaman, Sedat, Hikmet Günal, and Zeki Gökalp. 2012. "Variation of Clay Brick Colours and Mechanical Strength as Affected by Different Firing Temperatures." *Scientific Research and Essays* 7 (49): 4208–12. https://doi.org/10.5897/SRE12.248.

Karydis, Nikolaos. 2012. "The Vaults of St. John the Theologian at Ephesos: Visualizing Justinian's Church." *Journal of the Society of Architectural Historians* 71 (4): 524–51.

Karydis, Nikolaos. 2016. "The Evolution of the Church of St. John at Ephesos During the Early Byzantine Period." *Jahreshefte Des Österreichischen Archäologischen Institutes in Wien Band* 84: 97–128.

Krautheimer, Richard. 1986. *Early Christian and Byzantine Architecture*. 4th ed. New Haven and London: Yale University Press.

Kumar Mishra, Amit, Amit Mishra, and Anshumali. 2021. "Geochemical Characterization of Bricks Used in Historical Monuments of 14-18th Century CE

of Haryana Region of the Indian Subcontinent: Reference to Raw Materials and Production Technique." *Construction and Building Materials* 269: 121802. https://doi.org/10.1016/j.conbuildmat.2020.121802.

Kurugöl, Sedat. 2009. "18-19 YY. Osmanlı Harman Tuğlalarının Fiziko-Kimyasal, Petrografik ve Mekanik Özellikleri." In *Uluslararası Katılımlı Tarihi Eserlerin Güçlendirilmesi ve Geleceğe Güvenle Devredilmesi Sempozyumu-2*, 743–58. Diyarbakır: TMMOB İnşaat Mühendisleri Odası.

Kurugöl, Sedat, and Çiğdem Tekin. 2010. "Anadolu'da Bizans Dönemi Kale Yapılarında Kullanılan Tuğlaların Fiziksel, Kimyasal ve Mekanik Özelliklerinin Değerlendirilmesi." *Journal of the Faculty of Engineering and Architecture of Gazi Univeristy* 25 (4): 767–77.

Ladstaetter, Sabine, Mustafa Büyükkolancı, Evrim Ulusan, Umut Özdemir, and Bengü Sayar. 2015. "Ephesus-Nomination File." https://whc.unesco.org/uploads/nominations/1018rev.pdf.

Lopez-Arce, Paula, and Javier Garcia-Guinea. 2005. "Weathering Traces in Ancient Bricks from Historic Buildings." *Building and Environment* 40 (7): 929–41. https://doi.org/10.1016/j.buildenv.2004.08.027.

Luxan, M.P.;, F.; Madruga, and J. Saavedra. 1989. "Rapid Evaluation of Pozzolanic Activity of Natural Products by Conductivity Measurement." *Cement and Concrete Research* 19: 63–69.

MacDonald, William L. 1982. *The Architecture of the Roman Empire*. Yale University Press.

Malacrino, Carmelo G. 2010. *Constructing the Ancient World: Architectural Techniques of the Greeks and Romans*. Los Angeles: Getty Publications.

Mango, Cyril A. 1985. *Byzantine Architecture*. Milano: Electa Editrice.

Maniatis, Y., and M. S. Tite. 1981. "Technological Examination of Neolithic-Bronze Age Pottery from Central and Southeast Europe and from the Near East." *Journal of Archaeological Science* 8 (1): 59–76. https://doi.org/10.1016/0305-4403(81)90012-1.

Maritan, Lara, L. Nodari, C. Mazzoli, A. Milano, and U. Russo. 2006. "Influence of

Firing Conditions on Ceramic Products: Experimental Study on Clay Rich in Organic Matter." *Applied Clay Science* 31 (1–2): 1–15. https://doi.org/10.1016/j.clay.2005.08.007.

Mercangöz, Zeynep. 1997. "Efes ve Çevresinde Hristiyanlık (Ortaçağ Hristiyan Döneminde Efes ve Ayasuluk)." In *Birinci Uluslararası Geçmişten Günümüze Selçuk Sempozyumu*, 51–62. Selçuk Belediyesi Kültür Yayınları.

Mercangöz, Zeynep. 2005. "4. Yılında Kuşadası, Kadıkalesi/Anaia Kazısı." *Sanat Tarihi Dergisi* XIV–1: 205–23.

Mercangöz, Zeynep. 2007. "Emporion ve Kommerkion Olarak Anaia'nın Değişken Tarihsel Yazgısı." In *I. Uluslararası Sevgi Gönül Bizans Araştırmaları Sempozyumu*, 279–92. İstanbul: Vehbi Koç Vakfı.

Mercangöz, Zeynep. 2013. "Kadıkalesi/Anaia Ticari Üretiminin Latin Patronları." In *Bizanslı Ustalar-Latin Patronlar: Kuşadası Yakınındaki Kadıkalesi Kazıları Işığında Anaia Ticari Üretiminden Yansımalar*, 161–74. İstanbul: Ege Yayınları.

Mercangöz, Zeynep. 2018. "Doğu Akdeniz İslam Topraklarından Bir Bizans Kalesine: Kuşadası, Kadıkalesi'nde Orta Çağ İslam Seramikleri." *TÜBA-KED Türkiye Bilimler Akademisi Kültür Envanteri Dergisi* 17: 93–117.

Mercangöz, Zeynep, and Emine Tok. 2011. "Kuşadası Kadıkalesi 2010 Kazı Sezonu Çalışmaları." In *Kuşadası Kadıkalesi 2010 Kazı Sezonu Çalışmaları-2*, 353–72. Kültür ve Turizm Bakanlığı Kültür Varlıkları ve Müzeler Genel Müdürlüğü.

Mercangöz, Zeynep, Emine Tok, and Tümay Hazinedar Coşkun. 2012. "Kuşadası, Kadıkalesi Kazısı 2011 Yılı Çalışmaları." In *34. Kazı Sonuçları Toplantısı-2*, 275–88. Kültür ve Turizm Bakanlığı Kültür Varlıkları ve Müzeler Genel Müdürlüğü.

Mimaroğlu, Sinan. 2011. "Kuşadası, Kadıkalesi/ Anaia Kazısı'nda Ele Geçen Bizans Dönemi Günlük Kullanım Seramikleri." Ege University.

Mimaroğlu, Sinan. 2017. "Ayasuluk Tepesi ve St. Jean Anıtı Kazısı Buluntusu Ganos Amphoraları." In *Uluslararası XVIII. Ortaçağ ve Türk Dönemi Kazıları ve Sanat Tarihi Araştırmaları Sempozyumu*, 451–64. Aydın.

Mimaroğlu, Sinan, and Orçun Erdoğan. 2018. "The Place of the Commercial Amphorae Recovered During the Excavations at the Pilgrimage Church of St. John and at the

Ayasuluk Hill in the Byzantine Trade." In *SOMA 2018: XXII Symposium on Mediterranean Archaeology*. Rome.

Mirti, P., and P. Davit. 2001. "Technological Characterization of Campanian Pottery of Type A, B and C and of Regional Products from Ancient Calabria (Southern Italy)." *Archaeometry* 43 (1): 19–33. https://doi.org/10.1111/1475-4754.00002.

Mommsen, H. 2001. "Provenance Determination of Pottery by Trace Element Analysis: Problems, Solutions and Applications." *Journal of Radioanalytical and Nuclear Chemistry* 247 (3): 657–62.

"Monasteries of Daphni, Hosios Loukas and Nea Moni of Chios - Gallery - UNESCO World Heritage Centre." n.d. Accessed May 18, 2022. https://whc.unesco.org/en/list/537/gallery/.

Monteiro, S. N., and C. M.F. Vieira. 2004. "Influence of Firing Temperature on the Ceramic Properties of Clays from Campos Dos Goytacazes, Brazil." *Applied Clay Science* 27 (3–4): 229–34. https://doi.org/10.1016/j.clay.2004.03.002.

Moorey, P. R. S. 1999. *Ancient Mesopotamian Materials and Industries: The Archaeological Evidence*. Indiana: Eisenbrauns.

Moropoulou, Antonia, A. Bakolas, and K. Bisbikou. 1995. "Thermal Analysis as a Method of Characterizing Ancient Ceramic Technologies." *Thermochimica Acta* 2570: 743–53.

Moropoulou, Antonia, Ahmet Çakmak, and Kyriaki Polikreti. 2002. "Provenance and Technology Investigation of Agia Sophia Bricks, Istanbul, Turkey." *Journal of the American Ceramic Society* 85 (2): 366–72.

Munsell Colour (Firm). 2000. *Munsell Soil Colour Charts: Year 2000 Revised Washable Edition*. GretagMacbeth, Munsell Colour.

Navrátilová, Eva, and Pavla Rovnaníková. 2016. "Pozzolanic Properties of Brick Powders and Their Effect on the Properties of Modified Lime Mortars." *Construction and Building Materials* 120 (September): 530–39. https://doi.org/10.1016/j.conbuildmat.2016.05.062.

Oguz, Cem, Fikret Turker, and Niyazi Ugur Kockal. 2014. "Construction Materials Used in the Historical Roman Era Bath in Myra." *Scientific World Journal* 2014.

Onar, Vedat, Zeynep Mercangöz, Levent Kutbay, and Emine Tok. 2012. “Kuşadası Kadıkalesi (Anaia) Kazısında Ortaya Çıkarılan İşlenmiş Kemik Kalıntıları.” In *28. Arkeometri Sonuçları Toplantısı*, 83–90. Kültür ve Turizm Bakanlığı Kültür Varlıkları ve Müzeler Genel Müdürlüğü.

Ouahabi, M. El, L. Daoudi, F. Hatert, and N. Fagel. 2015. “Modified Mineral Phases During Clay Ceramic Firing.” *Clays and Clay Minerals* 63 (5): 404–13. https://doi.org/10.1346/CCMN.2015.0630506.

Ousterhout, Robert. 1999. *Master Builders of Byzantium*. Princeton University Press.

Özyıldırım, M., and A. A. Akyol. 2016. “Olba Tuğla Örneği: Arkeolojik ve Arkeometrik Yaklaşım.” *Seleucia* 6: 395–411.

Paama, Lilli, Ilkka Pitkãnen, and Paavo Perämäki. 2000. “Analysis of Archaeological Samples and Local Clays Using ICP-AES, TG-DTG and FTIR Techniques.” *Talanta* 51 (2): 349–57. https://doi.org/10.1016/S0039-9140(99)00281-7.

Papayianni, Ioanna, and Maria Stefanidou. 2000. “Characteristics of Bricks of Byzantine Period.” In *12th International Brick/Block Masonry Conference*, 1729–36.

Pavia, S. 2006. “The Determination of Brick Provenance and Technology Using Analytical Techniques from the Physical Sciences.” *Archaeometry* 48 (2): 201–18.

Pérez-Monserrat, Elena Mercedes, Lara Maritan, Enrico Garbin, and Giuseppe Cultrone. 2021. “Production Technologies of Ancient Bricks from Padua, Italy: Changing Colours and Resistance over Time.” *Minerals* 11 (7). https://doi.org/10.3390/min11070744.

Rat’ko, A. I., A. I. Ivanets, A. I. Kulak, E. A. Morozov, and I. O. Sakhar. 2011. “Thermal Decomposition of Natural Dolomite.” *Inorganic Materials* 47 (12): 1372–77. https://doi.org/10.1134/S0020168511120156.

Rathossi, C., and Y. Pontikes. 2010. “Effect of Firing Temperature and Atmosphere on Ceramics Made of NW Peloponnese Clay Sediments. Part I: Reaction Paths, Crystalline Phases, Microstructure and Colour.” *Journal of the European Ceramic Society* 30 (9): 1841–51. https://doi.org/10.1016/j.jeurceramsoc.2010.02.002.

Riccardi, M. P., B. Messiga, and P. Duminuco. 1999. “An Approach to the Dynamics of Clay Firing.” *Applied Clay Science* 15: 393–409.

RILEM. 1980. “Tests Defining the Structure.” *Materials and Construction* 13 (73).

Scalenghe, R., F. Barello, F. Saiano, E. Ferrara, C. Fontaine, L. Caner, E. Olivetti, I. Boni, and S. Petit. 2015. “Material Sources of the Roman Brick-Making Industry in the I and II Century A.D. from Regio IX, Regio XI and Alpes Cottiae.” *Quaternary International* 357: 189–206. https://doi.org/10.1016/j.quaint.2014.11.026.

Scatigno, Claudia, Nagore Prieto-Taboada, M. Preite Martinez, A. M. Conte, and Juan Manuel Madariaga. 2018. “A Non-Invasive Spectroscopic Study to Evaluate Both Technological Features and Conservation State of Two Types of Ancient Roman Coloured Bricks.” *Spectrochimica Acta - Part A: Molecular and Biomolecular Spectroscopy* 204: 55–63. https://doi.org/10.1016/j.saa.2018.06.023.

Şerifaki, Kerem. 2017. “Determination of Byzantine Wall Painting Techniques in Western Anatolia.” Unpublished PhD Thesis, Izmir Institute of Technology.

Setchell, J.S. 2012. “Colour Description and Communication.” In *Colour Design*, 99–129. Woodhead Publishing.

Singh, Pankaj, and Sukanya Sharma. 2016. “Thermal and Spectroscopic Characterization of Archeological Pottery from Ambari, Assam.” *Journal of Archaeological Science: Reports* 5: 557–63. https://doi.org/10.1016/j.jasrep.2016.01.002.

Stefanidou, Maria, Ioanna Papayianni, and V. Pachta. 2015. “Analysis and Characterization of Roman and Byzantine Fired Bricks from Greece.” *Materials and Structures/Materiaux et Constructions* 48 (7): 2251–60. https://doi.org/10.1617/s11527-014-0306-7.

Stubňa, Igor, and Rudolf Podoba. 2013. “Romanesque and Gothic Bricks from Church in Pác - Estimation of the Firing Temperature.” *Epitoanyag-Journal of Silicate Based and Composite Materials* 65: 48–51.

Taranto, Mirco, Luis Barba, Jorge Blancas, Andrea Bloise, Marco Cappa, Francesco Chiaravalloti, Gino Mirocle Crisci, et al. 2019. “The Bricks of Hagia Sophia (Istanbul, Turkey): A New Hypothesis to Explain Their Compositional

Difference." *Journal of Cultural Heritage* 38: 136–46. https://doi.org/10.1016/j.culher.2019.02.009.

Tarhan, İsmail, and İlker Işık. 2020. "An In-Depth Chemometric Study: Archaeometric Characterization of Ceramic Shards Excavated from the Sanctuary of Hecate at Lagina in Muğla (Turkey) by FTIR Spectroscopy and Multivariate Data Analysis." *Vibrational Spectroscopy* 111 (September). https://doi.org/10.1016/j.vibspec.2020.103172.

Tekin, Çiğdem, and Sedat Kurugöl. 2011. "Physicochemical and Pozzolanic Properties of the Bricks Used in Certain Historic Buildings in Anatolia." *Gazi University Journal of Science* 24 (4): 2011.

Thucydides. 1950. *The History of the Peloponnesian War*. New York: E. P. Dutton and Company, Inc.

Trindade, Maria José, Maria Isabel Dias, João Coroado, and Fernando Rocha. 2009. "Mineralogical Transformations of Calcareous Rich Clays with Firing: A Comparative Study between Calcite and Dolomite Rich Clays from Algarve, Portugal." *Applied Clay Science* 42 (3–4): 345–55. https://doi.org/10.1016/j.clay.2008.02.008.

Trindade, Maria José, Maria Isabel Dias, João Coroado, and Fernando Rocha. 2010. "Firing Tests on Clay-Rich Raw Materials from the Algarve Basin (Southern Portugal): Study of Mineral Transformations with Temperature." *Clays and Clay Minerals* 58 (2): 188–204. https://doi.org/10.1346/CCMN.2010.0580205.

TSE (Turkish Standards Institution). 2012. *TS EN 197-1: Cement Part 1: Composition, Specification and Conformity Criteria for Common Cements*.

Tucci, Pier Luigi. 2015. "The Materials and Techniques of Greek and Roman Architecture." In *The Oxford Handbook of Greek and Roman Art and Architecture*, 241–65. New York: Oxford University Press.

"Türkiye Kültür Portalı." n.d. Accessed May 17, 2022. https://www.kulturportali.gov.tr/.

Uğurlu Sağın, Elif. 2017. "Anadolu'da Roma Dönemi Yapı Tuğlalarının Özellikleri." *Journal of the Faculty of Engineering and Architecture of Gazi University* 32 (1): 227–36. https://doi.org/10.17341/gazimmfd.300612.

Uğurlu Sağın, Elif, and Hasan Böke. 2013. “Characteristics of Bricks Used in the Domes of Some Historic Bath Buildings.” *Journal of Cultural Heritage* 14 (3 SUPPL): 73–76. https://doi.org/10.1016/j.culher.2012.11.030.

Ulukaya, Serhan, Afife Binnaz Hazar Yoruç, Nabi Yüzer, and Didem Oktay. 2017. “Material Characterization of Byzantine Period Brick Masonry Walls Revealed in Istanbul (Turkey).” *Periodica Polytechnica Civil Engineering* 61 (2): 209–15. https://doi.org/10.3311/PPci.8868.

Valanciene, V., R. Siauciunas, and J. Baltusnikaite. 2010. “The Influence of Mineralogical Composition on the Colour of Clay Body.” *Journal of the European Ceramic Society* 30 (7): 1609–17. https://doi.org/10.1016/j.jeurceramsoc.2010.01.017.

Vieira, C. M.F., and S. N. Monteiro. 2007. “Effect of Grog Addition on the Properties and Microstructure of a Red Ceramic Body for Brick Production.” *Construction and Building Materials* 21 (8): 1754–59. https://doi.org/10.1016/j.conbuildmat.2006.05.013.

Vitruvius. 1914. *Vitruvius: The Ten Books on Architecture*. Translated by Morris Hicky Morgan. Cambridge: Harvard University Press.

Weng, Chih Huang, Deng Fong Lin, and Pen Chi Chiang. 2003. “Utilization of Sludge as Brick Materials.” *Advances in Environmental Research* 7 (3): 679–85. https://doi.org/10.1016/S1093-0191(02)00037-0.

Worrall, D. M. 1986. *Clays and Ceramic Raw Materials*. 2nd ed. Leeds: Springer Dordrecht. https://link.springer.com/book/9781851660049.

Wright, G.R.H. 2005. *Ancient Building Technology, Volume 2: Materials (2 Vols)*. Leiden: Brill.

Wright, G.R.H. 2009. *Ancient Building Technology, Volume 3: Construction (2 Vols)*. Leiden: Brill.

Yüksel, Fethi Ahmet, Nihan Sezgin Hoşkan, Mehmet Şafi Yıldız, and Zeynep Mercangöz. 2011. “Kuşadası-Kadıkalesi (Anaia) Arkeojeofizik Çalışmaları 2010.” In *27. Arkeometri Sonuçları Toplantısı*, 139–51. Kültür ve Turizm Bakanlığı Kültür Varlıkları ve Müzeler Genel Müdürlüğü.